Development of miniaturized disposable electrochemical systems intended for point of care blood analysis

Musa, Arnaud Emmanuel

Publication date:
2011

Document Version
Publisher's PDF, also known as Version of record

Development of miniaturized disposable electrochemical systems intended for point of care blood analysis

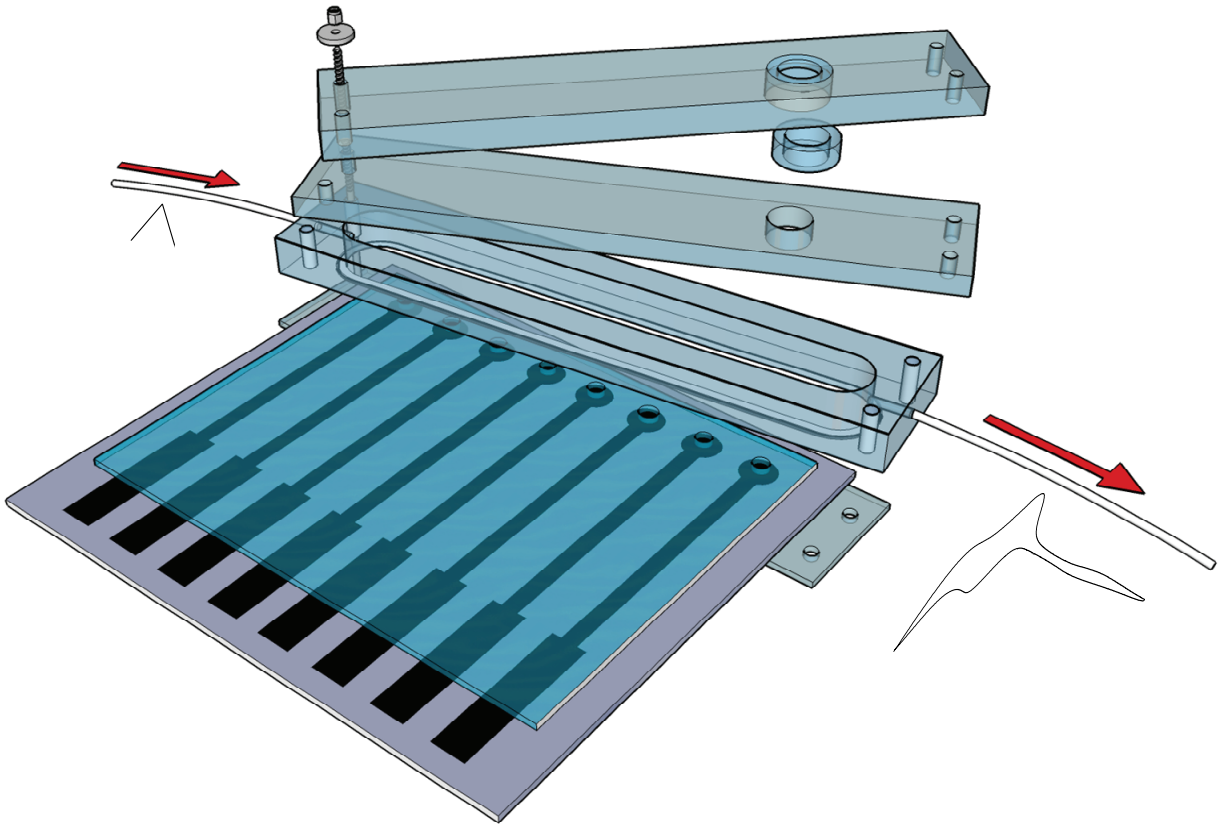

Arnaud E. Musa

Ph.D. Thesis

Technical University of Denmark – DTU
Department of Micro and Nanotechnology – DTU Nanotech

Development of miniaturized disposable electrochemical systems intended for point of care blood analysis

Arnaud E. Musa

Ph.D. Thesis

July 2011

Technical University of Denmark – DTU
Department of Micro and Nanotechnology – DTU Nanotech
Ørsted Plads - Building 344
2800 Kongens Lyngby
Denmark

Main supervisor

Jörg P. Kutter

Evaluation board

Jenny Emnéus (Technical University of Denmark, DTU Nanotech)
Janusz Plocharski (Warsaw University, Faculty of Chemistry)
Alberto Romano-Rodriguez (University of Barcelona, Electronics Department)

Date of the defense

September 30th, 2011

Abstract

Electrochemical systems are well established tools used to determine the presence of target analytes in a broad range of fields such as clinical, environmental, food, or industrial applications. Inexpensive, simple, versatile, and highly reproducible, the thick-film technology of screen-printing (SP) features several advantages and thus appeared as the evident fabrication process for the development of disposable electrochemical sensors in this project. Due to the popularity of this technology, a very expansive variety of SP products is currently available on the market, especially in terms of inks for electronically conducting materials and dielectric materials. However, the precise composition of these materials is kept as proprietary information from the manufacturers. In this thesis, an assortment of some of the most commonly used products was investigated. It was demonstrated that significant differences in terms of electrochemical, mechanical and electrical properties exist between these products. The effect of electrochemical and thermal treatments of the screen-printed materials was also investigated. This study resulted in the selection of an optimal electrochemical system used for further electrochemical investigations in this thesis.

Based on these electrochemical systems, the fabrication of potentiometric pH-sensors featuring a photo-curable polyurethane membrane as ion-selective-membrane (ISM) was then studied. The choice of the membrane was motivated by the fact that such material is very attractive from a technological point of view since compatible with standard photo-lithographic processes and thus easier to streamline than commonly used polyvinylchloride membranes.

Prior to the membrane deposition on the screen-printed electrodes, a series of electrode treatments were used in order to increase the double layer capacitance of the graphite based sensors and thereby increase their potential stability. Electrochemical activation by cyclic voltammetry and optimized thermal treatment of the graphite sensors were used. The final potentiometric pH-sensor was composed of a coated-wire electrode (CWE) and a quasi-reference electrode (QRE) and displayed the excellent pH response of -60.8 ± 1.7 mV/pH over a six day period, which is very close to the theoretical Nernstian value.

In order to further improve the stability of the CWEs, the conducting polymer PEDOT-PSS was deposited between the graphite electrode and the ISM to act as ion-to-electron transducing material. In this type of solid-state electrochemical system, the potential stability is defined by the redox capacitance instead of the double layer capacitance as in the case of CWEs. The dependence of the thickness of the PEDOT-PSS layer on the capacitance and the pH response of the final pH-sensor were investigated. It was observed that the thicker the PEDOT-PSS layer, the higher the capacitance of the sensor but, unexpectedly, the lower the pH-response of the final sensor. In order to support these results and understand them in depth, additional experiments are needed. Moreover, the choice of the CP as ion-to-electron transducer for pH-selective electrodes needs to

be investigated in more details. Alternatively, polymers that have proven to be suitable for such purpose such as polyaniline or polypyrrole could be used.

Finally, the development of a screen-printed voltammetric system for pH monitoring was attempted. The main characteristic of this system was that it integrated both sensing and reference electroactive species in the graphite matrix of the working electrode.
Sensors were fabricated by screen-printing a graphite paste loaded with phenanthraquinone (PAQ) as a pH-sensitive moiety (i.e., indicator species) and dimethylferrocene (Fc) as a pH-insensitive moiety. This represented a much simpler and faster technique compared to, for example, covalent chemical derivatization on carbon materials with electroactive species. Moreover, to my knowledge, the use of SP for the development of this type of voltammetric systems has surprisingly only been recently investigated by D. K. Kampouris et al. [1] despite its undeniable advantages.

Electrochemical measurements highlighted the promising performances of such electrochemical system. It was shown that the oxidation peak of the Q/QH_2 redox couple and the reduction peak of the Fc/Fc^+ redox couple could be successfully used to monitor pH. A super Nernstian pH response was displayed by the sensors which still remains not very well understood. However, the sensors responded to pH changes in a very reproducible way despite their very simple fabrication processes. Moreover, the developed voltammetric system presented the major advantage of limiting the potential issues stemming from the reference half-cell. Indeed, since the measurement principle was based on evaluating the difference between the redox peaks of the two electrochemical species, potential drift of the RE was thus not as crucial as for other common electrochemical setups.

[1] D. K. Kampouris, R. O. Kadara, N. Jenkinson, C. E. Banks, Analytical Methods, **2009**. 1: p. 25 - 28.

Resumé (in Danish)

Elektrokemiske systemer er veletablerede værktøjer, der anvendes til at bestemme tilstedeværelsen af specifikke stoffer indenfor en bred vifte af områder som kliniske, miljø-, fødevarer, eller industrielle applikationer. Billig, enkel, alsidig og yderst reproducerbar, tykfilm-teknologien i screen-printing (SP) har flere fordele og fremstod dermed som den åbenlyse fremstillings proces for udviklingen af de disponible elektrokemiske sensorer i dette projekt. På grund af populariteten af denne teknologi, findes der en meget bred vifte af SP-produkter på markedet, især i form af blæk til elektrisk ledende materialer og dielektriske materialer. Dog holdes den præcise sammensætning af disse materialer hemmelig af producenterne. I denne afhandling, blev et udvalg af nogle af de mest almindeligt anvendte produkter undersøgt. Det blev påvist, at der findes væsentlige forskelle i form af elektrokemiske, mekaniske og elektriske egenskaber mellem disse produkter. Effekten af elektrokemisk og termisk behandling af de screen-printede materialer blev også undersøgt. Denne undersøgelse resulterede i udvælgelsen af et optimalt elektrokemisk system, til anvendelse ved yderligere elektrokemiske undersøgelser i denne afhandling.

Baseret på disse elektrokemiske systemer, blev fremstillingen af potentiometriske pH-sensorer med en foto-hærdende polyurethan membran, som ion-selektiv-membran (ISM), undersøgt. Valget af membranen var motiveret ud fra, at et sådan materiale er meget attraktivt ud fra et teknologisk synspunkt, da det er kompatibelt med standard foto-litografiske processer og dermed nemmere at tilpasse end de almindeligt brugte polyvinylklorid membraner.

Forud for membran depositionen på de screen-printede elektroder, blev en række elektrode behandlinger anvendt med henblik på at øge kapacitansen af dobbelt laget i de grafit baserede sensorer og dermed øge deres spænningsstabilitet. Der blev brugt elektrokemisk aktivering ved cyklisk voltammetri og optimeret termisk behandling af grafit sensorerne. Den endelige potentiometriske pH-sensor var sammensat af en coated-wire elektrode (CWE) og en kvasi-reference elektrode (QRE) og viste i løbet af en seks dages periode, en fremragende pH følsomhed på -60,8 ± 1,7 mV / pH, hvilket er meget tæt til den teoretiske Nernstian værdi.

For yderligere at forbedre stabiliteten i CWE'erne, blev den ledende polymer PEDOT-PSS deponeret mellem grafitelektroden og ISM'en for at fungere som ion-til-elektron transducerende materiale. I denne type solid-state elektrokemisk system, er den potentielle stabilitet defineret af redox kapacitansen i stedet for dobbelte lags kapacitansen som er tilfælde ved CWEs. Afhængigheden af tykkelsen af PEDOT-PSS laget på kapacitansen og pH følsomheden ved den endelige pH-sensor blev undersøgt. Det blev observeret, at jo tykkere PEDOT-PSS lag, jo højere blev sensorens kapacitans, men uventet, jo lavere blev pH-følsomheden af den endelige sensor. For at understøtte disse resultater og forstå dem i dybden, er yderligere eksperimenter nødvendige. En yderligere detaljeret undersøgelse af valget af CP som ion-to-elektron transducer til pH-selektive elektroder er

desuden nødvendig. Alternativt kunne polymerer, der har vist sig at være velegnet til sådanne formål såsom polyaniline eller polypyrrole, anvendes.

Endeligt blev det forsøgt at udvikle et screen-printet voltametriske system til pH overvågning. Den vigtigste egenskab ved dette system var, at det integrerede både sensorer og reference elektroaktive komponenter i sensorelektrodens grafit matrix.
Sensorer blev fabrikeret ved at screen-printe en grafit pasta fyldt med phenanthraquinone (PAQ) som den pH-følsomme del (dvs. indikator komponenter) og dimethylferrocene (Fc) som den pH-ufølsomme del. Dette repræsenterede en meget enklere og hurtigere teknik i forhold til, for eksempel kovalent kemisk derivatisering på kulstof materialer med elektroaktive komponenter. Hertil kommer, så vidt jeg ved, at brugen af SP i fremstillingen af denne type voltametriske systemer overraskende først for nylig blevet undersøgt af DK Kampouris et al. [1] på trods af sine uomtvistelige fordele.

Elektrokemiske målinger fremhævede de lovende præstationer af disse elektrokemiske systemer. Det blev vist, at oxidationstoppen af Q/QH_2 redox parret og reduktionstoppen af Fc / Fc^+ redox parret med fordel kan anvendes til at overvåge pH. Sensorerne viste en super Nernstian pH-følsomhed, der stadig ikke er særlig godt forstået. Men sensorerne reagerede på pH-ændringer på en meget reproducerbar måde på trods af deres meget enkle fremstillingsprocesser. Desuden havde det udviklede voltametriske system den store fordel, at de spændingsmæssige problemer, der stammer fra reference halv-cellen, blev reduceret. Faktisk, eftersom målingen i princippet var baseret på bestemmelsen af forskellen mellem redox toppene af de to elektrokemiske komponenter, så var potentiel drift af RE ikke så afgørende som for andre sædvanlige elektrokemiske opsætninger.

[1] D. K. Kampouris, R. O. Kadara, N. Jenkinson, C. E. Banks, Analytical Methods, **2009**. 1: p. 25 - 28.

Preface

This thesis has been written as a partial fulfillment of the requirements for obtaining the Ph.D. degree at the Technical University of Denmark (DTU). This work has been carried out at DTU Nanotech, Department for Micro and Nanotechnology – DTU, from 2nd of February 2008 to 1st of July 2010.
This Ph.D. project was run in collaboration with Radiometer Medical, Copenhagen, Denmark.

The Ph.D. project has been supervised by:

- **Jörg P. Kutter**, Group Leader of the ChemLabchip group, DTU Nanotech, as main supervisor
- **Anders Wolff**, Associate Professor, DTU Nanotech, as main supervisor (from February 2008 to October 2008)
- **Monica Brivio**, Assistant Professor, DTU Nanotech, as co-supervisor (from February 2008 to December 2009)
- **Oliver Geschke**, Assistant Professor, DTU Nanotech, as co-supervisor (from February 2008 to April 2010)
- **Detlef Snakenborg**, Assistant Professor, DTU Nanotech, as co-supervisor (from February 2008 to May 2010)
- **Kasper Schweitz**, R & D Director, Radiometer Medical, as co-supervisor
- **Lars C. von Gersdorff**, Team leader Medical device development, Radiometer Medical, as co-supervisor

This Ph.D. project included two external periods of research in the group of Associate Professor F. Javier Del Campo at the Instituto de Microelectrónica de Barcelona IMB-CNM CSIC, on the Campus Universitat Autónoma de Barcelona, Spain.

Acknowledgements

First of all, I would like to acknowledge my previous and current supervisors for the guidance in their respective fields. Special thanks go to Jörg P. Kutter for his supervision and always optimistic approach to challenges during my project. Thanks to Anders Wolff, Monica Brivio, Detlef Snakenborg, Oliver Geschke, Kasper Schweitz, and Lars C. von Gersdorff, for giving me the opportunity to carry out this Ph.D. project.

I would also like to thank F. Javier del Campo, Natasha Abramova and M. Asunción Alonso-Lomillo for their priceless help and inspiring guidance during and after my stays in Spain.

I would like to acknowledge all my ChemLabChip friends, I truly appreciated working and sharing lunch breaks and breakfasts with you. In particular, I would like to thank Silja Senkbeil for the fun time in the office, amazing German cakes and her support. Thanks a lot to Guisheng Zhuang for his precious help on experiments in the clean room. I would like to thank Thomas Glasdam Jensen for his help on the Danish version of the abstract of this thesis and for the "last minute help". Thanks to Josiane Lafleur and Masahiro Motosuke for their priceless advice and support.

Thanks to my "CNM buddies" for their unbelievable hospitality. Special thanks to Neus Godino and Olga Ordeig who "convinced" me to do my external stays at CNM.

For many discussions and recommendations mostly electrochemistry related, I would like to gratefully thank Arto Heiskanen and Steen Skaarup.

I would like to thank all of my friends, in Denmark, France and Spain or wherever you are. Thanks Amine, Aga, Rodrigo, Marta, Debbie, Popiel, Gustavo, Rodolphe, Damien, Marie, Sebastien, Henrik, Benjamin, Jack, Anders, Jan, Jörg, Irakli, Kaushal, Indu, Pranjul, Jesper, Roman, Simone, Carlos, Diana, Sergio, Irene, Iñigo(s), Giordano, Juan Pablo(s), Sandra, I would probably not have enough pages to name all of you, but again thanks a lot for helping me forget about all the Ph.D. related stress.

Last but not least, I would like to dedicate this thesis to my family, Papa, Maman et Tom, for your love and constant care…

Table of contents

List of figures

List of tables

Main abbreviations

AC: alternating current
CE: counter electrode
CNC: computer numerical control
COP: cyclo olefin polymer
CV: cyclic voltammetry
CWE: coated-wire electrode
DI: deionized
DJRE: double-junction reference electrode
DL: double layer
Fc: ferrocene
ISE: ion-selective electrode
LTCC: low-temperature co-fired ceramic
OCP: open-circuit potential
PAQ: phenanthraquinone
PDMS: polydimethylsiloxane
PEDOT: poly(3,4-ethylenedioxythiophene)
PET: polyethyleneterephthalate
PMMA: polymethylmethacrylate
PSS: polystyrenesulfonate
PTFE: polytetrafluoroethylene
PUR: polyurethane
QRE: quasi-reference electrode
RE: reference electrode
SC: solid contact
SP: screen-printing
SPE: screen-printed electrode
SWV: square-wave voltammetry
UV: ultra violet
WE: working electrode

Chapter I Scope and outline of the thesis

1 Scope of the thesis

At the beginning of each chapter of the following thesis, the reader is introduced with the different motivations for the investigations carried out. Here, in the following section, a general description of the scope of the overall work presented in this thesis is given.

Electrochemical systems have rapidly evolved especially over the last 25 years. Electrochemical sensors feature high sensitivities, low cost, involve the use of simple setups and electronic equipment and thus low power consumption. Moreover, their high compatibility with advanced micromachining and microfabrication technologies have permitted them to replace some of the conventional cumbersome electrodes and electrochemical cells with easy to use miniaturized electrochemical systems [2]. As a matter of fact, most of these features stand for major advantages over many conventional laboratory systems (e.g., for techniques such as chromatography, spectroscopy, mass spectroscopy, etc.). Even though not completely replacing the above mentioned techniques mainly due their superior precision and detection limits, electrochemical systems have proven their remarkable compatibility with modern miniaturization techniques and have ultimately emerged as suitable for a broad range of applications, including industry, traffic, environmental, and medical monitoring [3]. Since the nineties and the introduction of the term miniaturized total analysis systems or μTAS by Manz et al. [4], coupling miniaturized electrochemical devices with advanced microfluidics techniques has been extensively investigated. As a result, this has ultimately offered the capability for developing portable diagnostic tools, hence revolutionizing the field of so called "Point-of-Care Medicine" [5,6]. More generally, the demand for clinical and industrial sensing systems has been in permanent increase and has led to the development of individual self monitoring devices. Consequently, the need for inexpensive, portable, disposable, yet highly accurate and rapid devices has been of crucial importance [7].
Most conventional electrochemical sensors feature bulky shapes and voluminous liquid compartments. Thus, this type of sensors presents many disadvantages, mainly due to the presence of a liquid electrolyte phase. Defined position of the sensor during storage, limited potential for miniaturization, pressure and temperature dependence, mechanical instability, inappropriate shape for measurement on surfaces and expensive production are examples of issues related to this type of sensors [8]. Most of those can be circumvented by the use of planar electrochemical sensors, which basically eliminate (or partly eliminate) the liquid component.

Available fabrication processes for development of planar electrochemical systems are thin-film and thick-film technologies and electroless plating (i.e., wet chemistry) ([8] and cited references). However, the most cost effective one is thick-film technology and especially the process of screen-printing (SP) [3,7]. Involving the use of simple inexpensive equipment and processes yet providing a highly reproducible fabrication method, SP has proven to be highly compatible for the development of disposable sensors ever since the nineties [9,10].

The development of this technology has pushed more and more manufacturers to produce screen-printed products. Nowadays, a very extensive range of screen-printing materials is available on the market. However, the precise composition and nature of these materials, for instance in terms of particle size, type of binder, additives, etc. are always regarded as proprietary information by their manufacturers [7]. A major concern rises from the fact that such parameters have proven to strongly affect the electrochemical properties of the fabricated sensors, as highlighted in the end of the nineties in pioneer works from J. Wang et al. [11,12] in which different SP graphite based materials were analyzed.

Compared to J. Wang et al.'s works, in this Ph.D., an updated selection of some of the most currently used commercial SP materials for both electronically conducting and dielectric patterns was thoroughly analyzed. The electrochemical, mechanical and electrical properties of these materials were investigated in detail. Moreover, the effects of the thermal curing and electrochemical activation of graphite SP pastes were also studied.

Furthermore, while the previous investigations on this topic were carried out on ceramic materials [12,13] and thus involved high process temperatures (sometimes up to 300 °C), for this project, low cost polymer materials, more suitable for mass production, were used.

Moreover, this study was ultimately done to obtain an optimal selection of materials and treatments for the development of a disposable solid-state potentiometric pH-sensor. Investigations were initiated by the development of coated-wire electrodes (CWEs). In this type of sensor, the potential stability depends on the double layer (DL) capacitance. Thus, in this Ph.D., different means to increase this DL were proposed. Moreover, in order to pursue this investigation, the use of a conducting polymer (CP) was introduced to act as ion-to-electron transducing material for further improvement of the sensor's properties. This was meant to further improve the potential stability of the sensor which in this case is defined by its redox capacitance [14].

In spite of the large success of electrochemical sensors in several different fields, a critical issue has restricted their use for certain industrial and biomedical applications: the unavailability of a reliable and durable miniature reference electrode (RE). Indeed, the miniaturization of electrochemical sensors has often been constrained to the working electrode and in many cases a commercial macroscopic reference electrode is used instead [15].

Many different promising solutions have been proposed. Examples of some of the most promising works published in the last 15 years have consisted in developing REs based on thin-film technology [15-19], SP technology [20-22], conducting polymers [23-30], nanofluidic channels acting as salt bridge [31], a solid crystalline KCl melt [32], polyacrylate microspheres composite [33], and non organic materials [34]. Different reviews of some of the microfabricated REs described in the literature have also been recently published [35,36].

However, as agreed by most who have been involved in the development of electrochemical systems, miniaturization and batch-fabrication of a reliable RE have been one of the most difficult challenges left in the field [9] and was even considered by many as being equal to the quest for the Holy Grail [37]. For instance, this has been one of the major challenges for industries such as

our collaborator *Radiometer Medical*, Copenhagen, where the development of disposable, reliable and stable REs for electrochemical medical devices is crucial.

As opposed to most of the previously mentioned works, which focused on researching for stable and reliable reference half-cells, here it was alternatively attempted to explore the fabrication of sensors featuring sensing half-cells with internal reference species. Thus, emphasis was not put on attempting to solve the uncountable potential issues stemming from the RE (e.g., complex or expensive fabrication, drift, membrane shrinkage or delamination, long conditioning times, etc.). Here, a different approach to circumvent those challenges was adopted and consisted in using a simple and low cost alternative type of electrochemical system featuring a sensing electrode incorporating both sensing and reference and a quasi-reference electrode (QRE).

Additionally, the sensors were made from screen-printed electrochemical platforms developed in this thesis. The development of this novel type of sensors and has surprisingly only been previously investigated by D. Kampouris et al. [1] on the bases of the pioneer work carried out by J. Hickman et al. [38].

2 Outline of the thesis

Chapter II starts by introducing with some of the key concepts and terms necessary to understand some of the fundamentals of electrochemistry. A brief description of electrochemical systems as well as some of the most commonly used electrochemical techniques is given.

Chapter III starts by describing the fabrication of low cost electrochemical systems by the thick-film process of SP. Then, the influence of various fabrication parameters on the electrochemical, electrical and mechanical properties to the developed sensors is investigated. Thus, choice of the SP materials and post-printing treatments of fabricated electrodes (both thermal and electrochemical) were optimized.
In the second part of this chapter, a brief description of the different micromachined polymer devices used in this thesis is given. These devices were developed for characterization and fabrication of electrochemical sensors.

In **chapter IV**, the development of electrochemical potentiometric pH-sensors based on thick-film electrodes is presented.
First, the fabrication of CWEs for pH monitoring is described. The results of this work were also reported in an article [39].
The second part of this chapter introduces with the use of a CP for ion-selective-electrodes (ISEs). The main focus of this investigation was to improve the general performances of the CWEs developed previously, by using a CP as an ion to electron transducing material.

Chapter V presents the fabrication of low cost voltammetric pH-sensors incorporating both sensing and reference electroactive species in the working electrode. The fabrication of these sensors was done by manual SP of graphite based inks incorporating a pH-sensitive moiety as the sensing component and a pH-insensitive moiety as the reference component.

In **chapter VI**, a summary of the conclusions drawn from the previous chapters is given with subsequent recommendations for future research and potential improvements.

3 References

[1] D. K. Kampouris, R. O. Kadara, N. Jenkinson, C. E. Banks, Analytical Methods, **2009**. 1: p. 25 - 28.

[2] J. Wang, Trends in Analytical Chemistry, **2002**. 21(4): p. 226-232.

[3] U. Guth, W. Vonau, J. Zosel, Measurement Science and Technology, **2009**. 20 (4): p. 1-14.

[4] A. Manz, N. Graber, H. M. Wildmer, Sensors and Actuators B, **1990**. 1(1-6).

[5] McLaughlin, J.A.D., *Point of Care Biomedical Sensors* in *Personalised Health Management Systems: The Integration of Innovative Sensing, Textile, Information and Communication Technologies*, C. D. Nugent, P. J. McCullagh, E. T. McAdams, A. Lymberis, Editor. **2005**, IOS Press. p. 25-34.

[6] A. J. Tüdős, G. A. J. Besselink, R. B. M. Schasfoort, Lab on a Chip, **2001**. 1(2): p. 83-95.

[7] J. P. Metters, R. O. Kadara, C. E. Banks, Analyst, **2011**. 136(6): p. 1067-1076.

[8] W. Vonau, U. Enseleit, F. Gerlach, S. Herrmann, Electrochimica Acta, **2004**. 49(22-23): p. 3745–3750.

[9] H. Suzuki, Electroanalysis, **2000**. 12(9): p. 703-715.

[10] O. Domínguez Renedo, M.A. Alonso-Lomillo, M.J. Arcos Martínez, Talanta, **2007**. 73(2): p. 202–219.

[11] J. Wang, B. Tian, V. B. Nascimento, L. Angnes, Electrochimica Acta, **1998**. 43(23): p. 3459-3465.

[12] J. Wang, M. Pedrero, H. Sakslund, O. Hammerich, J. Pingarron, The Analyst, **1996**. 121(3): p. 345-350.

[13] M. Rice, Z. Galus, R. N. Adams, Journal of Electroanalytical Chemistry, **1982**. 143(1-2): p. 89-102.

[14] J. Bobacka, A. Ivaska, A. Lewenstam, Chemical Reviews, **2008**. 108(2): p. 329-351.

[15] H. Suzuki, A. Hiratsuka, S. Sasaki, and I. Karube, Sensors and Actuators B, **1998**. 46(2): p. 104–113.

[16] H. Suzuki, T. Hirakawa, S. Sasaki, I. Karube, Sensors and Actuators B, **1998**. 46(22): p. 5069-5075.

[17] A. Simonis, H. Lüth, J. Wang, M. J. Schöning, Sensors and Actuators B, **2004**. 103(1-2): p. 429–435.

[18] H. J. Yoon, J. H. Shin, S. D. Lee, H. Nam, G. S. Cha, T. D. Strong, R. B. Brown, Sensors and Actuators B, **2000**. 64(1-3): p. 8–14.

[19] J. Ha, S. M. Martin, Y. Jeon, I. J. Yoon, R. B. Brown, H. Nam, G. S. Cha, Analytica Chimica Acta, **2005**. 549(1-2): p. 59–66.

[20] Ł. Tymecki, E. Zwierkowska, R. Koncki, Analytica Chimica Acta, **2004**. 526(1): p. 3–11.

[21] J.K. Atkinson, M. Glanc, P. Boltryk, M. Sophocleous, E. Garcia-Breijo, Microelectronics International, **2011**. 28(2): p. 49-52.

[22] A. W. J. Cranny, J. K. Atkinson, Measurement Science and Technology, **1998**. 9(9): p. 1557–1565.

[23] A. Kisiel, H. Marcisz, A. Michalska, and K. Maksymiuk, The Analyst, **2005**(130): p. 1655–1662.

[24] A. Kisiel, A. Michalska, K. Maksymiuk, Bioelectrochemistry, **2007**. 71(1): p. 75–80.

[25] A. Kisiel, A. Michalska, K. Maksymiuk, E. A. H. Hall, Electroanalysis, **2008**. 20(3): p. 318-323.

[26] N. H. Kwon, K. S. Lee, M. S. Won,Y. B. Shim, The Analyst, **2007**. 132(9): p. 906-912.

[27] C. C. Chen, J. C. Chou, Japanese Journal of Applied Physics, **2009**. 48(11): p. 111501.

[28] H. Jahn, H. Kaden, Microchimica Acta, **2004**. 146(2): p. 173–180.

[29] J. Ghilane, P. Hapiot, A. J. Bard, Analytical Chemistry, **2006**. 78(19): p. 6868-6872.

[30] Y. H. Liao, J. C. Chou, Journal of The Electrochemical Society, **2008**. 155(10): p. 257-262.

[31] J. Zhou, K. Ren, Y. Zheng, J. Su, Y. Zhao, D. Ryan, H. Wu, Electrophoresis, **2010**. 31(18): p. 3083-3089.

[32] W. Vonau, W. Oelßner, U. Guth, J. Henze, Sensors and Actuators B, **2010**. 144(2): p. 368-373.

[33] A. Kisiel, M. Donten, J. Mieczkowski, F. X. Rius-Ruiz, K. Maksymiuk,A. Michalska, Analyst, **2010**. 135(9): p. 2420-2425.

[34] J. Gabel, W. Vonau, P. Shuk, U. Guth, Solid State Ionics, **2004**. 169(1-4): p. 75–80.

[35] M. W. Shinwari, D. Zhitomirsky, I. A. Deen, P. R. Selvaganapathy, M. J. Deen, D. Landheer Sensors **2010**. 10 (3): p. 1679-1715.

[36] U. Guth, F. Gerlach, M. Decker, W. Oelßner, W. Vonau, Journal of Solid State Electrochemistry **2009**. 13(1): p. 27-39.

[37] R. P. Buck, E. Lindner, Analytical Chemistry, **2001**. 73(3): p. 88-97.

[38] J. J. Hickman, D. Ofer, P. E. Laibinis, G. M. Whitesides, M. S. Wrighton, Science, **1991**. 252(5006): p. 688-691

[39] A. E. Musa, F. J. del Campo, N. Abramova, M. A. Alonso-Lomillo, O. Domínguez-Renedo, M. J. Arcos-Martínez, M. Brivio, D. Snakenborg, O. Geschke, and J. P. Kutter, Electroanalysis, **2011**. 23(1): p. 115–121.

Chapter II Electrochemistry and electrochemical systems

1 Fundamentals

1.1 Introduction

Electrochemistry is the science concerned with the interrelation of electrical and chemical effects, namely, the relationship between the measurement of electrical quantities (current, potential, or charge) and chemical parameters [1,2]. In the following section, some of the fundamental terms and concepts commonly used to illustrate electrochemical reactions are briefly explained.

1.2 Electrical double layer

In electrochemical processes, interfacial charge transfer mechanisms are studied, most generally, taking place between a solid (electrode) and a liquid (electrolyte). In order to understand electrochemical phenomena, it is therefore necessary to have a close look at the different mechanisms occurring at this interface.

When a conducting solid is immersed into a solution, an array of charged particles and oriented dipoles is formed at the interface between the solid surface and the solution [3]. This region is called the electrical double layer (DL) and reflects the ionic zones formed in the solution to compensate for the charge on the electrode surface. In 1879, Helmholtz first introduced the term of electrical DL, which was mathematically described as a simple parallel-plate condenser (i.e., a capacitor) [4] in which a single layer of ions is adsorbed at the surface. Later, Gouy and Chapman intended to improve this model by introducing a diffuse model, in which anions and cations are unequally distributed in obedience to the laws of Poisson and Boltzmann [1,5]. Finally, Stern presented a model, which combined the two previous ones, describing an inner compact layer with a width of atomic dimension (i.e., Helmholtz layer) and an outer diffuse layer of semi-infinite dimension (i.e., Gouy-Chapman layer) [2]. Even though the theory of this latter model is almost a century old and has undergone additional modifications and refinements, it is still cited in many works, in almost all textbooks of electrochemistry and in many physical chemistry texts [2,5].

The electrical DL is often illustrated as being made of regions delimited by imaginary planes. A simplified illustration is shown in Figure 1. The region closest to the electrode surface contains solvent molecules and specifically adsorbed ions and is delimited by the plane passing through the centers of the specifically adsorbed ions and is named the inner Helmholtz plane (IHP). The region of nearest solvated ions is composed of non-specifically adsorbed ions and is known as the outer Helmholtz plane (OHP). Finally, the diffuse layer stands for the region extending from the OHP to

the bulk and contains the weakly adsorbed ions. The thickness of the diffuse layer varies according to the ionic concentration of the electrolyte, but is typically less than hundred angstroms [2].

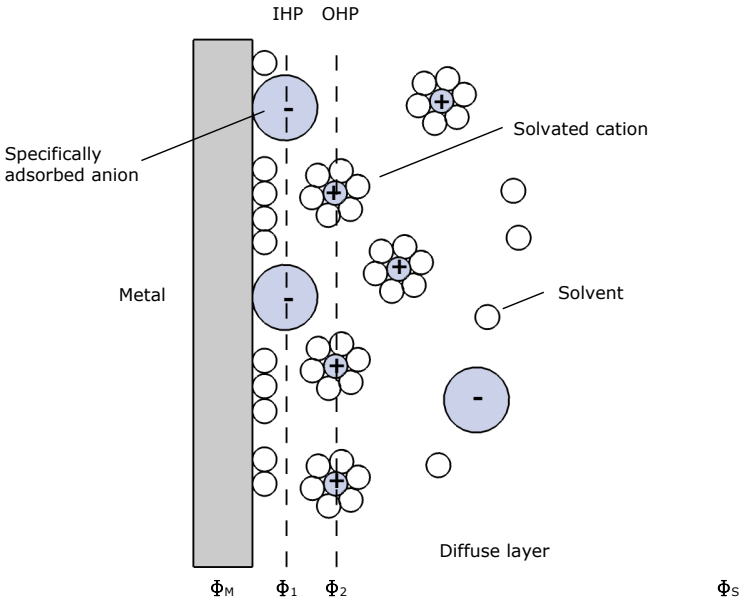

Figure 1: Illustration of the electrical DL structure. IHP is the inner Helmholtz plane, OHP is the outer Helmholtz plane, Φ_M, Φ_S, Φ_1 and Φ_2 are the electrostatic potentials of the metal surface, solution, IHP, and OHP, respectively.

Due to its structure, the electrical DL resembles a parallel-plate capacitor, for which the charge is proportional to the potential difference (Equation 1) [1].

$$q = CE \qquad \text{Equation 1}$$

Where q is the charge, C the capacitance and E the potential applied.

The total capacitance of the DL is often expressed as the sum of the capacitance of the compact and the diffuse layers (Equation 2) [1].

$$\frac{1}{C} = \frac{1}{C_H} + \frac{1}{C_G} \qquad \text{Equation 2}$$

Where C_H and C_G are the capacitances of the Helmholtz layer and the Gouy-Chapman layer, respectively.

Moreover, the electrochemical properties of a system differ according to the type of electrical perturbation it undergoes. For instance, whether a voltage step, a voltage ramp or a current step is applied to a system, the charging current (related to the capacitance) will be different [2].

1.3 Faradaic and non-faradaic processes

In an electrochemical cell, two types of current may flow, namely, the faradaic and the non-faradaic currents. The latter is due to adsorption and desorption of species taking place at the electrode/solution region resulting in rearrangement of the electrical DL structure [2]. Non-faradaic processes are directly related to Ohm's law and correspond to charging currents [6]. Those typically occur when a potential is applied at an electrode causing the formation of the electrical DL or when the electrode area or capacitances are changed [1]. On the other hand, faradaic processes occur when charges (e.g., electrons) are transferred across the electrode/solution interface thus, resulting in oxidation or reduction reactions of chemical species to occur [2].

For most investigations of electrode reactions, these faradaic processes are generally of primary interest and the non-faradaic ones are thus minimized. For instance, in the cyclic voltammetry experiments carried out in this thesis, non-faradaic contributions were minimized by subtracting the background currents.

1.4 Electrode reactions

The reactions occurring at the electrode surface can be fairly complicated and may involve several steps [1]. Simple electrode processes involve mass transport of the electroactive species to the electrode surface, electron transfer across the interface and transport of the product back to the bulk solution. However, additional chemical and surface reactions preceding or following electron transfer reactions and other surface reactions (i.e., adsorption) can also take place in more complex processes. Figure 2 depicts the general electrode reaction pathways.

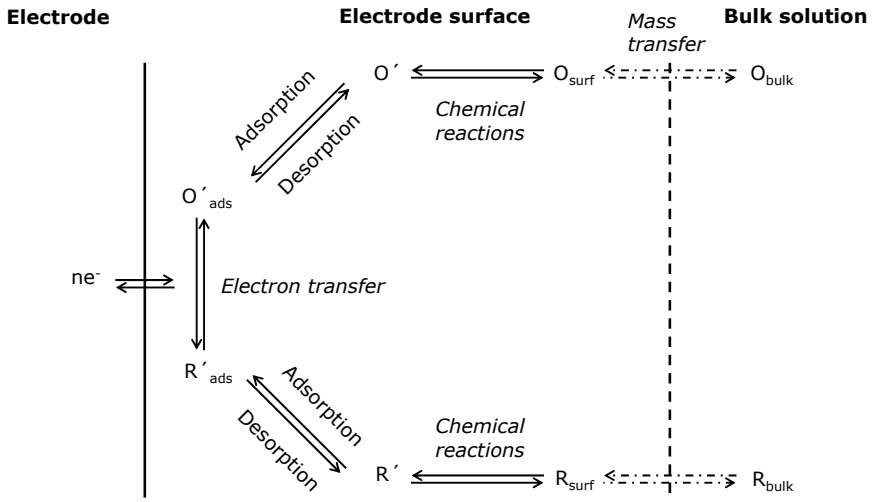

Figure 2: Typical electrode surface reaction (O and R are the oxidized and reduced species, n is the number of electron involved) adapted from [2].

The net rate of reaction, and thus the measured current, is determined by the slowest reaction. For instance, for simple processes, it is either mass transport or electron transfer reactions that govern the reaction rate and current. Mass transfer can occur via diffusion, migration and convection as depicted by the Nernst-Planck equation of the flux (Equation 3).

$$J_j(x) = -D_j \frac{\partial C_{j(x)}}{\partial x} - \frac{z_j F}{RT} D_j C_j \frac{\partial \phi(x)}{\partial x} + C_j \upsilon(x) \qquad \text{Equation 3}$$

Where J is the unidirectional flux of a species j. D, z, C are the diffusion coefficient, the charge and the concentration of the species j, respectively. F is the Faraday constant, υ is the rate at which the volume element moves and ϕ is the potential.

Usually, the main contribution to mass transport is diffusion. As a matter of fact, this has been the case for most of the electrochemical experiments carried out in this thesis: the test solutions were kept unstirred and high concentration supporting electrolytes were used in order to minimize the contribution of convection and migration, respectively. Moreover, the current also depends on the type of species measured as well as the experimental conditions (i.e., electrode material, media, operating potential, etc.) [1].

Generally speaking, in presence of fast electron transfer, the overall reaction is controlled by the rate at which the electroactive species are transported from the bulk to the electrode surface, and thus the current is said to be mass transport-limited. In this case, the thermodynamic laws (i.e., Fick's laws of diffusion and the Nernst-Planck relationship) are fulfilled and a so called Nernstian or reversible behaviour is observed. In the opposite case, if sluggish electron exchange is observed, the electrochemical process is characterized as irreversible.

2 Electrochemical systems

2.1 Introduction

Electrochemical sensors are often categorized as a subcategory of chemical sensors. They are well established and powerful tools commonly used as transducers for determining the presence and concentrations of chemical species in samples.
Since electrochemical sensors provide analytical results unaffected by the sample colour or turbidity, fast response times, and are often inexpensive, they have been used for a broad range of applications involving the detection of specific compounds contained in clinical, environmental, food or industrial samples [1,7]. The general properties of electrochemical sensors (i.e., sensitivity, selectivity and stability) very much depend on their operating conditions (i.e., temperature, pressure and chemical environment) [8].

In spite of not totally replacing traditional laboratory methods (i.e., spectrometric, mass spectrometric, or chromatographic techniques) still displaying better precision and detection limits, electrochemical sensors represent the most rapidly growing class of chemical sensors thanks to their miniaturization potential, design simplicity, low cost, and direct readout of transduction signals [8,9]. Another advantage of electrochemical sensors is that they can be applied on a very broad range of temperatures (i.e., – 30 to 1600 °C). Typically, classical electrochemical sensors used with aqueous or liquid electrolytes often work up to 140 °C, whereas solid-electrolyte based sensors can operate at temperatures higher than 500 °C [8].

The operating mechanisms of electrochemical systems are mainly based on measuring changes in electrical current and/or potential. Electrochemical sensors are generally classified according to their measuring principle which can be potentiometric, voltammetric, amperometric or impedimetric [8,10]. Numerous very good review articles discussing the different types of electrochemical sensors have recently been published [9,11-13]. In this thesis, the aim was mainly focused on the development of potentiometric systems and voltammetric systems for which a brief description is given in the following section.

2.2 Potentiometric systems

In potentiometric systems electrochemical techniques utilizing near zero currents are used. The equilibrium potential measured between two electrodes using a high impedance voltmeter is recorded to determine information about a target analyte in a sample [6].

In these systems, the working electrode (WE) generally features a membrane made of permselective ion-conducting materials which thus displays selectivity to a specific species transported through it [1]. Therefore, the WE is qualified as ion-selective-electrode (ISE). More details about the typical membrane composition are given in **chapter IV**. Typical ISEs feature an internal filling solution that contains the ion of interest at a constant activity (or concentration) in between the electronically conducting material of the electrode and the membrane.

The potential measured at the sensing electrode is not an absolute potential but a potential difference taken with respect to the potential of an electrode of reference, namely the reference electrode (RE). The RE is typically constructed in a similar fashion to the sensing electrodes, the main difference stems from the type of membrane separating the electrode system to the sample, which here is characterized as non specific to any particular species [14].
The reactions occurring at the surface of the electrodes can be characterized by the electrochemical process in Equation 4.

$$Ox + ne^- \Leftrightarrow Red \qquad \text{Equation 4}$$

Where Ox is the oxidized species, Red the reduced one and n the number of electrons exchanged.

Under equilibrium conditions and for reversible electrochemical systems, the Nernst equation (Equation 5) is used to establish the relationship between the activity of the electroactive species and the potential of the electrode.

$$E = E^O + \frac{RT}{nF} ln \frac{a_{ox}}{a_{red}} \qquad \text{Equation 5}$$

Where E is the half-cell potential, E^O is the standard potential, R the universal gas constant, T the temperature, and a_x the activity of the different species.

It is generally more convenient to consider concentrations rather than activities of the species.

These two parameters are related by the activity coefficient γ in Equation 6.

$$a_{ion} = \gamma_{ion}[ion] \qquad \text{Equation 6}$$

Thus, theoretically, at 25 °C, a ten fold change in activity of the target ion implies a 59.2 mV change in the potential of an ISE for a monovalent ion.
More emphasis on the fabrication of potentiometric ISEs will be given in **chapter IV**.

2.3 Voltammetric systems

In voltammetric sensors, the current is registered as a function of the potential (sweep) applied between a RE and a WE which causes the electroactive species in presence to react. For some specific applications involving high potentials (e.g. in large scale electrolytic or galvanic cells or in experiments involving non-aqueous solutions with low conductivities) the use of a third electrode (i.e., auxiliary counter electrode, CE) may be necessary [2]. In such cases, the current is in majority passed between the working and the counter electrodes.
The resulting current stands for a direct measure of the rate of the electron transfer reaction and can be used for quantification of the concentration of the analyte of interest [15]. Thus, voltammetric sensors are generally used to examine the concentration effect of a detecting species on the current-potential characteristics of the reduction or oxidation reaction involved [16]. Generally, more information and lower detection limits can be obtained. A major advantage of this type of sensors is that various species that react at different applied potentials can be detected almost simultaneously in the same experiment without prior separation [10].

In **chapter V**, additional details will be given on the particular type of voltammetric sensors developed.

3 Electrochemical techniques

3.1 Introduction

Quantitative as well as qualitative chemical analysis of various substances and media (i.e., liquids, gas and solids) can be performed using electrochemical methods. Based on very well established laws (such as Faraday's), electrochemical techniques allow fast, selective, and highly accurate analysis of small sample volumes [17]. Potential-controlled techniques stand for a major category of electrochemical techniques and consist in applying a potential at an electrode and measuring the resulting current. Different sub-categories of potential controlled techniques exist and can be differentiated by the type of excitation wave forms of the potential applied. In this thesis, potential sweep and potential step techniques were mainly used.

Cyclic voltammetry (CV) was extensively used for qualitative analysis of the electrochemical systems developed. Thus, a fairly deep description of this electrochemical method is first provided in the following section. A brief description of the other techniques used (i.e., chronoamperometry, square-wave voltammetry (SWV) and electrochemical impedance spectroscopy (EIS)) is then given.

3.2 Cyclic Voltammetry

CV falls into the category of potential sweep electrochemical techniques and is certainly one of the most commonly used ones. It is often the first experiment carried out in an electroanalytical study [1] to allow determination of qualitative, quantitative as well as thermodynamic and kinetic information about electrochemical systems [18].

CV consists in linearly sweeping the potential across the working and auxiliary electrodes, while recording the resulting current flowing through the cell, as it can be seen in Figure 3 A. The rate at which the potential is changed is called the scan rate (υ). The typical resulting current/voltage plot expected for a reversible redox couple is shown in Figure 3 B.
At the initial potential (E_1), no electrochemical activity is observed, whereas at the final potential (E_2), electrode reactions are controlled by mass transport. The potential is reversed and returned to E_1, which represents one cycle. Choice of the potentials is crucial, in order to determine whether the species is produced or consumed and if the reaction is controlled by kinetic or mass transport phenomena.

Immediate information that can be extracted from a CV experiment are the peak potentials ($E_{P,n}$) and peak currents ($I_{P,n}$) for the anodic (forward) and cathodic (backward) reactions.

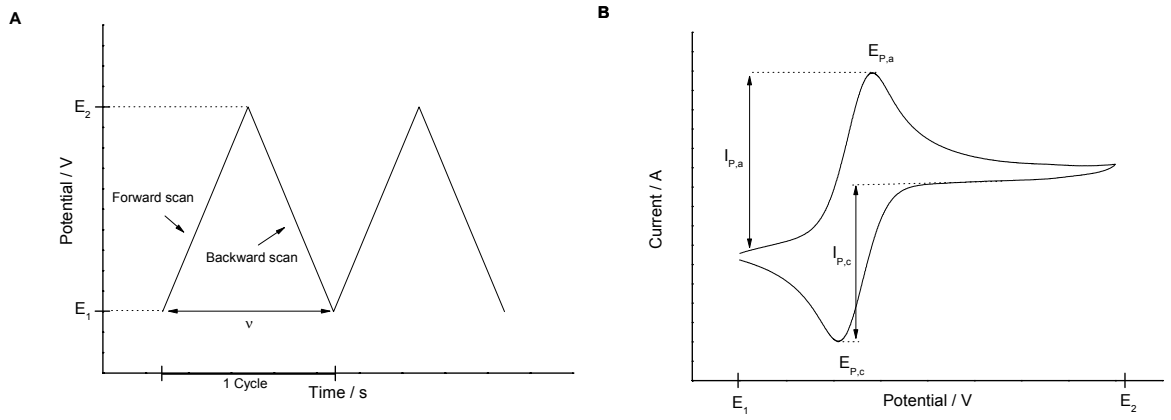

Figure 3: A. Cyclic voltammogram excitation wave form (υ is the scan rate, E_1 is the initial potential, E_2 is the final potential); B. response signal to one cycle of potential excitation wave for a reversible redox couple ($E_{P,n}$ are the peak potentials, $I_{P,n}$ are the peak currents, $_a$ stands for anodic and $_c$ for cathodic).

The shape of a voltammogram depends on the evolution of the concentration profiles resulting from the potential scan rate and diffusion mechanisms [6]. The evolution of the concentrations of oxidized and reduced species at the electrode surface induces diffusion phenomena between the bulk and the electrode.

Additionally, the current response depends on two main processes: movement of electroactive species at the electrode surface (mass transfer) and electron transfer reactions [19]. An electrochemical process is said to be reversible when the electrode reaction is limited by diffusion of the electrochemically active species (i.e., the kinetic reactions are fast). In such case, the peak current can be estimated by the Randles-Sevčik equation (Equation 7).

$$i_p = 0.4463nFAc\sqrt{\frac{nFD\upsilon}{RT}} \qquad \text{Equation 7}$$

Where n is the number of electrons, F is the Faraday constant (9.6485 x 10^4 C), A is the electrode area (in cm^2), c is the concentration (in mol cm^{-3}), D is the diffusion coefficient (in cm^2 s^{-1}), R is the molar gas constant (8.314 J mol^{-1} K^{-1}), T is the temperature (in K).

From this relationship, one can notice that the peak current is proportional to the concentration of the electroactive species, as well as to the square root of the scan rate (i.e., plotting i_p versus $\sqrt{\upsilon}$ results in a linear plot, from which the diffusion coefficient of the studied species can be estimated). Moreover, for a reversible process, the height of peak currents for anodic and cathodic reactions should be equal as depicted in Equation 8. However, the peak current ratio can be influenced by chemical reactions coupled to the electrochemical processes [20].

$$\left|\frac{i_{p,a}}{i_{p,c}}\right| = 1$$ Equation 8

Another characteristic of the voltammogram for reversible systems is that the number of electrons involved in the process can be determined from the difference between the peak potential values (Equation 9).

$$\Delta E_p = E_{p,a} - E_{p,c} = 2.218\frac{RT}{nF} = \frac{0.059}{n}(at 25°C)$$ Equation 9

Accordingly, a fast one-electron process exhibits a ΔE_p of about 59 mV.
The mid-point redox potential $E_{1/2}$ is centered between the peak potential values for anodic and cathodic reactions (Equation 10).

$$E_{1/2} = \frac{E_{p,a} + E_{p,c}}{2}(\approx E^{o'})$$ Equation 10

Where $E^{o'}$ is the formal reduction potential.

On the other hand, when the reaction rate is limited by the electron transfer rate, the reaction is said to be irreversible. In this case, the shape of the voltammogram is significantly different: the peak potentials tend to shift and broaden, resulting in larger peak separation (due to the fact that a greater overpotential value is needed to achieve the same rate of electron transfer [6]). The slower the electron transfer kinetics, the larger ΔE_p becomes [20]. Additionally, for irreversible systems, the peak current value is no longer proportional to the square root of the scan rate.

In this thesis, CV was mainly used for qualitative analysis of the electrochemical systems developed.

3.3 Chronoamperometry

As opposed to CV, chronoamperometry is a potential step technique. This technique consists in applying a potential step and recording the resulting current response [6]. The potential step typically ranges from a potential where no redox reaction occurs to a potential where a desired electrochemical reaction takes place.

For unperturbed solutions, where mass transfer of the electrochemical species to the electrode surface only occurs by diffusion, the current response can be modeled using a derivative of Flick's second law of diffusion for the concentration of the electrochemical species and is expressed in the Cottrell equation (Equation 11) [2].

$$i(t) = nFAC_o^* \sqrt{\frac{D}{t\pi}}$$ Equation 11

Where D is the diffusion coefficient for the oxidized species (in cm^{-2} s^{-1}), C_o^* is the bulk concentration of the species, and t is the time (in s).

Chronoamperometry is commonly used to determine the diffusion coefficient of electrochemically active species, provided that the concentration and the number of electrons involved are known. In this thesis, chronoamperometry was mainly used for activation of electrodes as an alternative to CV (**chapter III**).

3.4 Square-wave voltammetry

SWV is a pulse voltammetric method. It actually combines several advantages of other pulse voltammetric methods, such as the suppression of background current and high sensitivity of differential pulse voltammetry, the diagnostic capability of normal pulse voltammetry, and the ability to interrogate products directly as in reverse pulse voltammetry [2,6].

In a SWV experiment, the potential wave form applied at the working electrode is a symmetrical square wave, superimposed on a staircase (Figure 4). The current is sampled twice, during each square-wave cycle, once at the end of the forward pulse and once at the end of the reverse pulse. Three types of current/potential plots can be generated from this technique namely, forward current versus potential, reverse current versus potential, and difference current versus potential. For most analytical applications, the difference current plot is used, which yields a voltammogram displaying peaks for each electroactive species present in the analyzed solution. Furthermore, the peak height is proportional to the concentration of the different species [1]. Different theoretical models establishing the relationship between peak current and concentration can be found elsewhere [2,21,22].

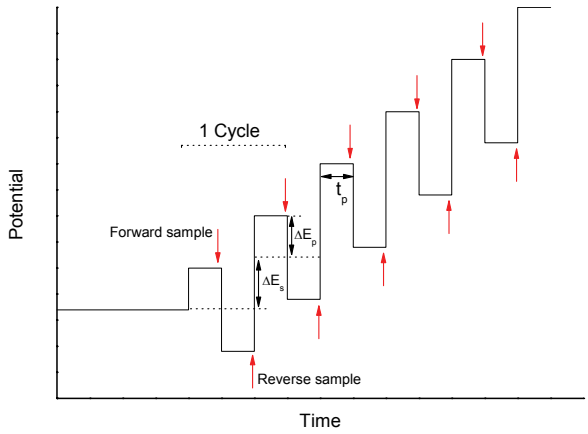

Figure 4: Square-wave potential waveform displaying the step height ΔE_S, the amplitude ΔE_P and the square-wave period t_P. The arrows represent the forward and reverse samples.

In the presented thesis, SWV was used as a means to locate the current peaks of different electroactive components and to assess eventual potential shifts with respect to the activity (or concentration) of a target species (**chapter V**).

3.5 Electrochemical Impedance Spectroscopy

Contrary to the electrochemical techniques previously described, where usually a transient signal is obtained as a response to either a potential or a current excitation that drives the electrode to a condition away from equilibrium, in impedance techniques, an alternating signal of infinitesimal magnitude is used to perturb the cell from its steady state [2]. This represents an essential advantage over these other techniques, especially when characterizing electrochemical systems for which large perturbations might induce inhomogeneous states (i.e., polymer films [23]). Often, EIS is used in parallel to voltammetric experiments to get a better understanding of an electrochemical system.

In EIS measurements, the impedance of a system (cell or electrode) is measured as a function of the frequency of the AC (alternating current) source and thus allows the determination of heterogeneous charge transfer parameters as well as information about the DL structure [2]. EIS is widely used for characterization of fundamental processes taking place at an electrode/electrolyte interface such as adsorption/film formation, rate of charge transfer or ion exchange and diffusion [24]. More recently, EIS has been used for kinetic studies of electroactive polymer films [23] and also as a diagnostic tool to investigate the functionality of electrochemical sensors. For instance, EIS has proven to be very effective for evaluating the degree of physical damage, biofouling, leaching of active components [25] as well as the potential stability of ion-selective electrodes (ISEs) [26] and solid-state REs [27].

In EIS, excitation voltage and current response signals are expressed as sinusoidal functions as displayed by Equation 12 and Equation 13.

$$E_t = E_o \sin(\omega t) \qquad \text{Equation 12}$$

Where E_t is the potential at a time t, E_O is the amplitude of the signal and ω is the angular frequency, which is 2π times the conventional frequency.

$$I_t = I_o \sin(\omega t + \phi) \qquad \text{Equation 13}$$

Where I_t is the current at a time t, I_O is the amplitude of the signal and ϕ the phase angle.

Combining the Ohm's law for the expression of the impedance with Euler's expressions for the voltage and current signals, the impedance can be expressed as displayed in Equation 14.

$$Z(\omega) = Z_o(\cos\phi + j\sin\phi) = Z_o e^{j\phi}$$ Equation 14

Where Z is the impedance and Z_o its amplitude.

The data obtained from an EIS experiment is often represented by plotting the imaginary part of the impedance versus its real part for different ω values and results in a so called Nyquist plot. Bode plots are also commonly used and represent the log of Z and ϕ against the log of ω [2].

The data of an EIS experiment is then analyzed by fitting it to an equivalent electrical circuit model (typically composed of common electrical element such as resistors, capacitors, and inductors).

In this thesis, EIS was used to mainly characterize the capacitance of conducting polymer based solid-state electrochemical sensors (**chapter IV**).

4 References

[1] J. Wang, *Analytical Electrochemistry*. 2nd ed. **2000**: Wiley-VCH.

[2] A. J. Bard, L. R. Faulkner, *Electrochemical methods, Fundamentals and Applications*. 2nd ed. **2001**: John Wiley Sons, Inc.

[3] D. C. Grahame, Chemical Reviews, **1947**. 41(3): p. 441-501.

[4] B. E. Conway, *Electrical Double-Layer and Ion Adsorption Behavior at Solid–Solution Interfaces*, in *Encyclopedia of Surface and Colloid Science*, P. Somasundaran, A. Hubbard, Editor. **2006**, Taylor & Francis: Columbia University, New York, USA.

[5] K. B. Oldham, Journal of Electroanalytical Chemistry, **2008**. 613(2): p. 131-138.

[6] C. G. Zoski, *Handbook of electrochemistry*. **2007**: Elsevier.

[7] H. Nam, G. S. Cha, T. D. Strong, J. Ha, J. H. Sim, R. W. Hower, S. M. Martin, and R. B. Brown, Proceedings of the IEEE, **2003**. 91(6): p. 870-880.

[8] U. Guth, W. Vonau, and J. Zosel, Measurement Science and Technology, **2009**. 20 (042002): p. 1-14.

[9] B. J. Privett, J. Ho Shin, and M. H. Schoenfisch, Analytical Chemistry, **2008**. 80(12): p. 4499–4517.

[10] C. M. A. Brett, Pure Applied Chemistry, **2001**. 73(12): p. 1969-1977.

[11] E. Bakker, M. Telting-Diaz, Analytical Chemistry, **2002**. 74(12): p. 2781-2800.

[12] Bakker, E., Analytical Chemistry, **2004**. 12(76): p. 3285-3298.

[13] E. Bakker, Y. Qin, Analytical Chemistry, **2006**. 12(78): p. 3965-3983.

[14] C. Anderson, K. V. Sin, *Reference electrode*. **1995**: US.

[15] G. Hanrahan, D. G. Patila, J. Wang, Journal of Environmental Monitoring, **2004**. 6(8): p. 657-664.

[16] C. C. Liu, *Electrochemical Sensors*, in *The Biomedical Engineering Handbook*, Bronzino, J. D., Editor. **2000**, CRC Press LLC: Boca Raton.

[17] V. S. Bagotsky, *Fundamentals of electrochemistry*. 2nd ed. 2006: A. J. Wiley & Sons, Inc. .

[18] J. T. Maloy, Journal of Chemical Education, **1983**. 60(4): p. 285-289.

[19] G. A. Mabbott, Journal of Chemical Education, **1983**. 60(9): p. 697-702.

[20] P. T. Kissinger, Journal of Chemical Education, **1983**. 60(2): p. 702-706.

[21] M. Lovrić, *Square-wave voltammetry*, in *Electroanalytical Methods*, Scholz, F., Editor. **2010**, Springer: Berlin Heidelberg. p. 121-145.

[22] L. Ramaley, M. S. Krause Jr., Analytical Chemistry, **1969**. 41(11): p. 1362-1365.

[23] M. M. Musiani, Electrochimica Acta, **1990**. 35(10): p. 1665-1670.

[24] B. Pejcic, R. De Marco, Electrochimica Acta, **2006**. 51(28): p. 6217-6229.

[25] A. Radu, S. Anastasova-Ivanova, B. Paczosa-Bator, M. Danielewski, J. Bobacka, A. Lewenstam, and D. Diamond, Analytical Methods, **2010**. 2: p. 1490-1498.

[26] J. Bobacka, Analytical Chemistry, **1999**. 71(21): p. 4932-4937.

[27] A. Kisiel, H. Marcisz, A. Michalska, and K. Maksymiuk, The Analyst, **2005**(130): p. 1655–1662.

Chapter III Fabrication of electrochemical systems

1 Development of miniaturized potentiometric systems

1.1 Introduction

Adapted from the microelectronics industry, the thick-film process of screen-printing (SP) is one of the most commonly used techniques to deposit coatings in the sub-millimeter range. SP is an inexpensive, simple, versatile and highly reproducible large-scale production technique [1-3]. It consists in pressing a thixotropic fluid (i.e., a SP ink or paste) through a mesh screen to transfer patterns on a substrate. Typically, printed patterns can be controlled by the design and mesh of the screen used, and have thicknesses in the range of 20 to 100 μm, which is thicker than those obtained by other printing methodologies. This technology is thus denominated "thick-film technology" [4]. Originally used on ceramic materials due to their good mechanical, chemical and especially, thermal properties, nowadays SP is also applied on a broader range of substrates including paper, fabrics and plastics [5,6]. An important application of this technology is the fabrication of planar components for miniaturized electrochemical sensors, which have proven their suitability in biomedical, environmental and industrial applications [7-10].

One of the main benefits of the SP technology is that the materials used (especially the SP ink formulations) can be chosen from a broad and diverse range of commercial products, which is definitely beneficial for the development of mass produced low-cost sensors. However, the precise composition of these inks is often kept as proprietary information by the manufacturers [11] and very different performances can be obtained from one ink to another. For instance, graphite inks are commonly used for the fabrication of planar electrochemical sensors due to their relatively low cost, good electrical conductivity, suitability for functionalization [12], low background currents [13] and a wide potential range [14]. These inks principally consist of a carbon powder combined with water-immiscible, non-conducting liquids (i.e., polymer binder) and other additives (e.g., for dispersion, printing or adhesion enhancement) [11,15] but their exact composition is often unknown to the user. This is an important factor since the quality and precise composition of graphite inks (e.g., size, type, and loading of the carbon particles) vary from one to another and thus may result in final screen-printed sensors with very different electroanalytical performances. As an example, J. Wang et al. investigated the influence of the type of carbon materials on the electrochemical properties of fabricated screen-printed sensors [11,16]. However, these works studied the behavior of carbon sensors on ceramic substrates and thus implied, in some cases, fabrication processes with very high temperatures (up to 300 °C). In the work described in this thesis, the aim was mainly focused on developing low cost, disposable devices. Thus, the use of polymer materials and, consequently, SP processes at low curing temperatures were preferred.

To a certain extent, the same may apply to the dielectric materials used as passivation layers to protect these electrochemical systems since those can also differ in their composition as well as in their post printing curing treatment. While the influence of the electrically conducting material on the final sensor performances was investigated in a few papers [11,15], to my knowledge, the same study has not been carried out on the possible influence of the dielectric material.

Accordingly, in the first part of the following chapter, the fabrication of low cost screen-printed electrodes on polymer substrate after selection of the optimum materials for the electrically conducting and the dielectric materials is presented. Moreover, the development of electrochemical sensors with even further improved performances was also investigated by optimization of thermal and electrochemical treatments of the SP materials via thermal curing and activation processes, respectively. The properties of the developed sensors were followed by electrochemical, electrical and mechanical measurements.

1.2 Experimental

In order to obtain the best performance for the final electrochemical systems, selection of the right SP materials (i.e., for the electronically conducting materials and dielectric materials) was made by characterizing the electrochemical, electrical and mechanical properties of different developed electrodes. Moreover, adjustment of the curing and electrochemical treatments of SP pastes was also investigated. In this following section, the equipments, chemicals, materials and methods used to achieve this study are described.

1.2.1 Instrumentation

The screen-printed electrodes (SPEs) were produced with a *DEK 248* screen-printing machine (*DEK*, UK). We designed three different polyester *DEK 230* screens featuring the appropriate stencil patterns for printing the relevant layers of the electrochemical systems. The screens were aligned semi-automatically using the *DEK align-4-vision* system.

The electrochemical measurements were carried out with a *CH700 series* electrochemical workstation (*CH Instruments*, USA) controlled by a *Windows* based PC. For the measurements, the electrodes developed were used as working electrodes, in combination with a double junction Ag/AgCl (3 M KCl) reference electrode or DJRE (*Metrohm*, Spain) and a glassy carbon rod as counter electrode. All experiments were conducted inside a home made Faraday cage.

The electrical properties of the SPEs were followed by electrical resistance measurements using a *Metex M3850D* digital multimeter (*Metex Instruments*, USA).

The mechanical properties of the sensors were investigated by taking images of their surface with a *PLμ non-contact confocal imaging profiler* system attached to a *Nikon* microscope controlled using *PLμ* proprietary software (*Sensofar*, Spain) and a *Leo 1530* (*Zeiss,* Spain) Scanning-Electron-Microscope. A stylus profiler *Dektak 8* (*Bruker AXS*, UK) was also used for determination of the thickness of the different screen-printed layers.

1.2.2 Chemicals

The reagents used for the electrochemical characterization of the sensors (i.e., KNO_3 and $K_4Fe(CN)_6$) were of analytical grade and were used as received from *Sigma-Aldrich*, Spain, without further purification. Stock solutions were prepared weekly with deionized (DI) water of minimum resistivity of 18 MΩ cm.

1.2.3 Electrodes

- ***Materials***

SP was done using inks chosen from various manufacturers (i.e., *Acheson Colloids Company*, The Netherlands, *DuPont*, UK, *Gwent*, UK, *Heraeus*, Germany, *Electro-Science Laboratories* Inc., USA and *Cytec Industries Inc*, USA) on 500 μm thick polyethylene terephthalate (PET) sheets (*HiFi Industrial Film*, France) as substrates.
Following, a short description of the different types of SP materials used is given.

Graphite pastes were used for the fabrication of electrical wires (conducting leads) and electrodes active areas. They were purchased from three different manufacturers: *Acheson, DuPont,* and *Gwent*. The paste formulations mainly differed in their overall solid content, resistivity and viscosity. Principally, the *Gwent* had a higher solid content compared to the *DuPont* and *Acheson*. However, the *Gwent* pastes were also the least viscous (3.5 – 6.1 Pa s) compared to the *DuPont* and *Acheson* (20 - 50 and 60 - 125 Pa s, respectively). Unfortunately, none of the manufacturer data sheets provides the exact composition of their pastes.
The different curing treatments (temperature and time) investigated to cure the graphite pastes are summarized inTable 1.

Silver (Ag) pastes were also used for electrode wires.

A Silver/silver chloride (Ag/AgCl) paste was used for the fabrication of QREs.
Various types of **dielectric** materials were used for the passivation layer protecting the wires and electrodes. Those differed in the type of curing treatment: the *Acheson ED 452SS* was screen-

printed and UV-cured, whereas the *ESL 242-SB*, the *DuPont 5018*, and the *Gwent D2071120D1* materials were screen-printed and thermally cured. Finally, the *Cytec Ebecryl*® dielectric was manually deposited on the electrical leads of the electrodes and UV-cured (as depicted further down in Figure 5C).

Table 1: Curing treatments used in this study for the fabrication of graphite SPEs (bold numbers are curing conditions recommended by the respective manufacturers)

SP ink	*Curing temperature (ºC)*	*Curing time (min.)*
Gwent C10903P14	**60**	**30**
	60	60
	75	30
DuPont 7102	**120**	**5**
	120	10
	135	5
Acheson Electrodag® (ED) PF-407 A	**120**	**20**
	120	40
	135	20

For more clarity, the different inks used in this thesis as well as their main characteristics are listed in Table 2.

Table 2: SP inks (used as received from the various manufacturers, without further purification)

Ink type	*Supplier and origin*	*Reference*	*Curing treatment*	*Content information*
Graphite	**Acheson** Colloids Company, The Netherlands	Electrodag® (ED) PF-407 A	Thermally cured	34.5-37.5 % (solid content)
	DuPont, UK	7102		
	Gwent, UK	C10903P14		43-47 % (solid content)
Ag	**Acheson** Colloids Company, The Netherlands	Electrodag® (ED) 418	Thermally cured (120 °C, 20 min)	
Ag/AgCl	**Acheson** Colloids Company, The Netherlands	Electrodag® (ED) 6037 SS	Thermally cured	60/40 (Ag to AgCl ratio)
Dielectric	**Acheson** Colloids Company, The Netherlands	Electrodag® - ED 452-SS	UV cured	
	DuPont, UK	5018		
	Electro-Science Laboratories (**ESL**), Inc., USA	242-SB	Thermally cured	
	Gwent, UK	D2071120D1		
	Cytec Industries Inc, USA	Ebecryl® 270	UV cured	

- ***Chip design***

The electrochemical systems developed were screen-printed on PET sheets by sequential printing of the electrically conducting and dielectric materials and consisted in two different configurations.

A first chip design consisted in eight individual graphite electrodes (Figure 5). The electrical paths and electrodes (Figure 5 A) were protected with a dielectric material as passivation layer (Figure 5 B and Figure 5 C) leaving openings for the active part of the electrodes and the electrical pads for connection to a measuring apparatus.

A second generation of chips consisted in the same geometry as the previous ones, the only difference being that the electrodes leads were made of silver instead of graphite (Figure 6 A). The active part of the electrode was, however, still in graphite (Figure 6 B). For these chips, an identical design of passivation layer was used to protect the electrodes (Figure 6 C).

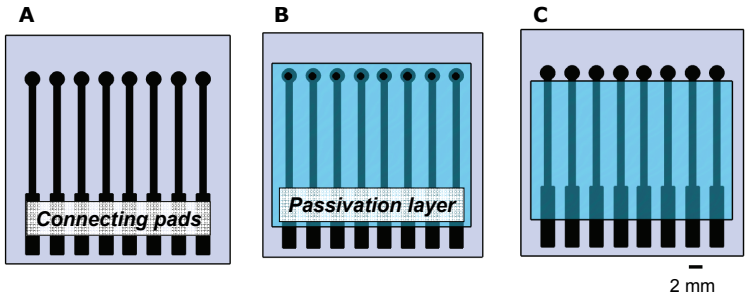

Figure 5: Electrode configuration (1st generation): A. Printing of the electrical paths and electrodes; B. Printing of the insulating layer *452-SS* and *242-SB*; C. Printing of the insulating layer *Ebecryl® 270*.

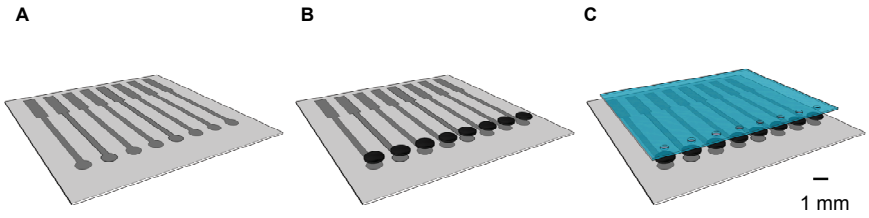

Figure 6: Electrode configuration (2nd generation): A. Printing of silver electrical paths; B. Printing of graphite working electrodes; C. Printing of the insulating layer.

1.2.4 Electrochemical methods

Electrochemical characterization of the SPEs was carried out by CV in 1 mM $K_4Fe(CN)_6$, 0.1 M KNO_3, at a scan rate υ ranging from 25 to 500 mV s^{-1}.
For more reproducibility of the experiments and determination of the quantitative values (i.e., peak currents, peak potentials and thus, I_a/I_c and ΔE_p), the CV measurements were carried out on triplicates, at a fixed scan rate of 100 mV s^{-1}.

Electrochemical activation of electrodes was carried out by CV or chronoamperometry. The difference being that in chronoamperometry a potential step is applied at the working electrode and not a triangular potential wave like in CV. The activation treatment by CV consisted in ten scans, ranging from -2 to 2 V, at υ = 50 mV s^{-1}, in a 0.1 M KNO_3 solution. The activation step by chronoamperometry consisted in ten potential steps, ranging from 0 to 2 V, in a 0.1 M KNO_3 solution.

Unless otherwise stated, all potentials are given with respect to the DJRE.

All the experiments were conducted at 22 ± 2 °C.

For more information regarding the theory behind the electrochemical experiments, the reader is referred to **chapter II**.

1.3 Results and discussion

In a preliminary work [17], I demonstrated that the curing treatment suggested by the ink manufacturer definitely needed further investigation. In this work, which will be introduced later in **chapter IV**, SPEs were fabricated using a carbon ink from *Acheson* and dried using two different curing treatments: 90 °C for 30 minutes and 120 °C for 20 minutes. Analysis of the mechanical and electrical properties and sensitivity of the resulting sensors (after direct deposition of the ion-selective membrane or ISM on the SPE) revealed that the second curing treatment provided the sensors with better overall performances. This motivated me to investigate a broader range of curing treatments (changing both curing temperature and time) and more SP materials in order to allow the final electrochemical system to display the best performances possible.

In the following section, the study of the electrochemical properties of various types of fabricated SPEs is first presented. For this investigation, experimental parameters such as the type of graphite and dielectric materials and type of curing and electrochemical treatments were varied resulting in the fabrication of a total of nine different types of SPEs (45 electrode-sheets were printed in total).

CV was used as a means to qualitatively characterize the different electrodes by investigating the mechanisms and kinetics of reactions taking place at their surface. Then, electrical resistance measurements and surface analysis (i.e., surface roughness measurements and characterization of electrode dimensions) were carried out on the SPEs for broader assessment of their properties.

All the fabricated electrodes were characterized with these techniques which thus resulted in a very amount of experimental data. In this thesis, emphasis is put on the major results which are here summarized. Furthermore, for more reproducibility of the data, the experiments carried out to verify the influence of each experimental parameter were repeated at least on triplicates. For clarity matters, the results for only one sample per experimental parameter are shown in the following chapter, especially for the CV measurements that could have resulted in messy overlapping of voltammograms. However, supplementary voltammograms can be found in the **Appendix** section.

1.3.1 Performance of graphite electrodes

1.3.2 Graphite ink influence

First, electrodes were printed and characterized by investigating the three different graphite pastes. Those were printed according to the curing treatments recommended by their respective manufacturers (Table 1) and protected with the same dielectric material (i.e., *ED 452SS*). The electrochemical behavior of the SPEs was then analyzed by CV. Typical voltammograms obtained for the different pastes are shown in Figure 7.

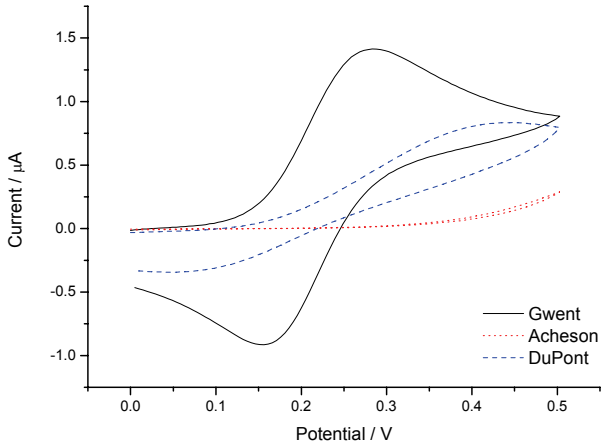

Figure 7: Cyclic voltammograms (υ: 100 mV s^{-1}, in 1 mM $K_4[Fe(CN)_6]^{4-}$, 0.1 M KNO_3) of the different graphite electrodes (i.e., *Acheson, DuPont,* and *Gwent*).

The *Gwent* electrodes undoubtedly displayed the best voltammograms with polarization curves characteristic for macro-electrodes, with defined anodic (forward) and cathodic (backward) peaks. From these voltammograms, the average peak separation value ΔE_p was found to be 0.135 ± 0.012 V and the peak current ratio i_p (i_a/i_c) was 1.12 ± 0.03. Moreover, as depicted in Figure 8, a linear relationship was obtained when plotting peak current values (anodic and cathodic) versus the square root of the scan rate. These information confirmed that a reversible process (i.e., with fast electron transfer and thus, diffusion controlled) takes place at the *Gwent* electrode surface.

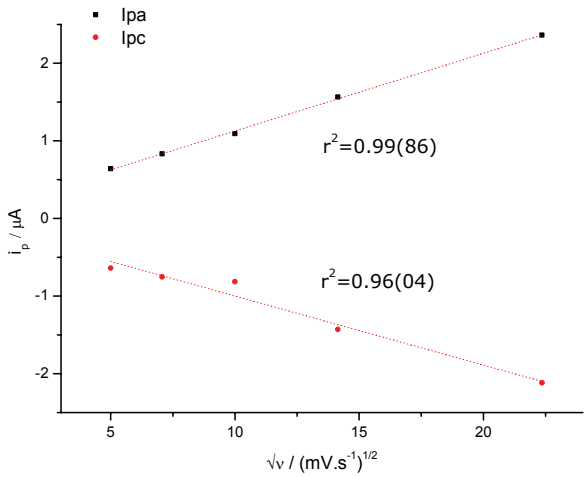

Figure 8: Characterization of a Gwent graphite electrode: relationship between anodic (I_{Pa}) and cathodic (I_{Pc}) peak currents and scan rate values (υ from 25 to 500 mV s^{-1}). The linear fits (straight lines) are also displayed.

On the other hand, the voltammograms of the *Acheson* and *DuPont* electrodes barely showed any peaks at all, making the qualitative analysis of the electrochemical reactions taking place at their surface difficult if not impossible.

From profilometer measurements (Figure 9), the thickness of the different SPEs was estimated to 16.0 ± 1.5, 9.1 ± 0.6 and 7.4 ± 0.7 µm (n= 4 samples) for the *Gwent*, *DuPont*, and *Acheson*, respectively. These values can be related to the general composition of the SP pastes. For instance, the larger thickness of the *Gwent* electrodes can be explained by the high solid content of this paste (43 to 47 % compared to 34.5 to 37.5 % for the Acheson) which implies that more material would remain on the substrate after the curing step.

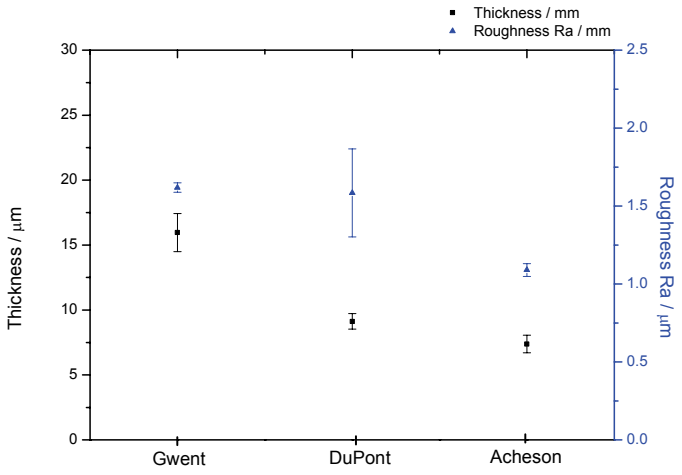

Figure 9: Thickness (n=4 samples) and roughness (n=6 samples) measurements of screen-printed carbon electrodes.

Analysis of the surface roughness of the different electrodes revealed average roughness values of 1.62 ± 0.03 µm, 1.58 ± 0.28 µm and 1.09 ± 0.04 µm (n=6 samples), for the *Gwent*, *DuPont* and *Acheson* electrodes, respectively (Figure 9).

Generally, in the development of electrochemical systems, precise control of the electrode surface properties is necessary since those principally define the phenomena occurring when the electrode is put in contact with another phase (e.g., sample, other part of the electrode, etc.). In this thesis, as will be described later in **chapter IV**, a CP and/or polymer membrane were eventually deposited on the graphite electrodes for the fabrication of ISEs. Thus, a strong adhesion of the membrane on the electrode surface was required and this was favored by having a rough surface providing mechanical interlocking sites for the membrane. In that sense, the *Gwent* ink definitely stood for the most suitable SP graphite material.

The electrical resistance measurements of the various pastes were also significantly different from one paste to another. As seen in Figure 10, 1.24 ± 0.05 kΩ, 2.50 ± 0.07 kΩ and 0.77 ± 0.04 kΩ (n=4 samples) were obtained for the bare (without passivation layer applied) *Gwent*, *DuPont* and *Acheson* electrodes, respectively.

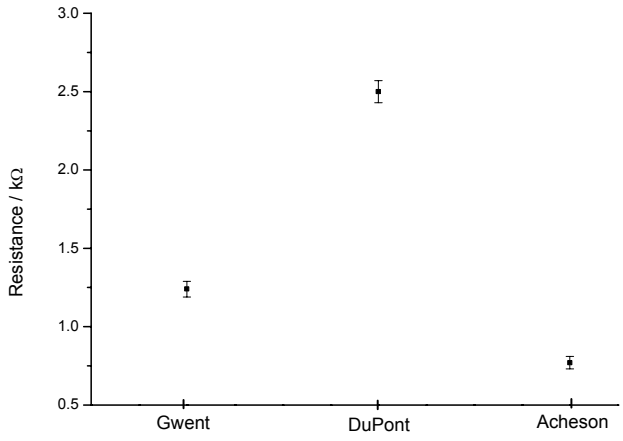

Figure 10: Electrical resistance of the bare electrodes (no passivation layer) fabricated from various manufacturers (n=4 samples).

These two series of experiments clearly showed that the electrodes made with the *DuPont* graphite paste resulted in the most spread data both in terms of surface roughness and electrical resistance measurements. While *Gwent* and *Acheson* pastes displayed relatively small and identical standard deviation values, *DuPont*'s were significantly larger and thus, could definitely cause reproducibility issues for the final sensor.

The *Acheson* electrodes featured the smoothest surfaces as well as the least resistive electrical leads. This was unexpected since according to the information from the manufacturers' data

sheets, the *Acheson* paste features a lower solid content (34.5 to 37.5 %) and a higher curing temperature than the *Gwent* (120 °C and 60 °C, respectively). Thus, one could have expected the *Acheson* paste to result in more porous and/or more resistive electrodes.

As a result, the *Gwent* electrodes undoubtedly displayed the best electrochemical properties with voltammograms revealing diffusion controlled processes occurring at their surface. Additionally, the high surface roughness of these electrodes might also stand for an advantage for the fabrication of the final sensor, by presenting a surface more inclined for further deposition and stronger adhesion of a coating layer. Moreover, this may also enhance the final stability of the sensor, by increasing the contact area between the electrode and the coating layer, thereby increasing the DL capacitance of the sensor.

1.3.3 Dielectric material influence

The *Gwent* electrodes displaying the best overall properties, their properties were further investigated after protecting them with various types of dielectric materials. Thus, *452-SS, 242-SB* and *Ebecryl* dielectrics were deposited on *Gwent* graphite electrodes which were then characterized by CV. The main results are summarized in Figure 11. The voltammograms of the *Acheson* and *DuPont* electrodes coated with different dielectric materials are shown for comparison in **Appendix A**.

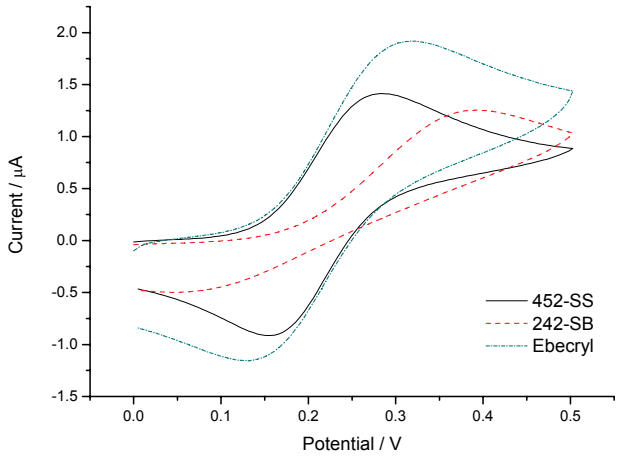

Figure 11: Cyclic voltammograms (υ: 100 mV s^{-1}, in 1 mM $K_4[Fe(CN)_6]^{4-}$, 0.1 M KNO_3) of *Gwent* graphite electrodes protected with various passivation layer materials (*452-SS*, *242-SB* and *Ebecryl*).

From the obtained polarization curves, one could notice that the electrodes with the screen-printed and UV-cured dielectric material (*452-SS*) displayed the most reversible behavior: larger and

sharper peak currents and lower overpotentials values compared to the ones of the *242-SB* coated electrode were obtained.
The increase of capacitive and faradaic current in the voltammograms of the electrodes with the manually deposited dielectric (*Ebecryl*) compared to the screen-printed ones (*452-SS* and *242-SB*), highlighted the difference in surface area between these two types of electrodes (see electrode designs depicted in Figure 5 B and C).

Analysis of confocal images confirmed that the electrode diameters were 1.04 ± 0.01, 1.09 ± 0.01, and 1.17 ± 0.01 mm (n=2 samples), for the electrodes coated with *ED 452 SS*, *242 SB,* and *Ebecryl*, respectively. Thus, due to different coverage of the dielectric material on the electrodes, the electrodes with screen-printed dielectrics were, respectively, 13 and 7 % smaller than the electrodes with the manually deposited one.

Additionally, characterization of the electrical properties of the electrodes revealed that all electrodes coated with the screen-printed and thermally cured passivation layer (*242 SB*) had a resistance much higher than the other ones. In fact, the electrical resistance values of the *Acheson, DuPont* and *Gwent* electrodes protected with this dielectric type were respectively, 8, 6, 3 times higher than the same electrodes left bare (i.e., not coated with a dielectric material). On the other hand, electrodes protected with *ED-452 SS* featured identical resistance values to the ones obtained for bare electrodes. Limited information from the manufacturer's data sheets regarding the exact composition of the graphite and dielectric pastes did not allow us to explain these results in details. However, one can assume that the thermal curing of the passivation layer and/or the nature of the solvents and binders contained in *242-SB* might degrade the structure of the graphite electrode wires.

1.3.4 Curing treatment influence

Post printing, the *Gwent* electrodes underwent different curing treatments and their properties were investigated. The voltammograms of the *Acheson* and *DuPont* electrodes are shown for comparison in **Appendix B**.

Characterization of the electrochemical behavior of the *Gwent* electrodes cured at different temperatures and times (Figure 12) allowed to confirm that curing of the paste at 60 °C for 30 minutes (denoted later as *treatment 1*) yields the most reversible electrochemical behavior. This was emphasized by the sharper peak currents and slightly lower overpotential values obtained compared to the ones of the electrode pastes cured at 60 °C for 60 minutes (denoted as *treatment 2*) as well as the ones cured at 75 °C for 30 minutes (denoted as *treatment 3*).

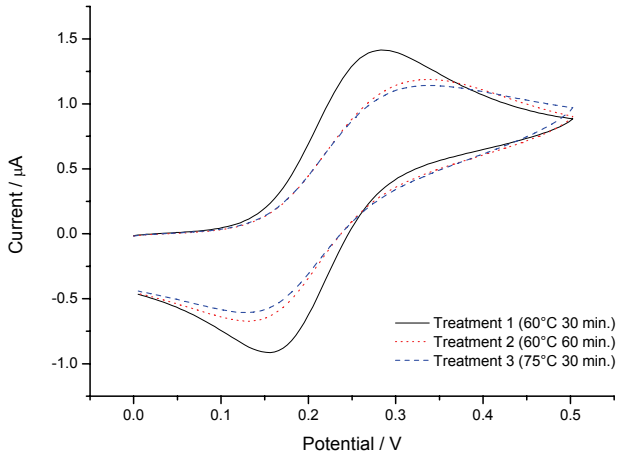

Figure 12: Cyclic voltammograms (υ: 100 mV s^{-1}, in 1 mM $K_4[Fe(CN)_6]^{4-}$, 0.1 M KNO_3) of *Gwent* graphite electrodes cured at different temperatures and times.

Furthermore, the peak current ratio i_a/i_c under these optimal curing conditions (i.e., treatment 1) was 1.12 ± 0.03, whereas 1.39 ± 0.08 and 2.08 ± 0.60 (n=3 samples) were obtained for the electrodes that underwent *treatment 2* and *treatment 3*, respectively.

However, as also observed elsewhere [11], the peak potential separations ΔE_p obtained in our study were much greater than the expected theoretical Nernst value of about 59 mV for a 1 electron transfer reaction. Here, we obtained greater values, typically, 135, 163, and 201 mV for *treatment 1*, *treatment 2* and *treatment 3*, respectively. This decrease in the electron transfer reactivity can probably be attributed to the presence of non-metallic components in the pastes (e.g., binders), affecting the redox activity.

1.3.5 Electrochemical activation influence

The effects of electrochemical activation treatments on the SPEs properties were also investigated. Electrochemical treatment was meant to clean the electrode pastes of impurities. As described earlier (**chapter II**), two electrochemical methods were investigated on the SPEs: CV and chronoamperometry.

Figure 13 depicts the typical activation effect observed on the electrochemical behavior of the *Gwent* electrodes. The voltammograms of *Acheson* and *DuPont* electrodes are shown for comparison in **Appendix C.** For these graphite pastes, the electrochemical treatment had even more drastic effects.

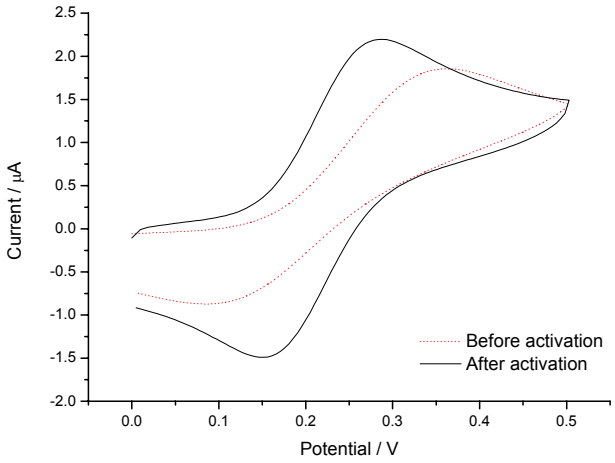

Figure 13: Example of cyclic voltammograms (υ: 100 mV s^{-1}, in 1 mM $K_4[Fe(CN)_6]^{4-}$, 0.1 M KNO_3) depicting the typical effect of the electrochemical activation of a *Gwent* graphite electrode (here the *Ebecryl* dielectric material was used).

The activation step resulted in significant increases of both capacitive and faradaic current which mainly reflected the roughening of the electrode surface and thus, a net increase in active surface area. For the same reasons as previously stated, this demonstrated that electrochemical treatment of the electrodes could definitely be beneficial for enhancing the performances of the final sensor.
It was also observed that activation treatment of the electrodes by CV or chronoamperometry led to identical effects.

1.3.6 Characterization of silver / graphite electrodes

In order to decrease the electrical resistance of the final sensors, SPEs were fabricated with a different material for the electrical leads. Silver was chosen for the leads whereas graphite was used for the electrodes (see design depicted in Figure 6).
Sensors were printed under the selected optimal parameters (i.e., use of *Gwent* graphite paste cured at 60 °C for 30 minutes and coated with the UV-cured dielectric material *242-SB*) and then characterized by CV (Figure 14).

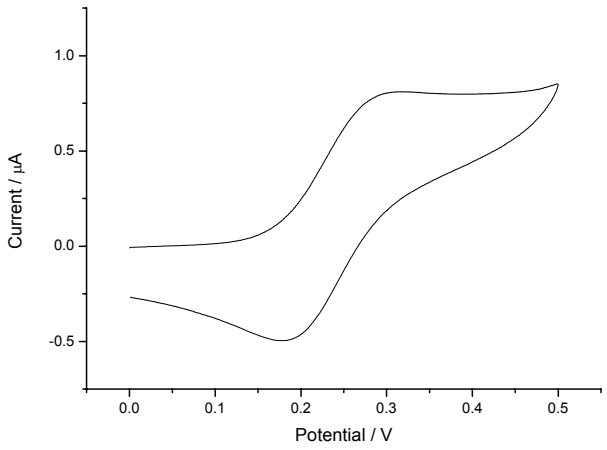

Figure 14: Example of cyclic voltammogram (υ: 100 mV s^{-1}, in 1 mM $K_4[Fe(CN)_6]^{4-}$, 0.1 M KNO_3) of Ag/C based electrodes (coated with *242-SB*)

The voltammograms obtained for the silver/graphite electrodes had a similar shape as the one of all in graphite electrodes. Typical ΔE_p was found to be 0.120 V and i_a/i_c was equal to 1.37.
Regarding the electrical properties of the sensors, the ohmic resistance values obtained for the silver/graphite electrodes were as expected, significantly lower than the ones of the all in graphite sensors, since they decreased by three orders of magnitude.

1.4 Conclusions

A very broad range of SP materials is currently available on the market, which definitely favors the fast development of low cost, mass produced sensors. However, in this study, significant differences were shown to exist within a variety of SP materials available, which do not appear evident from the information provided by their manufacturers.

Here, it was demonstrated that in the development of screen-printed electrochemical systems, optimization of fabrication parameters such as the choice of the SP inks (i.e., type, composition, etc.) and post printing treatments (i.e., thermal and electrochemical) is crucial. These parameters greatly affect the electrochemical, electrical and mechanical properties of the resulting sensors, which were here, investigated by CV, electrical resistance measurements, and various surface analysis experiments.

From this study, the optimal materials for the fabrication of the electrochemical system were found to be the *Gwent* graphite paste for the electrodes and the UV-cured passivation layer *ED 452 SS*. Typical voltammograms for macro electrodes were obtained for the *Gwent* ink based sensors and

witnessed that reversible electrochemical processes (i.e., diffusion controlled) occur at their surface.

Investigation of the influence of the curing treatment of the graphite inks confirmed that precise curing temperature and time vary from paste to paste and that optimization of such parameters was necessary. Moreover, it was discovered that type as well as curing method of the protecting dielectric material had a significant impact on the overall electrodes properties. Covering the electrodes with the UV-cured dielectric material resulted in sensors with unaffected electrochemical, electrical and mechanical properties. This was drastically different for the SPEs coated with thermally cured dielectrics, whose properties were greatly altered.

Further improvement of the properties of the sensors was obtained after electrochemical activation treatment. This resulted in increasing the overall active surface area of the carbon electrodes and thus improving their electrochemical performance.

While some of the obtained results could be explained, some still remain unclear mainly due to the lack of information from the manufacturer's data sheets. Consequently, in order to reduce as much as possible the effect of the uncertainty of the quality and content of the SP materials on the properties of the final printed system, a solution could be to develop home made SP paste formulations.

In addition, to complete this study and carry out an even more thorough investigation, one could evaluate the influence of the electrode geometry on the electrochemical response using computer simulations. This part was, however, considered as beyond the scope of the presented study.

2 Fabrication of polymer devices for electrochemical systems

2.1 Introduction

In the following section, a description of the fabrication of polymer devices used to characterize the electrochemical systems developed in this thesis is given.

- ***Polymer materials***

The use of polymer materials for the fabrication of devices was mainly motivated by the fact that they offer many different material properties and their fabrication processes are easy and allow fast and simple prototyping and manufacturing [18]. For instance, polymethylmethacrylate (PMMA) and polydimethylsiloxane (PDMS) are two of the most common polymer materials for microfluidic device fabrication and were used in this thesis. Advantages of PMMA include its low cost, optical transparency, amenability to fabrication and modification, and biocompatibility [19]. Likewise, PDMS is well known for its excellent structural (ability to reproduce mold structures with sub 0.1 µm fidelity), chemical and physical properties [20] making it an excellent candidate for microfluidic devices. For instance, PDMS has proven to be very suitable for medical devices [18]. Cyclic olefin polymer (COP) was also used for some of the polymer parts in this Ph.D. thesis. COP has quite recently emerged as extremely attractive material for microfluidic applications due to its excellent optical properties, low water absorption, and exceptionally good resistance to different solvents [21].

In the work described in the following section, these polymer materials were mainly used with rapid prototyping fabrication technologies such as micromachining, PDMS casting, laser ablation and thermal bonding for the fabrication of various devices.

- ***Direct micromachining***

Employing direct micromachining methods is a competitive approach to fabricate miniature parts from polymer materials in a fast and low cost way. Moreover, it presents a financial advantage in the initial investment for the production of prototypes, compared with series production methods like injection molding.

Micromilling is a downscaled version of the conventional machining process and was used in this thesis due to its rapidity, low cost and flexibility to create various structures on and from polymer parts [22]. Here, micromilling was used to structure microchannels, molds for PDMS parts, fluidic interconnections and other macro-size parts.

Laser ablation is another direct machining technique used in this thesis. It is a very fast technique used to structure parts and consists in using the power of a laser to remove material from a substrate. The laser first heats up the material to be ablated which decomposes and then evaporates. The resolution of the resulting ablated structures typically depends on the substrate and the type of laser (especially its wavelength) however, typical resolutions are in the range of 50 to 200 µm [23,24]. In this thesis, laser ablation was used as a means to cut or structure polymer parts in a rapid and reproducible way.

- ***PDMS-casting***

Fabrication of microfluidic devices in PDMS via soft-lithography (i.e., replica molding) has proven to be a fast and low cost rapid prototyping technique used in several applications (medical analysis, environmental monitoring, chemical and biochemical analysis, fundamental research, etc.) [25,26]. PDMS-casting consists in pouring the curable elastomer (obtained by mixing a base and a curing agent) into a master (mold) resulting in a PDMS replica of the structures of the master [20]. Here, PDMS-casting was used to fabricate reversible sealing parts such as O-rings, gaskets or microfluidic chambers.

- ***Bonding process and surface modification***

When irreversible assembly of polymer parts was needed, thermal assisted bonding was used. This bonding process consists in heating the polymer parts to be bound at a temperature close to the glass transition temperature (T_g) of the polymer, while applying a pressure to achieve intimate contact, with inter-diffusion of polymer chains between the surfaces, ultimately leading to a strong bond [21].

Prior to bonding, the polymer parts can undergo several types of surface modification treatment (e.g., via chemical treatment, surface grafting, plasma treatment and application of UV light) in order to enhance the bonding process. For instance, UV-exposure treatment of polymer parts is commonly used to enhance mechanical interlocking of polymer chains between the surfaces to be bound and ultimately, improve bonding through the generation of electrostatic interactions [21]. This surface treatment results in photo-degradation of the polymer (mainly due to photo-oxidation and scission of polymer chains) causing the formation of lower molecular weight radicals and reduction in T_g at the exposed surface. However, since the thickness of the affected polymer layer is determined by the optical absorption length, the thermo-mechanical properties of the bulk polymer are not affected by UV exposure (i.e., no significant deformation of the channels or reduced bond strength [27]). This surface treatment was used here prior to bonding PMMA parts.

2.2 Experimental

In the following part, the different setups and materials used for polymer device fabrication are described. For each fabrication process, the general experimental parameters used in this thesis are also given.

2.2.1 Instrumentation

A computer numerically controlled (CNC) micromilling machine (*Folken Industries*, USA) with tungsten-carbide micro-cutting tools (*Kyocera*, USA) with diameters ranging from 100 to 500 µm were used for most of the microfabricated polymer parts.
A 150 W CO_2-laser (*Synrad*, USA) was used to structure polymer parts.
A UV light source (*DYMAX*, USA) and a bonding press (*P/O/Weber*, Germany) were used to assemble polymer parts.

2.2.2 Polymer materials

The following polymer materials were used:

- PMMA sheets (*Nordiskplast*, Denmark) of thicknesses ranging from 1 to 5 mm.
- PDMS (*Dow Corning,* Denmark).
- COP films (*Zeon*, Germany) 100 µm thick.
- Polytetrafluoroethylene (PTFE) tubing (*Bola*, Germany) of inner diameter 0.8 mm and 1.6 mm of outer diameter.

2.2.3 Experimental parameters

- ***Micromilling***

Micromilling of PMMA and COP parts was done with milling and drilling tool (cutters) of diameters varying from 100 to 500 µm. In order to obtain an optimal milled or drilled structure, several parameters had to be optimized according to the type of material structured. Among those, the speed of rotation of the cutter (spindle speed), the speed at which the tool cuts the material

(surface cutting speed), the speed of vertical penetration of the tool in the material (feed rate) and the depth of cut had to be adjusted.

- ***PDMS-casting***

PDMS was obtained by mixing the base and curing agent in a volume ratio of 10:1. PDMS was degassed for 1 h under vacuum in a desiccator before being poured in the micromilled PMMA molds and cured at 80 °C for 3 h.

- ***Surface modification of PMMA and thermal fusion bonding***

The bonding process of PMMA parts consisted in two different optimized steps:

First, the PMMA parts were activated with UV-light. They were placed bonding side up, 12 cm below the UV-light source for 90 s. Prior to this exposure and as per manufacturer's instructions, the light source was warmed up for 5 min.

Following UV exposure, the PMMA layers were placed between two glass plates and placed in the bonding press (heating plates set at 85 °C). The applied pressure was 0.5 kN cm^{-2}. After 1 h the heating plates were turned off and the bonding assembly was allowed to cool to room temperature in the press.

2.3 Results and discussion

In the following section, a presentation and brief discussion of the different polymer based devices developed in this thesis are given.

2.3.1 Microfluidic flow cell

In order to reduce sample volumes and facilitate electrochemical characterization of the developed sensors, a fluidic flow-cell (volume < 1ml) was fabricated (Figure 15). This cell was composed of PMMA parts (Figure 15, layers 2, 4 and 6) structured by micromilling, and PDMS parts (Figure 15, layers 3 and 5) made by PDMS-casting. The PDMS parts were designed in order to reversibly seal the fluidic cell on the chip to be analyzed. For instance, the fluidic chamber part (Figure 15, layer 3) featured a small ridge (200 µm wide x 100 µm high) at its bottom providing a leak proof sealing with the electrochemical chip.

The top part of the fluidic cell featured a plug (Figure 15, layers 4, 5 and 6) designed to permit the easy introduction of a macro-electrode (i.e., RE or CE) in the fluidic chamber. Moreover, if the use of an additional macro-electrode was not necessary, the top part of the cell could also be easily closed by replacing layers 4, 5 and 6 in Figure 15 by a simple PMMA lid.

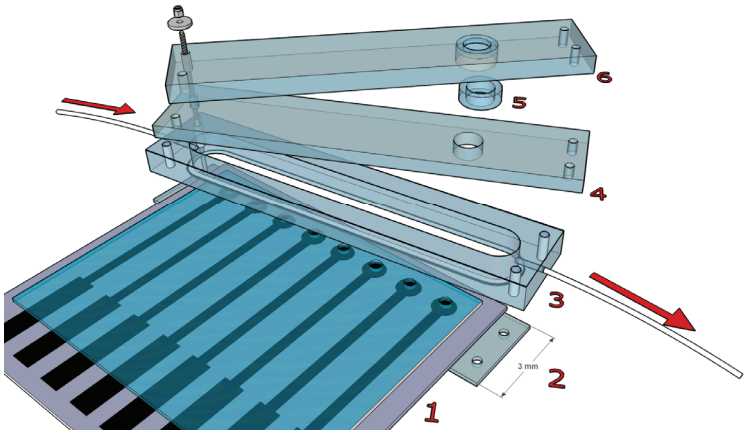

Figure 15: Microfluidic flow cell for SPEs: 1. developed chip with SPEs. 2. PMMA bottom part. 3. PDMS chamber with fluidic tubing. 4. PMMA middle part. 5. PDMS o-ring. 6. PMMA top part (with insertion plug for RE or CE).

2.3.2 Fluidic interconnection

A fluidic interconnection module (Figure 16) was fabricated in order to be able to dispense different solutions in the fluidic-cell described earlier. It was composed of from thermally bonded micromilled PMMA parts and PTFE tubing.

The design and dimensions of the micromilled channels of the microfluidic network were ranging from 200 to 500 µm (Figure 16 B) and were chosen to limit back-flow and cross contamination between the channels.

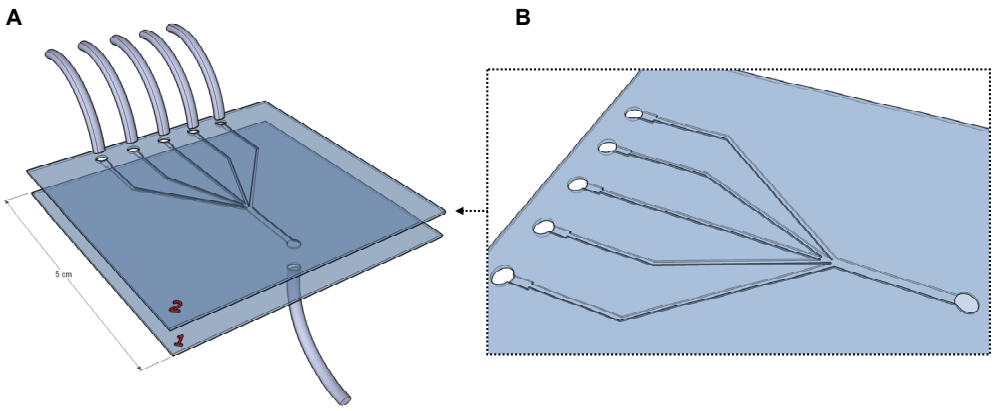

Figure 16: A. Fluidic interconnection module: 1. bottom PMMA part with outlet port leading to the microfluidic cell. 2. Top PMMA part with microfluidic channels and inlet ports. B. Zoom on the microfluidic network.

2.3.3 Manual screen-printing platform

In order to be able to quickly fabricate sensors, a manual SP setup (Figure 17) was designed and fabricated. It was composed of an reversibly assembled PMMA parts for the bottom and top layers (Figure 17, layers 1 and 3) and a COP part for the SP screen (Figure 17, layer 2). The PMMA layers were structured by micromilling. COP layers featuring the inverse of the patterns to be printed (e.g., circular holes of 1.2 mm in diameter) were either micromilled or CO_2-laser ablated.

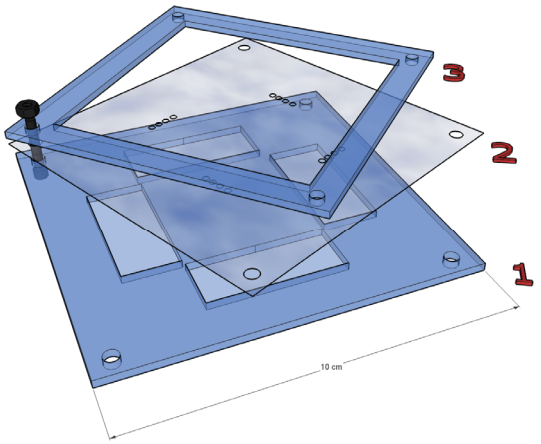

Figure 17: Manual screen-printing device: 1. PMMA bottom part with placement slots for 4 chips. 2. COP foil screen with CO_2-lasered patterns. 3. PMMA top frame.

2.4 Conclusions

A combination of micro-fabrication technologies suitable for low cost, fast prototyping has permitted the development and fabrication of different types of devices for both the fabrication and the characterization of the electrochemical systems developed in this thesis. Thus, a fluidic cell, a fluidic interconnect unit and a manual SP platform were designed and fabricated.

3 References

[1] Ł. Tymecki, S. Glab, R. Koncki, Sensors **2006**. 6: p. 390-396.

[2] M. Prudenziati, B. Morten, Microelectronics Journal, **1992**. 23(2): p. 133-141.

[3] C. A. Galán Vidal, J. Munoz, C. Dominguez, and S. Alegret, Trends in Analytical Chemistry, **1995**. 14(5): p. 225-231.

[4] J. P. Metters, R. O. Kadara, C. E. Banks, Analyst, **2011**. 136(6): p. 1067-1076.

[5] Ł. Tymecki, E. Zwierkowska, R. Koncki, Analytica Chimica Acta, **2004**. 526(1): p. 3–11.

[6] S. Laschi, I. Palchetti, G. Marrazza, M. Mascini, Journal of Electroanalytical Chemistry, **2006**. 593: p. 211–218.

[7] O. Domínguez Renedo, M.A. Alonso-Lomillo, and M.J. Arcos Martíinez, Talanta, **2007**. 73: p. 202–219.

[8] J. P. Hart, S. A. Wring, Trends in Analytical Chemistry, **1997**. 16(2): p. 89-103.

[9] M. Tudorache, C. Bala, Analytical and Bioanalytical Chemistry, **2007**. 388: p. 565–578.

[10] R. O. Kadara, N. Jenkinson, and C. E. Banks, Sensors and Actuators B, **2009**. 138: p. 556–562.

[11] J. Wang, B. Tian, V. B. Nascimento, L. Angnes, Electrochimica Acta, **1998**. 43(23): p. 3459-3465.

[12] H. Kahlert, Journal of Solid State Electrochemistry, **2008**. 12 (10): p. 1255-1266.

[13] C. Apetrei, I. Mirela Apetrei., J. Antonio De Saja, and M. Luz Rodriguez-Mendez Sensors, **2011**. 11(2): p. 1328-1344.

[14] C. G. R. Heald, G. G. Wildgoose, L. Jiang, T. G. J. Jones, R. G. Compton, ChemPhysChem, **2004**. 5(11): p. 1794–1799.

[15] M. Rice, Z. Galus, R. N. Adams, Journal of Electroanalytical Chemistry, **1982**. 143(1-2): p. 89-102.

[16] J. Wang, M. Pedrero, H. Sakslund, O. Hammerich, J. Pingarron, The Analyst, **1996**. 121(3): p. 345-350.

[17] A. E. Musa, F. J. del Campo, N. Abramova, M. A. Alonso-Lomillo, O. Domínguez-Renedo, M. J. Arcos-Martínez, M. Brivio, D. Snakenborg, O. Geschke, and J. P. Kutter, Electroanalysis, **2011**. 23(1): p. 115–121.

[18] H. Becker, C. Gärtner, Analytical and Bioanalytical Chemistry, **2008**. 390(1): p. 89-111.

[19] Y. Chen, L. Zhang, G. Chen, Electrophoresis **2008**. 29 (9): p. 1801-1814.

[20] J. C. McDonald, G. M. Whitesides, Accounts of chemical research, **2002**. 35(7): p. 491-499.

[21] C. W. Tsao, D. L. DeVoe, Microfluidics and Nanofluidics **2009**. 6(1): p. 1-16.

[22] C. R. Friedrich, P. J. Coane, M. J. Vasile, Microelectronic Engineering, **1997**. 35(1-4): p. 367-372.

[23] C. G. Khan Malek, Analytical Bioanalytical Chemistry, **2006**. 385(8): p. 1351–1361.

[24] C. G. Khan Malek, Analytical Bioanalytical Chemistry, **2006**. 385(8): p. 1362-1369.

[25] J. C. McDonald, D. C. Duffy, J. R. Anderson, D. T. Chiu, H. Wu, O. j. Schueller, G. M. Whitesides., Electrophoresis, **2000**. 21(1): p. 27-40.

[26] D. C. Duffy, J. C. McDonald, O. J. A. Schueller, G. M. Whitesides, Analytical Chemistry, **1998**. 70(23): p. 4974–4984.

[27] R. Truckenmuller, P. Henzi, D. Herrmann, V. Saile, W. K. Schomburg, 17th IEEE International Conference on Micro Electro Mechanical Systems, **2004**: p. 761-764.

Chapter IV Ion-selective electrodes

A. Coated-wire electrodes

1 Introduction

Potentiometric ion sensors represent an important subcategory of electrochemical sensors which measure the difference in potential between an indicator electrode, also known as ion-selective electrode (ISE), and a reference electrode (RE) [1].

In the 1970^{s}, a major step forward was made in the field of electrochemical sensors with the invention of a special type of ISEs, namely the coated-wire electrodes (CWE) [2]. As opposed to conventional macro ISEs, CWEs are made by direct deposition of an ion-selective membrane (ISM) on an electronic conductor thus, eliminating the presence of internal solution making them very simple and robust systems [3]. On the other hand, these systems can be subject to potential instabilities caused by the lack of a well defined redox couple at the interface between the electrode and the ISM. For CWEs, the potential is actually defined by their double layer (DL) capacitance. Consequently, when dealing with this type of systems, increasing the DL capacitance is necessary in order to enhance their potential stability [2].

More generally, the elimination of an internal liquid phase is adopted in solid contact (SC) ISEs. This category of sensors presents major advantages over conventional glass ISEs. For example, from the manufacturing point of view, SC ISEs are very attractive systems since they are compatible with low cost and mass production technologies (they can involve a combination of thin and thick-film technologies [4]) and can be monitored with relatively simple measuring electronic apparatus [5,6]. Moreover, they can adopt planar geometries, they are maintenance free and easily miniaturized [4]. Thus, it is essentially for these reasons that SC ISEs stand for a very suitable type of electrochemical systems for a broad range of practical applications [2]. On the other hand, their operating mechanisms are more complex than those of conventional ISEs and their underpinning thermodynamic mechanisms (i.e., internal boundary potentials) are difficult to harness [7]. On top of that, the performance of SC ISEs is often limited by the adhesion of the membrane to the electrode, as seeping of electrolyte between the electrode surface and the membrane impairs the sensor [8-10].

In the following chapter, the development of a solid-state potentiometric system intended for clinical applications is presented. In addition to responding fast to concentration changes, biomedical sensing systems must meet very stringent quality requirements in terms of accuracy, reliability and stability.

First, in the following chapter, a preliminary study was carried out on the fabrication of a first type of sensor, namely some CWE featuring a photo-cured pH-sensitive polymer membrane. The

membrane preparation was optimized by N. Abramova et al. [11], from their experience in the development of urethane diacrylate polymer membrane matrices for ion-sensitive field-effect transistor (ISFET) sensors [12-14] as well as from their knowledge in microtechnology for mass production of chemical sensors [15]. This ISM originally developed for H^+-ion sensitive ISFET has proven to display a selectivity in front of sodium ions suitable for clinical and biomedical applications and a lifetime of more than three months. In this chapter, the innovative use of this photocurable polyurethane (PUR) membrane was motivated by the fact that PUR is very attractive from a technological point of view due to its compatibility with standard photo-lithographic processes which makes it easier to streamline than commonly used polyvinylchloride (PVC) membranes [16]. Moreover, as discussed in [11], such PUR membrane contains only small amounts (< 0.05%) of intrinsic impurities (which can alter the final sensor sensitivity, limit of detection, and selectivity) and is compatible with the addition of lipophilic salts for cation as well as anion-selective sensors.

In order to improve the final sensor stability, different means of increasing the contact area between the ISM and the electronic contact to increase their DL capacitance but also to enhance the adhesion between the two phases was investigated (more details in **chapter III**). As opposed to what is claimed in the literature, the sensors developed did not suffer from drift and potential instabilities but instead displayed very good overall performances.

Later, in **chapter IV**, the development of SC ISEs was attempted. For this, an electroactive material displaying mixed electronic and ionic conductivity was used to serve as an ion-to-electron transducing material between the electronic conductor and the ISM.

The reader is asked to bear in mind that the work described in **part A** of this chapter was done chronologically prior to the investigation carried out on the development of SPEs described in **chapter III**. Thus, optimization of the fabrication parameters of the SPEs was not yet achieved. Here, the influence of only few parameters was studied and actually was the origin of the deeper investigations described in **chapter III**.

2 Experimental

In the following section, a description of the different equipments, materials, chemicals and methods used in this thesis for the fabrication and characterization of pH sensitive ISEs is provided.

2.1 Instrumentation

The potentiometric measurements were carried out with a *CHI 700 series* electrochemical workstation (*CH Instruments*, USA) controlled by a Windows based PC. The electrodes developed were used as working electrodes against Ag/AgCl DJRE (3M KCl) (*Metrohm*, Spain). The pH value of solutions was monitored with a commercial pH-meter *model 827* and a pH glass electrode *(Metrohm*, Spain). All experiments were conducted inside a Faraday cage.

The images of the surfaces of the samples and the roughness measurements were obtained with a *PLμ* non-contact confocal imaging profiler system attached to a *Nikon* microscope controlled using PLμ proprietary software (*Sensofar*, Spain) and a *Leo 1530* (*Carl Zeiss*, Germany) Scanning-Electron-Microscope (SEM).

Curing of the ISMs was done within a specially designed chamber under nitrogen flow. The samples were exposed to the UV-irradiation of a spot lamp system *PC 5000* (*Dymax*, Germany) with an irradiation intensity of 62 mW cm^{-2} (wavelength = 365 nm).

2.2 Chemicals

For the preparation of the ISM, the ionophore tridodecylamine (HI-I), lipophilic additives potassium tetrakis(p-chlorophenyl)borate, (K-TpClPB), tetradodecylammonium tetrakis(4-chlorophenyl)borate (*ETH 500*) and plasticizer di-(n-hexyl)-itaconate octyl[2-(trifluoromethyl)phenyl]ether (OTFMPh) were purchased from *Fluka*, Spain. The aliphatic urethane diacrylate oligomer (*Ebecryl 270*) and cross-linker hexanediol diacrylate (HDDA) were bought from *UCB Chemicals*, Spain. The photoinitiator 2,2´-dimethoxyphenylacetophenone (IRG 651) was from *Ciba-Geigy*, Switzerland.

All other reagents used were of analytical grade and were used as received from *Sigma-Aldrich*, Spain, without any further purification. Stock solutions were prepared weekly with deionized (DI) water of minimum resistivity of 18 MΩ cm.

2.3 Electrochemical measurement

Here, the different experimental protocols used for the characterization of the potentiometric systems composed of a H^+-sensitive electrode and an Ag/AgCl QRE are described. A presentation of the method used to characterize the sensor response in presence of Na^+ ions (i.e., selectivity test) is also provided.

- ***Cyclic voltammetry experiments***

Randles-Sevčik analysis was carried out on CV experiments run in 1 mM $K_4Fe(CN)_6$, 0.1 M KNO_3, at a scan rate (υ) ranging from 25 to 500 mV s^{-1}.

- ***Potential stability and reproducibility of the QREs***

First, the Ag/AgCl QREs were cleaned with deionized (DI) water, dried under mild airflow, and dipped into a stirred potassium dihydrogen phosphate solution (0.04 M KH_2PO_4) also containing potassium chloride (0.06 M KCl). The pH of the solution was set to 7.00 by addition of potassium hydroxide (0.1 M KOH). The potential of these electrodes was recorded for five minutes versus the DJRE. The average and standard deviation of the potential during the steady state regime (last minute of each measurement) were taken. This measurement was repeated daily, over a period of seven days in order to characterize the electrode stability. The reproducibility of the measurements was verified by repeating this protocol four times for each sample. In between each measurement, the electrodes were rinsed with DI water and dried under mild air stream.

- ***Potentiometric pH-response of the ISEs***

The response of the ISEs to pH change was characterized in a test buffer solution (0.04 M KH_2PO_4, 0.06 M KCl) whose pH was raised to 7.00 by adding 0.1 M KOH. The open-circuit potential (OCP) of each characterized electrode was recorded during ten minutes in buffer solution vs. DJRE. The solution was then titrated by adding 500 µl of 0.1 M KOH solution every five minutes (five additions were made) on a pH range of 7.00 to 7.63. The pH values were followed with a laboratory pH-meter and pH glass electrode.

- ***Selectivity test of the ISEs to Na^+***

The potentiometric response to pH in presence of sodium was studied in a test buffer containing 100 mM Tris with 140 mM sodium chloride (NaCl). The solution was titrated by adding 500 µL aliquots of a 140 mM HCl, 140 mM NaCl mixture, every five minutes.

For this series of tests, the outer jacket of the DJRE used was filled with lithium acetate.

2.4 Fabrication of ion-selective electrodes

2.4.1 Thick-film electrodes

Different transducers were fabricated based on an eight-electrode configuration on 500 µm thick PET films. The technology used for the fabrication of these electrochemical systems was presented with more details in **chapter III**.

The fabricated chips consisted of eight *Acheson* graphite electrodes (Figure 18 A). The Ag/AgCl ink was printed over four of them to serve as QREs (Figure 18 B). Next, the final electrode geometry was defined by printing a dielectric material over the substrates (Figure 18 C). This dielectric coating was also meant to provide further protection of the devices.

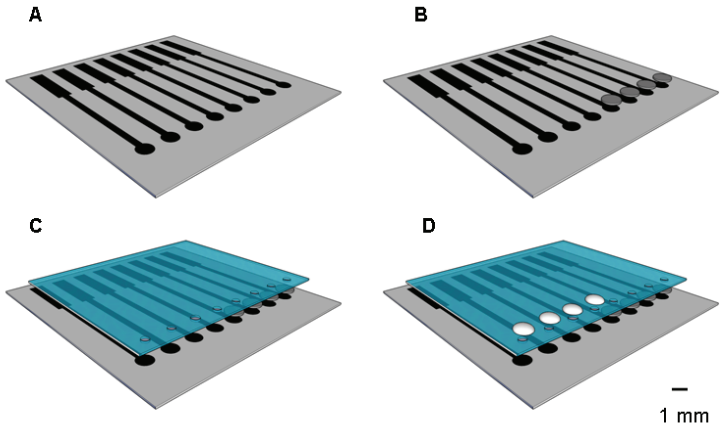

Figure 18: Fabrication steps of the potentiometric systems A. Printing of graphite electrical paths and working electrodes; B. Printing of the Ag/AgCl QREs; C. Printing of the insulating layer; D. Deposition of the ISMs.

Some other sets of SPEs featuring an alternative type of dielectric layer merely covering the connection pads were also prepared (Figure 5 C).

Different curing treatments of the screen-printed pastes (for both the QREs and ISEs) were investigated: 30 minutes at 90 °C and 20 minutes at 120 °C.

Moreover, for the fabrication of the QREs, different material configurations were investigated: Ag/AgCl electrodes printed directly on PET sheet, Ag/AgCl on Ag tracks, and Ag/AgCl on graphite tracks.

An electrochemical activation treatment of the graphite electrodes was used and meant to clean them of impurities. This activation step consisted in ten CV scans, ranging from -2 to 2 V, at a scan rate of 50 mV s^{-1}, in a 0.1 M KNO_3 solution.

2.4.2 Formulation of ion-selective membrane

ISMs are usually prepared from a mixture of a high molecular weight polymer, a plasticizer, an ionophore and lipophilic cationic or anionic salts, dissolved in an organic solvent [17]. The ISM used in the work described here was based on a photocured PUR matrix with neutral carriers. Its composition was optimized [11] and consisted of 0.3 g of a main polymer mixture (i.e., aliphatic urethane diacrylate oligomer, cross-linker HDDA and photoinitiator IRG 651) dissolved in 0.2 ml of THF. Other components namely 2.2 wt. % of ionophore (HI-I), 40 wt. % of plasticizer (OTFMPh), and 10 mol % of lipophilic salt (KTpClPhB) were then added to this solution and the final cocktail was homogenized in an ultrasonic bath. The solution was left in a fume hood for several hours until the solvent was evaporated.

The ISEs were produced by depositing 1 µl of the membrane cocktail over the electrode surface (see Figure 18 D). The membranes were cured by being exposed to UV-light for 200 seconds under nitrogen flow. The resulting electrodes could be dry stored for several days before use, but once immersed into a solution the membranes had to be kept hydrated.

3 Results and discussion

In the following section, the development of screen-printed ISEs and the investigation of their properties and performances are discussed.

3.1 Fabrication of the screen-printed electrodes

For this work, the electrode-sheets were screen-printed as previously described by successive SP of three layers of different materials (i.e., electrical connector layer, electrode material and passivation layer).

The printed electrodes were well reproduced on the PET sheets: the Randles-Sevčik analysis of cyclic voltammograms confirmed a typical electrode size of 1.0 ± 0.1 mm^2, corresponding to the area of the screen patterns of 1.0 mm^2.

Confocal images and stylus profiling of the SPEs (Figure 19) revealed typical thicknesses of 7 ± 1 µm and 36 ± 3 µm (n=4 samples) for the screen-printed electronically conducting material and the dielectric material, respectively.

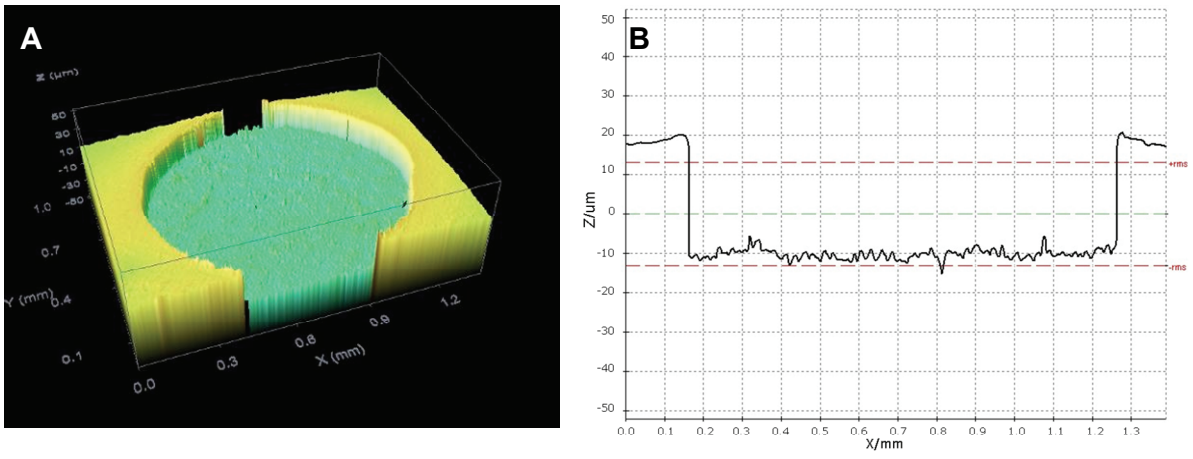

Figure 19: A. Typical confocal image of a graphite electrode. B. Profile of the electrode surface.

3.2 Performance of the screen-printed electrodes

3.2.1 Ag/AgCl quasi-reference electrodes

As previously described, different configurations of QREs were fabricated: Ag/AgCl on PET sheet, Ag/AgCl on Ag tracks, and Ag/AgCl on graphite tracks. The best performance, especially in terms of electrode potential stability was obtained using Ag/AgCl on graphite tracks printed on the PET sheets. Therefore, this configuration of materials was used for the QREs.

The curing treatment of the QREs was optimized by successively curing the graphite and then the Ag/AgCl layers for 20 minutes at 120 °C. SEM images (Figure 20) and confocal images of the topography of different samples revealed that the Ag/AgCl electrodes cured 20 minutes at 120 °C presented a rougher surface ($Ra_{(Ag/AgCl\ 120)}$= 3.3 ± 0.5 µm (n=8 samples)) than the ones cured 30 minutes at 90 °C ($Ra_{(Ag/AgCl\ 90)}$= 2.5 ± 0.5 µm (n=8 samples)). This indicated that a higher curing temperature was very likely to remove more of the non metallic components contained in the pastes, leaving rougher electrode surfaces.

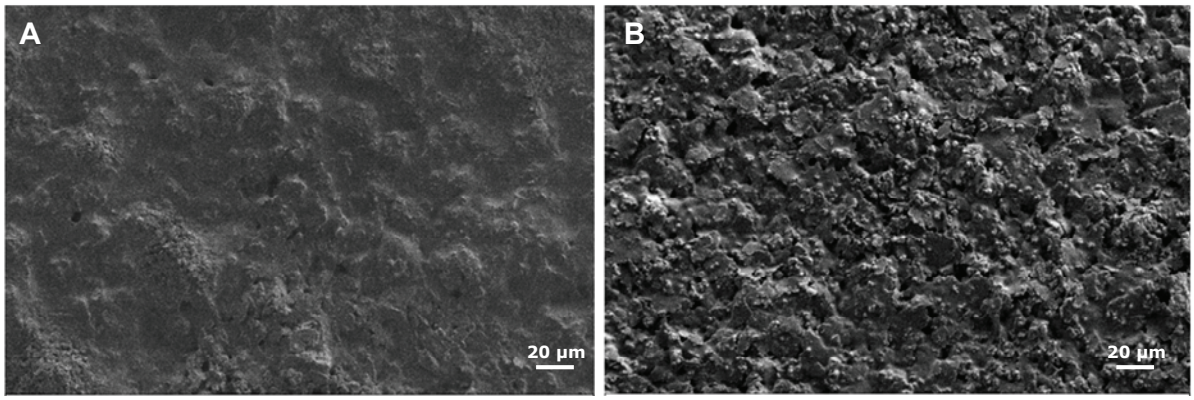

Figure 20: SEM images: A. Surface of an Ag/AgCl QRE cured 30 minutes at 90 °C. B. Surface of an Ag/AgCl QRE cured 20 minutes at 120 °C.

From experiments carried out daily over a week, the standard deviation of the potential of these electrodes was ± 0.8, 1.1, and 1.7 mV for three individual QREs. Assuming that this type of electrode was used as RE in combination with a strictly Nernstian pH-electrode, this deviation would represent an error of 0.02 pH units only. Thus, this experimental error value makes the developed QRE potentially suitable for biomedical applications and, by extension, to any other application with less stringent stability requirements. This was further confirmed by a series of reproducibility tests carried out on triplicates: their average OCP after four consecutive experiments was 26.2 ± 0.2 mV, 26.8 ± 0.3 mV and 26.7 ± 0.1 mV, respectively. For medical applications, the maximum allowed uncertainty of the RE for monovalent ions is ± 0.50 mV, including deviations stemming from junction potentials, sample matrix and boundary-layer phenomena [18]. Therefore, the developed QREs were in principle suitable for medical applications, and were then used in combination with the developed screen-printed pH-sensor in saline solutions of controlled composition. One possible application for this system could be, for instance, the control of the saline solutions used in dialysis equipment.

3.2.2 pH-electrode

The aim of the work described here was to develop a potentiometric pH-electrode with a sensitivity as close as possible to the theoretical Nernstian behavior. Prior to the deposition of the pH-membrane formulation on the electrodes, different material configurations for the fabrication of the electrochemical system were first investigated: bare graphite SPEs, electrochemically activated graphite SPEs, and heat cured graphite SPEs. Last, some selectivity tests to sodium were performed.

- **Non pre-treated (bare) graphite electrodes based sensors**

Characterization of the sensors made by direct deposition of ISM on non pre-treated graphite SPEs revealed an average potentiometric response to pH of -40.0 ± 2.4 mV/pH over the seven day period (Table 3), which is far from the theoretical Nernstian response of -59.2 mV/pH.

Table 3: Potentiometric response of the pH-electrode without pretreatment.

Day	*Slope (mV/pH)*	r^2
1	**-38.0**	0.99(98)
4	-40.3	0.99(74)
5	-40.4	0.99(72)
6	-43.7	0.99(16)
7	-37.6	0.99(70)

- **Electrochemically activated graphite electrodes based sensors**

In order to improve the pH sensitivity of the sensors, the effects of electrochemical activation of the graphite electrodes prior to drop casting the ISM were investigated by CV. Typical effects of the electrochemical activation of the graphite electrodes are shown in Figure 21. An increase of capacitive and faradaic current was observed which reflected the roughening of the electrode surface and thus a net increase in the electrode active surface area.
The increase in roughness due to electrochemical activation was confirmed by confocal microscopy and surface roughness measurements $Ra_{(activated)}$= 1.7 ± 0.5 µm (n=8 samples) and $Ra_{(non\ activated)}$= 1.0 ± 0.1 µm (n=8 samples).

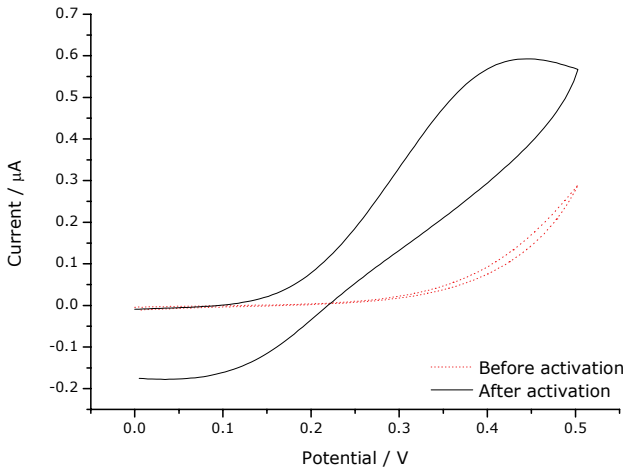

Figure 21: Example of cyclic voltammograms (scan rate: 100 mV s^{-1}, in 1 mM $K_4Fe(CN)_6$, 0.1 M KNO_3) of a graphite electrode before and after electrochemical activation treatment.

Following electrochemical activation, the electrodes were coated with the ISM cocktail and their potentiometric response to pH changes was -51.7 ± 5.9 mV/pH over the seven day period (Table 4). This revealed that the activation step improved the potentiometric response of the electrodes (getting closer to the Nernstian behavior).

Table 4: Potentiometric response of the electrochemically activated pH-electrode.

Day	*Slope (mV/pH)*	r^2
1	**-53.6**	0.99(94)
4	-48.3	0.99(90)
5	-52.0	0.99(92)
6	-44.4	0.99(98)
7	-60.1	0.99(44)

It was believed that the violence of hydrogen bubble generation from the electrochemical activation process resulted in an increase of the surface roughness of the electrodes. The electrochemical treatment enhanced the adhesion of the polymer membranes on the electrode surface and thus provided the electrodes with an improved sensitivity to pH changes. Indeed, increase in surface roughness may favor the attachment (better mechanical interlocking) of the membrane to the electrodes consequently providing the sensors with more stability and higher pH sensitivity.

- **Thermally treated graphite electrodes based sensors**

Since a high resistivity of SPEs may be detrimental to the overall sensor performance and may require more expensive electronic components, the effect of curing treatment on the overall resistivity of the SPEs was explored.

Analysis of electrode surfaces by confocal microscopy and SEM revealed that the electrode shape was better defined after curing the electrodes 30 minutes at 90 ºC than curing them 20 minutes at 120 ºC. Curing the pastes 20 minutes at 120 ºC resulted in a thinner passivation layer and allowed the resistivity of the devices to decrease from 2.31 to 1.65 kΩ. On average, the resistance of the electrodes cured 20 minutes at 120 °C was 33 % lower than the ones cured 30 minutes at only 90 °C. As it has also been discussed elsewhere [19], this is likely due to the fact that more of the non metallic components present in the pastes either decompose or evaporate when using higher curing temperatures. This mechanism may have caused an increase of the carbon content of the pastes and ultimately led to an increase of their conductivity. However, curing at temperatures beyond 120 ºC did not lead to further decrease in resistivity.

The samples that underwent this thermal treatment were then activated by CV before drop-casting of the ISM. The thermal treatment followed by electrochemical activation of the electrodes allowed the pH response of the ISEs to rise to an average value of -52.8 ± 3.7 mV/pH over the seven days period -52.1 ± 1.2 mV/pH after the two first days (Table 5).

Table 5: Potentiometric response of the thermally treated pH-electrode.

Day	*Slope (mV/pH)*	r^2
1	**-48.6**	0.99(94)
2	**-59.5**	0.99(92)
3	-53.9	0.99(96)
6	-51.2	0.99(94)
7	-51.7	0.99(84)
8	-51.7	0.99(86)

- **Passivation layer influence**

The last step in the optimization of the pH-sensors was the verification of the passivation layer influence around the electrodes. Some other sets of SPEs (electrodes cured 20 minutes at 120 °C and subsequently electrochemically activated as described above) were prepared and featured the passivation layer design depicted in Figure 5 C. ISMs were then drop-casted on the electrodes. Their average potentiometric pH response was -53.5 ± 3.7 mV/pH over four days. Despite displaying a slightly better potentiometric response than the electrodes featuring the passivation layer based on the layout depicted in Figure 5 B, the appearance of the ISMs changed after being immersed in the test solution for a couple of days. While one would expect the membranes to swell due to water intake during the hydration phase [20,21], they surprisingly seemed to shrink and slightly delaminate. These phenomena were tentatively explained by the fact that the ISM may preferentially adhere to the passivation layer material compared to the PET substrate, and therefore the absence of the dielectric passivation layer around the electrodes may result in poorer adhesion of the membranes and a shorter electrode lifetime.

- ***Selectivity test***

An important requirement for the pH-electrode was to be insensitive to the presence of possibly interfering ions. Thus, the potentiometric pH response of the ISEs was studied by titration in sodium containing solutions. These experiments showed that the presence of sodium did not interfere with the pH response of the sensors. During seven consecutive days of measurement the pH-electrode displayed a pH response of -55.1 ± 3.5 mV/pH which was close to its response in absence of sodium.

3.2.3 Ion-selective electrode versus quasi-reference electrode

In the previous sections, the development and individual fabrication and characterization of a QRE and a pH-electrode were described. Both of them were stable and reliable over a target period of at least seven days and were thus integrated on the same platform (PET film) and then characterized. The typical potentiometric response of this system during titration and its corresponding calibration plot are displayed in Figure 22. As noticed from this figure, the response time of the system was very short since a stable potential was reached less than a minute after titration.

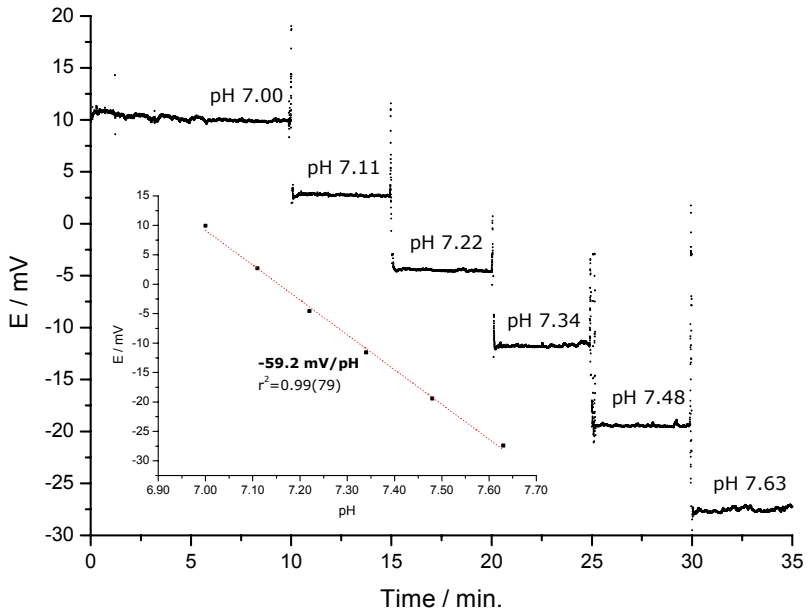

Figure 22: Example of titration plot of 0.04 M KH_2PO_4, 0.06 M KCl with 0.1 M KOH and its related calibration plot (insert graph) of the potentiometric system pH-electrode VS. Ag/AgCl QRE (8^{th} day of measurement).

Table 6 summarizes the potentiometric response of the two electrodes integrated on the same substrate over an eight-day period.

Table 6: Potentiometric response of the pH-electrode versus the QRE.

Day	*Slope (mV/pH)*	r^2
1	**-44.1**	0.99(38)
2	**-49.4**	0.99(96)
5	-62.8	0.99(70)
6	-61.6	0.99(50)
7	-59.7	0.99(80)
8	-59.2	0.99(78)

From day five to day eight, the average potentiometric response of the electrochemical system was -60.8 ± 1.7 mV/pH, which was exceptionally close to the theoretical Nernstian behavior.

As seen in all previous experiments, the ISMs developed required a preconditioning phase by immersion in the test solution for at least two days before reaching a steady potentiometric response. During this period, water is actually transported through the polymer membrane of the ISE until a steady state condition is reached [20]. In order to greatly decrease the preconditioning time, one could think of storing the sensors in containers with humid atmospheres before use [22].

In this last series of experiments, it was noticed that the sensitivity to pH of the potentiometric system was slightly higher than for the ISE characterized versus a commercial RE. This could be attributed to the fact that here the use of a QRE (thus, no internal electrolyte) may have affected the potentiometric response of the sensors, due to changes in ionic strength of the solution. However, enhancing the performance of the electrochemical system by replacing the QRE with a commercial RE would tremendously increase the overall chip costs, which was against the target of this project to develop a disposable and low cost point-of-care-system.

3.2.4 Gwent graphite electrode

As a comparison, sensors based on *Gwent* graphite electrodes (instead of *Acheson*) were also fabricated.

Moreover, to attempt shortening the conditioning phase of the sensors, the buffer solution pH 7.0 previously used was replaced by the same buffer solution but pH 4.5. The potentiometric response of these sensors was recorded over seven days (Table 7). The typical average pH response of these sensors was -50.0 ± 1.0 mV/pH after two days of hydration, whereas the pH response in presence of sodium was -49.3 mV/pH.

These results definitely showed an improvement in terms of stability of the sensors' day to day sensitivity. The potentiometric sensitivity was, however, slightly lower than for the *Acheson* based electrodes. This difference in potentiometric response of the sensors made of different graphite

materials confirmed that the electrode material definitely has an impact on the final sensor performance

Table 7: Potentiometric response of a Gwent graphite based pH-electrode.

Day	*Slope (mV/pH)*	r^2
3	-51.0	0.99(82)
4	-50.9	0.99(80)
5	-48.5	0.99(62)
6	-50.1	0.99(92)
7	-49.7	0.99(96)

4 Conclusions

SP has proven to provide simple, fast and low cost platforms for disposable potentiometric electrochemical systems.

While the effect of the electrochemical pre-treatment of different SP pastes for ISEs has been investigated, for instance, by G. Cui et al. [23], the effect of the thermal electrode pre-treatment has only rarely been considered [24]. In our work, combining electrochemical and thermal treatments of SPEs considerably improved the performance of QREs and ISEs. Indeed, the post printing curing step of the electrode pastes (Ag/AgCl QREs and graphite WEs) of 20 minutes at 120 °C decreased the electrodes electrical resistance, very likely due to thermal decay of the plastic/non-conducting components of the ink. This preliminary study actually set the basis for pursuing investigations on a broader range of curing treatments and on other SP materials (**chapter III**).

The optimized QREs made of Ag/AgCl on graphite tracks printed on the PET sheets presented an excellent potential stability over seven days (± 1.2 mV, for n=3 samples) and would possibly be suitable for a broad range of applications, particularly in the medical field.
Direct contact between an electronically conducting material and the ion conducting membrane may result in blocking of the interface since no continuous flow of charge can be established between the two phases. This could possibly cause an increase of the overall resistance of the electrode and ultimately lead to larger noise levels. Moreover, the potential appearance of a liquid layer between the membrane and its solid contact may also result in potential drifts [25,26]. However, it has been demonstrated [27] that ISEs like the ones presented in this thesis (CWEs), can display performances very close to the ones of ISEs with an internal electrolyte. Moreover, in this study, this method provided a fast, simple and low cost ISE production process and such potential drifts were actually insignificant during the test period.

Electrochemical activation by CV of the graphite working electrodes prior to the deposition of ISMs proved to be largely beneficial. This electrochemical treatment further helped removing some of the impurities contained in the graphite paste. In addition, hydrogen bubble generation resulted in an increase of the surface roughness of the electrodes (and thereby, an increase in their surface area), which enhanced the adhesion of the polymer membranes and led to higher pH sensitivity ISEs.

All in all, it was believed that both thermal and electrochemical treatments contributed in increasing the active surface area of the SPEs, resulting in sensors with increased DL capacitance and thus enhanced sensitivity and stability.

The passivation layer material used to protect the electrodes also played an important role in improving the adhesion of the pH-membranes on the electrodes. Surrounding the electrodes with a layer of dielectric material not only prevented electrode delamination but also allowed the membranes to adhere more strongly to their surface (i.e., adhesion of the membrane was stronger on the passivation layer than directly on the PET substrate), increasing their stability and hence the sensor lifetime.

Last, the optimized QRE and pH-electrode were integrated on the same PET substrate. The potentiometric response to pH of the final system was in good agreement with the theoretical Nernstian behavior. After two days of hydration, the average pH response of a typical system was -60.8 ± 1.7 mV/pH, over a six day period. This pH-response was very close to ideal Nernstian behavior.

B. Solid-state ion-selective electrodes

1 Introduction

In order to further improve the potential stability of CWEs, the introduction of a hydrogel-electrolyte phase between the electrical conducting material and the ISM has proven to be advantageous. In such systems, the liquid electrolyte solution of the classical ISEs is replaced by a hydrogel electrolyte which thus ascribes a better defined pathway for ion-to-electron transduction than for CWEs.

Currently, electroactive materials showing mixed electronic and ionic conductivity to establish a well defined ion-to-electron transduction process at the electrode/ISM interface are emerging. Conducting polymer (CP) materials are some of the most promising materials [2,28]. The multifunctionality of CPs is mainly due to the formation of charge carriers in the polymer backbone [29] as well as the incorporation of counterions (doping ions) or other neutral molecules to maintain electroneutrality into the polymer matrix [30]. Therefore, the properties of the CP depends on its degree of oxidation (i.e., p-doping) or reduction (i.e., n-doping) [30], which then defines if the polymer would act as an electron-to-cation or an electron-to-anion transducers [31].
The transduction process occurring in CPs is very similar to the process taking place at the liquid electrolyte of a conventional ISE or at the hydrogel-contact of other ISEs [32]. The selectivity of CP based SC ISE is mainly determined by the ISM [30]. The basic operating principles of SC ISEs based on p-doped CP as ion-to-electron transducer are depicted in Figure 23. The high redox capacitance of CP is another reason why these materials are particularly appropriate as SC materials. Indeed, high capacitance of the ion-to-electron transducing material has proven to be necessary to stabilize the electrode potential [26]. Over the past few years, several different types of CPs have been used as ion-to-electron transducers in order to tremendously improve the performances of SC ISEs [2]. Polypyrrole, polythiophene, and polyaniline are examples of CPs widely used for various applications as listed in excellent recent review articles [29,30,32].

In this thesis, the CP chosen was the commercially available product poly(3,4-ethylene-dioxythiophene) (PEDOT) doped with an excess of poly(4-styrenesulfonate) (PSS) counterions stabilizing the colloidal particles [33]. While most other CPs are electrochemically deposited, the PEDOT-PSS solution used can be directly drop-casted on a substrate. This stands for an important advantage and is in particular crucial for mass production of sensors [2,29]. This choice was also supported by the fact that PEDOT is one of the most stable CPs available today [34,35]. Furthermore, it was demonstrated that PEDOT is very suitable as a SC material for a broad range of applications ([26] and cited references) mainly due to its low sensitivity to O_2 and CO_2 compared with other CPs [36]. For instance, this type of PEDOT-PSS was successfully used for all solid-state K^+-selective and Ca^{2+}-selective electrodes [33,34].

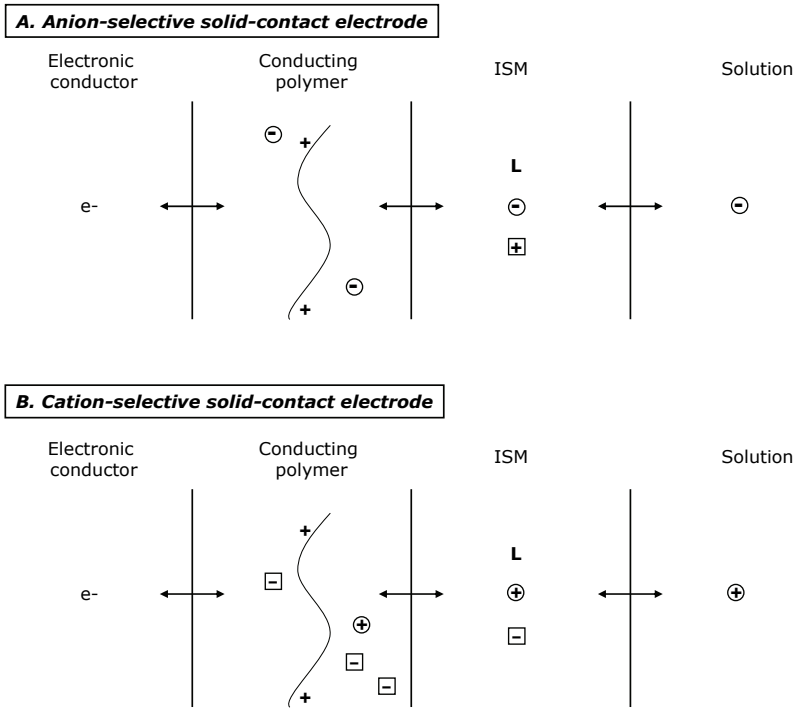

Figure 23: Operating principle of CP based ISEs for: A. Anion-selective SC ISE. B. Cation-selective SC ISE. L is the ion-recognition site (fixed or mobile). Primary ions are circled whereas counterions are squared (adapted from [32])

In the following work described, PEDOT-PSS was casted on the optimized SPEs developed in **chapter III**. The ISM previously developed in this chapter was then drop-casted on the PEDOT-PSS in order to form pH-ISEs.

2 Experimental

Most of the instrumentation, chemicals, materials and electrochemical techniques used in the following section are the same as the ones from the first part of the chapter. Thus, only the necessary additional information are given here.

2.1 Instrumentation

The fluidic flow cell and microfluidic interconnection module described in **chapter III** were used for the pH-measurements.

2.2 Chemicals

Poly(3,4-ethylenedioxythiophene)-poly(styrenesulfonate) (PEDOT-PSS), high conductivity grade (conductivity of 150 S cm^{-1} for a 18 µm thick film), was bought from *Sigma-Aldrich*.

2.3 Electrodes

The SPEs optimized in **chapter III** were used in the following experiments. The PEDOT-PSS and the ISM were sequentially drop-casted on the SPEs.

First, PEDOT-PSS was deposited on the SPEs with a 0.5 µl micropipette by contact printing. The CP layer was then dried at room temperature for 24 h, without light. For the following study, four different types of sensors were made: with 0, 1, 2, and 4 layers of PEDOT-PSS.

The ISM cocktail was then deposited on the PEDOT-PSS electrodes with the same method as previously described in this chapter.

2.4 Electrochemical methods

EIS was performed in the frequency range 0.1 Hz-10 kHz with an excitation amplitude of 10 mV. The impedance spectra were fitted to the equivalent circuit of shown in Figure 24 for further analysis.

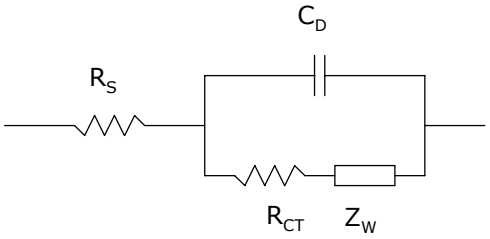

Figure 24: Randles cell: equivalent circuit used to fit the EIS data. R_S, C_D, R_{CT}, and Z_W are the solution resistance, the DL capacitance, the charge transfer resistance and the Warburg impedance, respectively.

3 Results and discussion

In the following section, the development of SC ISEs for pH monitoring is described. First, the influence of the thickness of PEDOT-PSS on the general properties of sensors was investigated. Then, the pH response of the PEDOT-PSS based SC ISEs was studied.

3.1 General properties of the PEDOT-PSS layers

Analysis of the thickness of the PEDOT-PSS sensors revealed average values of 4.3 ± 0.6, 6.5 ± 0.9 and 13.2 ± 1.6 µm, for the 1, 2, and 4 PEDOT-PSS layers, respectively (n=4 samples).

Then, electrochemical impedance spectra of each PEDOT-PSS based sensor were taken. Typical spectra obtained are displayed in Figure 25. One could notice that the thicker the PEDOT-PSS layer on the graphite electrode, the closer to the 90° capacitive line their impedance plot got. Additional experiments need to be carried out to further explain this phenomenon.

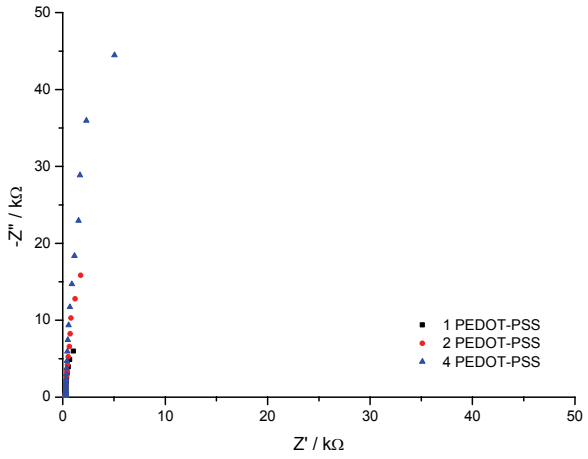

Figure 25: Impedance spectra of graphite/PEDOT-PSS electrodes in 0.1 M KCl.

After fitting the data from the electrochemical impedance spectra to the equivalent circuit displayed in Figure 24, the capacitance values for each type of electrode were obtained (Figure 26).

This series of experiments emphasized the influence of the number of PEDOT-PSS layers (or thickness of the PEDOT-PSS layer) on the capacitance of the CP based electrode. The capacitance values for 0, 1, 2 and 4 layers of PEDOT-PSS were typically 0.04 (DL capacitance), 40.4, 99.4, and 247.4 µF, respectively. This revealed a linear relationship between the number of PEDOT-PSS layers and the capacitance of the sensors. This was an important information since for solid-state

ISEs, a high capacitance of the SC material is needed in order to improve the final stability of the sensor [26].

The linear fit of the plot of the sensor capacitance values versus the number of PEDOT-PSS layers deposited gave a straight line with a correlation factor of r^2= 0.98. This showed that the reproducibility of the deposition process of PEDOT-PSS layers was good. The sensor to sensor reproducibility was in addition highlighted by the similar capacitance values obtained from three different electrodes on which one layer of PEDOT-PSS was deposited: the average capacitance value was 40.4 ± 4.8 µF.

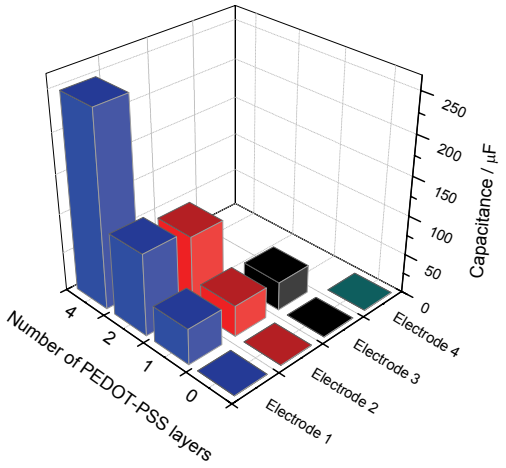

Figure 26: Influence of the number of PEDOT-PSS layers on the capacitance of the sensors.

3.2 pH response

The pH-membrane was deposited on the PEDOT-PSS electrodes and the pH response of the different sensors was recorded (Figure 27). From this figure, the influence of the presence of the CP on the pH response of the different sensors could definitely be observed. The pH sensitivity of the electrodes featuring 0, 1, 2 and 4 layers of PEDOT-PSS as SC material was -10.8, -8.5, -6.4 and -2.0 mV per pH unit, respectively. Therefore, one could notice that the thicker the PEDOT-PSS layer, the lower the pH response of the pH-sensor. Similar results were already observed in other investigations [37,38] for polypyrrole as SC material.

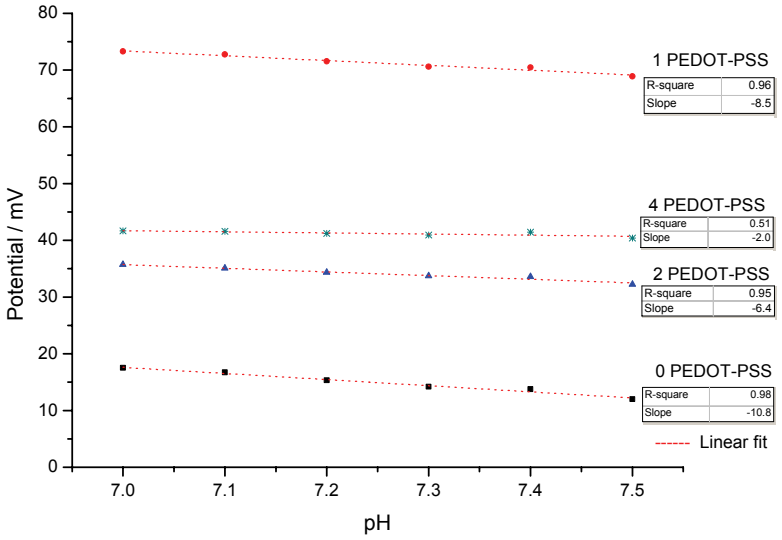

Figure 27: pH response of SC ISEs based on various numbers of PEDOT-PSS layers.

The pH response of the different sensors was very low, even for the CWE sensors (i.e., sensor without PEDOT-PSS layer), which previously had displayed sensitivities close to the Nernstian predicted value. Indeed, as demonstrated in **Part A** of this chapter and as also reported in other works [11,39], the ISM used normally features excellent properties in terms of pH sensitivity, selectivity and stability over time. Thus, it was suspected that the properties of the pH-membrane might have been affected. The ISM cocktail was synthesized at the Center for Microelectronics of Barcelona, IMB-CNM (CSIC), Barcelona, Spain and shipped to Denmark where the SC ISEs were developed. At its arrival, the vial containing the membrane preparation looked damaged. The membrane composition might, unfortunately, have been altered and might have been responsible for the low response of the sensors. Another reason could be that PEDOT might have been partly reduced which could have decrease its conductivity and thus altered its property to act as an ion-to-electron transducing material.

Even so, the effect of changing the pH of the test solution up and down (i.e., from pH 7.00 to pH 7.50 and back to pH 7.00) on the potentiometric response of the sensors was also studied (Figure 28).

These experiments also displayed the lower pH sensitivity of the PEDOT-PSS based sensors compared with the CWEs. This could tentatively be explained by the fact that PEDOT-PSS may not be the optimal material for pH ISEs. On one hand, PEDOT-PSS was chosen for its superior stability, its low cost, and its easy manufacturing procedures compared with other CPs, which made it one of the best candidates for the fabrication of sensors for mass production. Moreover, it was recently successfully used for the development of a similar type of low cost screen-printed sensors for K^+-ISEs [35]. On the other hand, based on the experiments carried out in this thesis, the quality of PEDOT-PSS to act as an electron-to-proton transducer material remains doubtful.

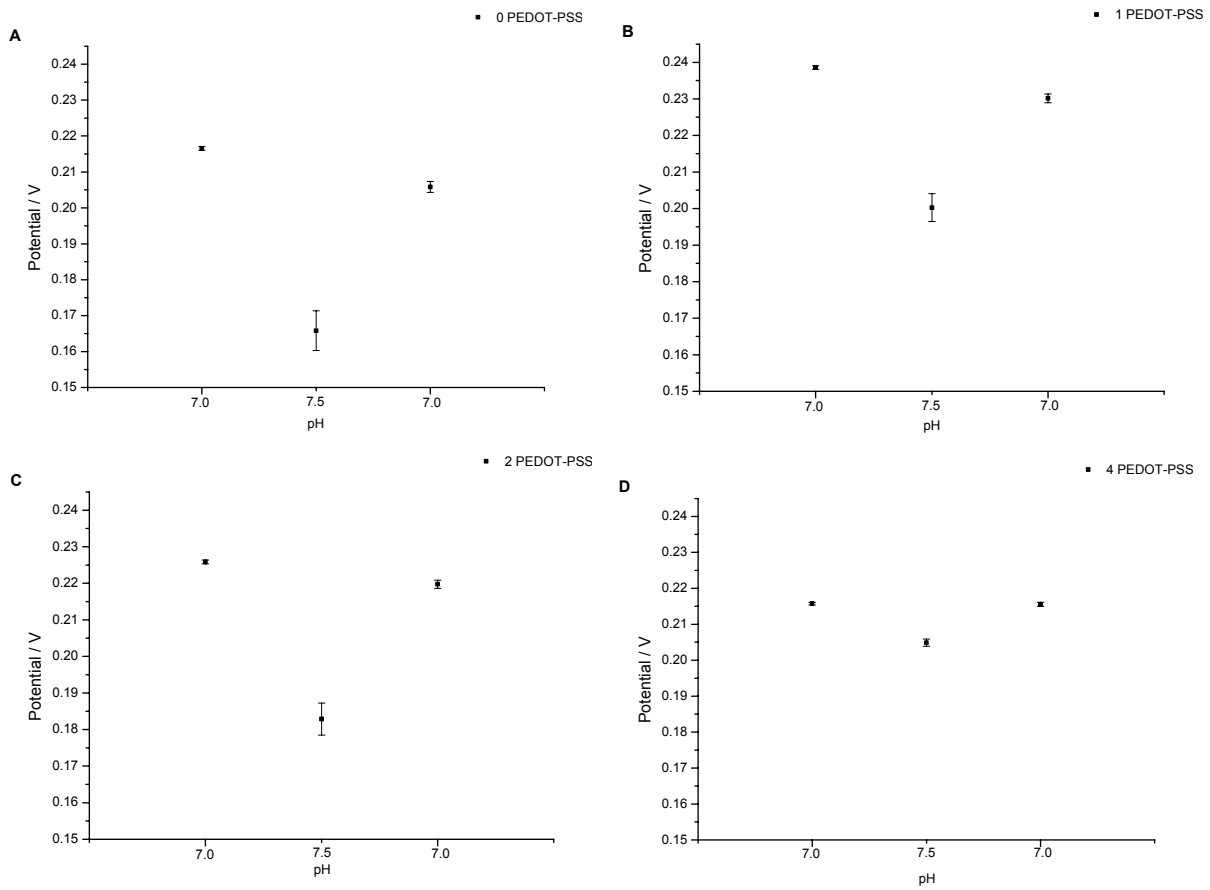

Figure 28: Influence of the number of PEDOT-PSS layers on the pH response of the SC ISEs. Plots A, B, C and D are for 0, 1, 2, and 4 layers of PEDOT-PSS, respectively.

While more investigations need to be carried out to confirm the previous statements, other CPs such as polypyrrole or polyaniline might be more appropriate for pH monitoring ([32] and cited references). Besides, it was previously observed that the PEDOT-PSS can have the tendency to swell and disintegrate [40] in aqueous solutions which thus might result in affecting its efficiency to act as a proper SC material. A way to further improve the stability of PEDOT-PSS was previously proposed [33] and consisted in ionically (physically) crosslinking the excess of negative charges in the CP solution (i.e., from PSS) with multivalent cations (e.g., Mg^{2+}, Ca^{2+}, $Fe^{2+/3+}$ and $Ru(NH_3)_6^{2+/3+}$) in order to decrease the water solubility of the PEDOT-PSS.

From the experiments carried out in this thesis, it was generally observed that major differences exist between the pH responses of the sensor without PEDOT-PSS (Figure 28 A) and the sensors with PEDOT-PSS (Figure 28 D). It was clearly shown that the sensor without SC material (i.e., CWE) responded much more significantly to the first pH change (i.e., from pH 7.00 to pH 7.50) compared with the PEDOT-PSS based sensor. However, after changing the pH of the sample back to the initial value, the potential of the CWE did not directly return to its initial value and/or might

need more time to equilibrate. In the case of the sensor with the thick PEDOT-PSS layer, the potential exactly returned to its initial value. This may be attributed to the elimination of the potential formation of a water layer in between the electrode material and the ISM as described earlier [4,41], which would allow faster equilibration processes.

4 Conclusions

After developing CWEs for pH monitoring, the fabrication of solid-state ISEs was attempted. The conducting polymer PEDOT-PSS was used to act as an ion-to-electron transducing material between the screen-printed graphite electrode and the ISM. The commercial product PEDOT-PSS was chosen supported by its confirmed superior stability in all-solid-state arrangements and its deposition process very suitable for mass production.

While improved performances were expected compared with the CWEs, the SC ISEs displayed pH sensitivities much lower than the predicted Nernstian value of approximately -59.2 mV per pH unit. Alteration of the composition of the ISM preparation (during transportation of the chemical) was suspected as a potential reason for the low pH response. Thus, additional experiments and especially, formulation of a new pH sensitive membrane would be necessary to be able to draw more precise conclusions.

Further investigation of the role of PEDOT-PSS as SC material for SC pH-sensors would also be required. Alternatively, the use of CP materials that have already proven to be suitable for such purpose (e.g., polypyrrole or polyaniline) might need to be attempted. Nonetheless, a correlation between the thickness of the SC material and the pH response of the sensors was shown. The thicker the PEDOT-PSS layer, the lower the pH response of the sensor. However, it was also generally observed that the SC ISE provided a more reproducible potential response than the CWE.

C. References

[1] C. A. Burtis, R. Ashwood, *Fundamentals of Clinical Chemistry*. 5th ed. **2001**: W. B. Saunders Company. 105-113.

[2] J. Bobacka, A. Ivaska, A. Lewenstam, Chemical Reviews, **2008**. 108(2): p. 329-351.

[3] R. W. Cattrall, H. Freiser, Analytical Chemistry, **1971**. 43(13): p. 1905-1906.

[4] E. Lindner, R. E. Gyurcsányi, Journal of Solid State Electrochemistry, **2009**(13): p. 51–68.

[5] E. Lindner, R. P. Buck, Analytical Chemistry, **2000** 72: p. 336-345.

[6] S. Joo, R. B. Brown, Chemical Reviews, **2008**. 108: p. 638–651.

[7] M. Vamvakaki, N. A. Chaniotakis, Analytica Chimica Acta, **1996**. 320(1): p. 53-61.

[8] E. Lindner, V. V. Cosofret, S. Ufer, R. P. Buck, W. J. Kao, M. R. Neuman, and J. M. Anderson, Biomedical Materials Research, **1994**. 28: p. 591-601.

[9] G. S. Cha, D. Liu, M. E. Meyerhoff, H. C. Cantor, A. Rees Midgley, H. D. Goldberg, and R. B. Brown, Analytical Chemistry, **1991**. 63(17): p. 1666-1672.

[10] H. Nam, G. S. Cha, T. D. Strong, J. Ha, J. H. Sim, R. W. Hower, S. M. Martin, and R. B. Brown, Proceedings of the IEEE, **2003**. 91(6): p. 870-880.

[11] N. Abramova, A. Bratov, Talanta, **2010**. 81(1-2): p. 208-212.

[12] A. Bratov, N. Abramova, J. Munoz, C. Dominguez, S. Alegret, and J. Bartroli, Analytical Chemistry, **1995**. 67(19): p. 3589-3595.

[13] A. Bratov, N. Abramova and C. Domínguez, Analytica Chimica Acta, **2004**. 514(1): p. 99-106

[14] N. Abramova, A. Ipatov, S. Levichev, and A. Bratov, Talanta **2009**. 79: p. 984–989.

[15] C. Jimenez, A. Bratov, N. Abramova, and A. Baldi, *Encyclopedia of Sensors*, ed. C.A. Grimes, E.C. Dickey, and M.V. Pishko. 2006, Pennsylvania, USA American Scientific Publishers. 151–196.

[16] N. Abramova, A. Bratov Sensors, **2009**. 9: p. 7097-7110.

[17] W. Morf, W. Simon, *Ion Selective electrodes in analytical chemistry*, ed. H, Freiser. 1978: Plenum Press, New York, London. 211-286.

[18] G. J. Kost, C. Hague, *In Vitro, Ex Vivo, and In Vivo Biosensor Systems, Handbook of Clinical Automation, Robotics and Optimization*. Vol. 648. 1996: John Wiley & Sons, Inc., Chichester.

[19] J. Wang, M. Pedrero, H. Sakslund, O. Hammerich, J. Pingarron, The Analyst, **1996**. 121(3): p. 345-350.

[20] A. Lynch, D. Diamond, P. Lemoine, J. Mc Laughlin, and M. Leader, Electroanalysis, **1998**. 10(16): p. 1096-1100.

[21] P. Lemoine, P. Mailley, M. Hyland, J. M. McLaughlin, E. McAdams, J. Anderson, A. Lynch, D. Diamond, and M. Leader, Journal of Biomedical Materials, **2000**. 50: p. 313-321.

[22] V. V. Cosofret, M. Erdösy, E. Lindner, T. A. Johnson, R. P. Buck, W. J. Kao, M. R. Neuman, and J. M. Anderson, Analytical Letters, **1994**. 27(15): p. 3039-3063.

[23] G. Cui, J. H. Yoo, J. S. Lee, J. Yoo, J. H. Uhm, G. S. Cha, and H. Nam, The Analyst, **2001**. 126: p. 1399–1403.

[24] R. O. Kadara, N. Jenkinson, and C. E. Banks, Sensors and Actuators B, **2009**. 138: p. 556–562.

[25] M. Fibbioli, W. E. Morf, M. Badertscher, N. F. de Rooij, and E. Pretsch, Electroanalysis, **2000**. 12.

[26] J. Bobacka, Analytical Chemistry, **1999**. 71(21): p. 4932-4937.

[27] S. Walsh, D. Diamond, J. McLaughlin, E. McAdams, D. Woolfson, D. Jones, and M. Bonner, Electroanalysis, **1997**. 9(17): p. 1318-1324.

[28] E. Pretsch, Trends in Analytical Chemistry, **2007**. 26(1): p. 46-51.

[29] A. Michalska, Analytical and Bioanalytical Chemistry, **2006**. 384(2): p. 391-406.

[30] J. Bobacka, A. Ivaska, A, Lewenstam, Electroanalysis, **2003**. 15(5-6): p. 366-374.

[31] H. Jahn, H. Kaden, Microchimica Acta, **2004**. 146(2): p. 173–180.

[32] J. Bobacka, Electroanalysis, **2006**. 18(1): p. 7-18.

[33] M. Vázquez, P. Danielsson, J. Bobacka, A. Lewenstam, A. Ivaska, Sensors and Actuators B, **2004**. 97(2-3): p. 182-189.

[34] A. Michalska, K. Maksymiuk, Analytica Chimica Acta, **2004**. 523: p. 97–105.

[35] H. Xu, X. Yang, Y. Wang, J. Zheng, Z. Luo, G. Li, Measurement Science and Technology, **2010**. 21: p. 1-5.

[36] M. Vázquez, J. Bobacka, A. Ivaska, A. Lewenstam, Sensors and Actuators B, **2002**. 82(1): p. 7-13

[37] K. K. Shiu, F. Y. Song, K. W., Lau, Journal of Electroanalytical Chemistry, **1999**. 476(2).

[38] B. Lakard, O. Segut, S. Lakard, G. Herlem, T. Gharbi, Sensors and Actuators B, **2007**. 122(1): p. 101-108.

[39] A. E. Musa, F. J. del Campo, N. Abramova, M. A. Alonso-Lomillo, O. Domínguez-Renedo, M. J. Arcos-Martínez, M. Brivio, D. Snakenborg, O. Geschke, and J. P. Kutter, Electroanalysis, **2011**. 23(1): p. 115–121.

[40] S. Ghosh, O. Inganäs, Journal of Electrochemical Society, **2000**. 147(5): p. 1872-1877.

[41] R. De Marco, J. P. Veder, G. Clarke, A. Nelson, K. Prince, E. Pretsch, E. Bakker, Physical Chemistry Chemical Physics, **2008**. 10: p. 73-76.

Chapter V Voltammetric sensors with internal reference

1 Introduction

The main aim of the work described in the following chapter was to investigate the fabrication of low cost voltammetric systems featuring reference and sensing function on the same electrode, namely, a sensing half-cell incorporating both indicator and reference species.

The sensors developed in the following study were intended for pH monitoring and featured phenanthraquinone (denoted as PAQ) as a pH-sensitive moiety (i.e., indicator species) and dimethylferrocene (denoted as Fc) as a pH-insensitive moiety (i.e., reference species). The redox reaction of PAQ and Fc are shown in Equation 12 and Equation 13, respectively.

$$Fc^{+} + e^{-} \Leftrightarrow Fc$$ Equation 15

$$Q + 2e^{-} + 2H^{+} \Leftrightarrow QH_2$$ Equation 16

The measurement method used for this type of voltammetric system was based on evaluating pH changes by monitoring the deviation in peak potential of the redox pH-sensitive component (PAQ), with respect to the redox active pH-insensitive species (Fc). The idealized response of such a voltammetric system is displayed in Figure 29.

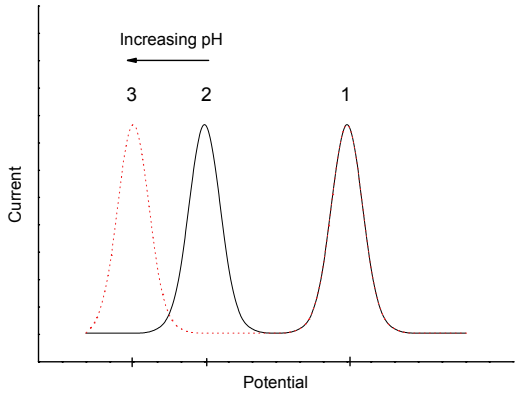

Figure 29: Idealized response of a voltammetric sensor featuring both sensing and reference molecules, for two different target species activities (e.g., here pH). 1: overlapped peaks revealing the presence of the reference redox component (e.g., pH-insensitive molecule such as Fc); 2 and 3: peaks revealing the presence of an indicator redox component (e.g., pH-sensitive molecule such as PAQ).

This type of system presented several very attractive advantages compared to other electrochemical systems. First, since the difference in the peak potential position of the two redox species from the sensing electrode versus a common reference half-cell is taken into account, even if potential of the latter happened to be altered (e.g., by drifting), the measurements should

theoretically not be affected (since the peak position of both redox species would equally shift). Thus, this technique would permit the use of a simple, inexpensive QRE as reference half-cell avoiding the use of bulky and expensive macro RE or complicated multi layer or membrane based RE systems, which could, moreover, involve issues such as shrinkage, delamination, long conditioning times, etc. This definitely stands for a major advantage for the development of low cost electrochemical sensors, which was, moreover, comforted by the fact that finding the perfect, reliable and stable RE has been considered by many as being equal to the quest for the Holy Grail [1]. Here, the aim was not focused on solving the major issues involved with the instability, potential drift and other flaws coming from reference half-cells, but instead a way to circumvent those using this alternative type of electrochemical system featuring a sensing electrode with internal reference was investigated.

In addition, with the voltammetry technique just described, the height of the peak current was not as significant as in typical voltammetric measurements where this height is used for determining the concentration of a target species. Here, the location of the peak currents (i.e., the potential) was only needed for analysis.

To my knowledge, the fabrication of screen-printed voltammetric pH-sensors of this type was only investigated by D. K. Kampouris et al. in 2009 [2]. Inspired by this work and a few other ones based on the use of quinone and ferrocene components for electrochemical systems [3-5], I intended pursuing the development of this type of low cost voltammetric microsensors for a narrower application range. More precisely, I aimed at developing screen-printed microsensors that could be used on a narrower pH-range (i.e., the physiological pH range).

In order to verify whether this could work, I used manual SP of graphite pastes incorporating the two redox species on SPEs previously fabricated and optimized (work described in **chapter III**). This was intended to allow the development of microsensors in a fast and very simple way however, still keeping in mind that the results might be affected by a certain lack of reproducibility.

2 Experimental

In the following section, a description of the experimental setups, materials and conditions is given.

2.1 Instrumentation and materials

Fabrication and optimization of the SPEs, fabrication of the manual SP device, polymer materials and fluidic flow cell (volume < 1ml) used in the following chapter are described in more details in **chapter III**.

A SP squeegee (*Speedball Art Product Company*, US) was used for manual SP. Dust free cellulose polyester wipes (*Sitix IMTEX*, Denmark) were used to polish the sensors surface.
The mechanical properties of the sensors were investigated by taking images of their surface with a *Nikon Eclipse L 200* optical microscope (*Nikon*, Denmark). A stylus profiler *Dektak 8* (*Bruker AXS*, UK) was also used for determination of the thickness of the different screen-printed layers.

2.2 Chemicals

1,1'-Dimethylferrocene, 95% and 9,10-Phenanthrenequinone, 95% as well as the reagents used for the electrochemical characterization of the sensors (of analytical grade) were used as received from *Sigma-Aldrich*, Denmark, without further purification. Stock solutions were prepared weekly with deionized (DI) water of minimum resistivity of 18 MΩ cm.

2.3 Electrodes

- ***SP materials***

For the electrodes, the graphite (*C10903P14)* and Ag/AgCl (*C2040308D2*) inks were obtained from *Gwent*, UK. For the dielectric material, *242-SB* (*Electro-Science Laboratories (ESL), Inc.*, USA) was used. 500 µm thick PET sheets (*HiFi Industrial Film*, France) were utilized as substrate material.

- ***Manual SP process***

The chips fabricated were made of the same configuration as the ones described earlier in **chapter III** and consisted of eight electrodes, including four graphite electrodes (i.e., the WE) and four

Ag/AgCl electrodes (i.e., the QREs). On top of the graphite electrodes were screen-printed the voltammetric sensors (Figure 30).

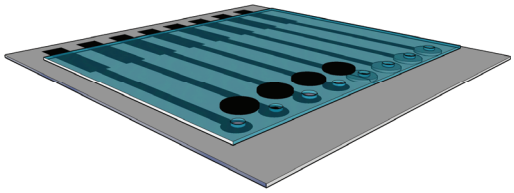

Figure 30: Electrode configuration of the voltammetric sensors.

The first part of the investigation consisted in attempting to print the modified SP graphite inks (i.e., incorporating the redox electrochemical species) on top of the SPEs by manual screen-printing for fast fabrication of low cost electrochemical systems. Thus, a manual SP setup was designed and fabricated. It was composed of an assembly of different polymer materials (i.e., PMMA platform and frame and a 100 µm thick COP screen) structured by either micromilling or CO_2-laser ablation (**chapter III**).

Four SPEs were placed in slots in the bottom layer of the setup, helping aligning the screen patterns on top of the working electrodes. The different layers were then clamped by mounting the top frame. By depositing approximately 100 mg of the graphite paste preparation, the electrodes were printed by drawing the paste across the screen patterns with a SP squeegee (four passes provided optimal results).

After printing, the graphite patterns were cured at 40° C for 15 minutes. This low temperature curing process was used in order not to alter the chemicals loaded in the ink via thermal degradation [2]. After curing, the sensors were left overnight at room temperature for further drying. The electrode patterns were then gently polished with a dust free wipe and rinsed with DI water.

- ***PAQ/Fc incorporated SP graphite paste***

Based on the work previously mentioned [2], different graphite paste compositions with different weight to weight ratios of electrochemically active components were investigated. Ratios of 1:6 and 1:6 of PAQ and Fc to graphite ink were first used. Later (see SWV experiments), ratios of 2:6 and 1:6 of PAQ and Fc to graphite ink were also used.

2.4 Electrochemical methods

Electrochemical characterization of the SPEs was carried out by CV at a scan rate ranging from 25 to 500 mV s^{-1}. For the CV experiments, the fabricated sensor was used as WE in combination with a Pt CE, and either a DJRE or a fabricated Ag/AgCl QRE.

SWV was used with a frequency ranging from 10 to 100 Hz, a step potential of 1 mV and an amplitude of 10 mV. Moreover, derivative voltammetry was used to optimize the location of the peak potentials. This method was introduced to precisely determine the peak positions in the square-wave voltammograms by taking the first derivative of the voltammograms [6]. For the SWV experiments, the fabricated sensor was used as WE in combination with a Pt CE, and an Ag/AgCl DJRE.

Unless otherwise stated, all potentials are stated with respect to the DJRE.

All the experiments were conducted at 22 ± 2 °C.

3 Results and discussion

In the following section, characterization of the main mechanical and electrochemical properties of the manually fabricated SP electrodes is described.

To verify the quality of the fabrication technique used, graphite patterns without electroactive species loaded were first printed and analyzed. Their general properties such as dimensions, thickness and roughness were followed by optical microscopy and stylus profilometry. The electrochemical properties of the electrodes were also investigated by CV.

Next, the development of the voltammetric pH-sensors incorporating sensing and reference electrochemical species in SP graphite pastes is presented.

3.1 Manual screen-printing of graphite electrodes

3.1.1 General properties

After curing treatment, analysis of the dimensions of the graphite electrodes by optical microscopy revealed well reproduced printed patterns with an average diameter of 1.23 ± 0.01 mm (n=3 samples) which was in good agreement with the diameter of the micromilled (or laser ablated) holes in the screen (i.e., theoretical diameter of the milled holes of 1.2 mm, see **chapter III**). The average thickness of the printed patterns was 64.1 ± 4.5 μm (n=3 samples), which revealed the expected shrinkage of the paste caused by the thermal treatment.

Profilometer measurements showed an average surface roughness of 1.3 ± 0.1 μm (n=3 samples). This was very close to the roughness values previously obtained in **chapter III** for semi-automatically fabricated SPEs (i.e., 1.62 ± 0.03 μm). Here, the slightly smoother surface obtained could be attributed to the removal of less non metallic material from the lower temperature curing step or to the additional polishing step. As expected, the reproducibility of the manual printing process was lower than the semi-automatic one, which is, for example, highlighted by the higher deviation values.

3.1.2 Electrochemical performance

The electrochemical properties of the printed patterns were then investigated by CV. Typical voltammograms obtained for the manually printed graphite electrodes are shown in Figure 31 A.

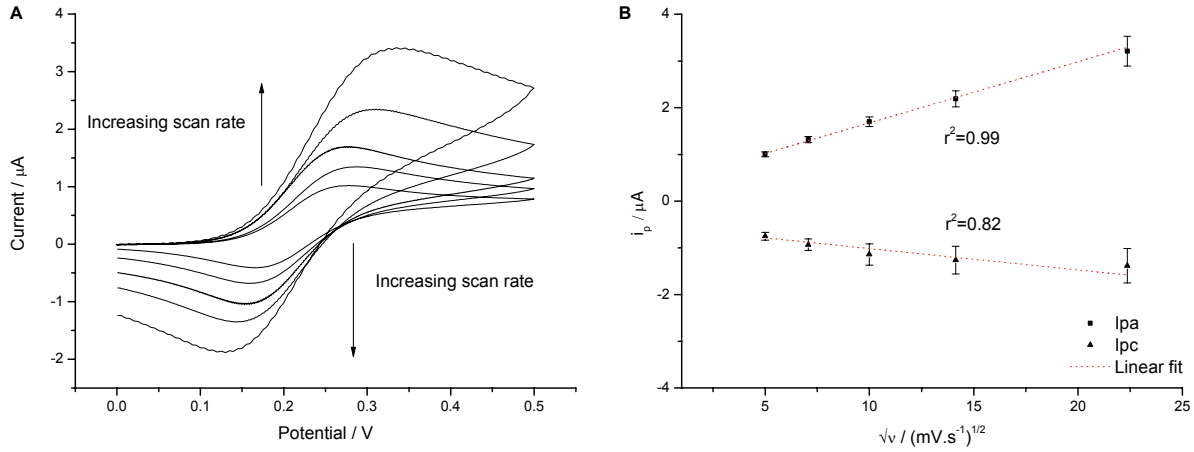

Figure 31: A. Overlaid cyclic voltammograms of a manually screen-printed graphite electrode in 1 mM $K_4[Fe(CN)_6]^{4-}$, 0.1 M KNO_3 recorded at varying scan rates (υ from 25 to 500 mV s^{-1}). B. Corresponding plot of the relationship between anodic peak current I_{Pa} (▪) and cathodic peak current I_{Pc} (▲) and various scan rate values (n=3 samples).

The electrodes displayed good voltammograms with polarization curves characteristic for macro-electrodes, featuring well defined anodic and cathodic peaks. From voltammograms carried out on a broad range of scan rates (25 to 500 mV s^{-1}), the average peak separation value ΔE_p was typically 0.15 ± 0.04 V whereas the peak current ratio i_p was 1.4 ± 0.2. Those values were very close to the ones previously obtained for the semi-automatically screen-printed *Gwent* electrodes (**chapter III**) and confirmed that both the curing treatment and the fabrication method used here provided very good results. Moreover, as depicted in Figure 31 B, a linear relationship was obtained when plotting the peak currents versus the square root of the scan rate. Those confirmed that a reversible process (i.e., with fast electron transfer and thus a diffusion controlled process) takes place at the surface of the manually printed electrodes.

3.2 Voltammetric pH-sensors with internal reference

3.2.1 Preliminary characterization

For preliminary investigations, three types of sensors were printed: one type with only Fc incorporated in the graphite paste, one type with only PAQ incorporated in the graphite paste and one type with both Fc and PAQ incorporated in the graphite paste.

By CV, the electrochemical properties of the sensors were investigated. The experiments were carried out on a three electrode setup (the sensors were characterized against a commercial Ag/AgCl DJRE and a commercial Pt CE) in two buffer solutions with different pH in a beaker (volume analyzed ~ 10 ml).

- ***PAQ incorporated graphite electrodes***

The cyclic voltammograms of the electrodes incorporating only the PAQ compounds showed a strong anodic peak on the forward scan and a shoulder on the backward scan both revealing the presence of also a cathodic peak (Figure 32 A). This witnessed the presence of the redox couple Q/QH_2.

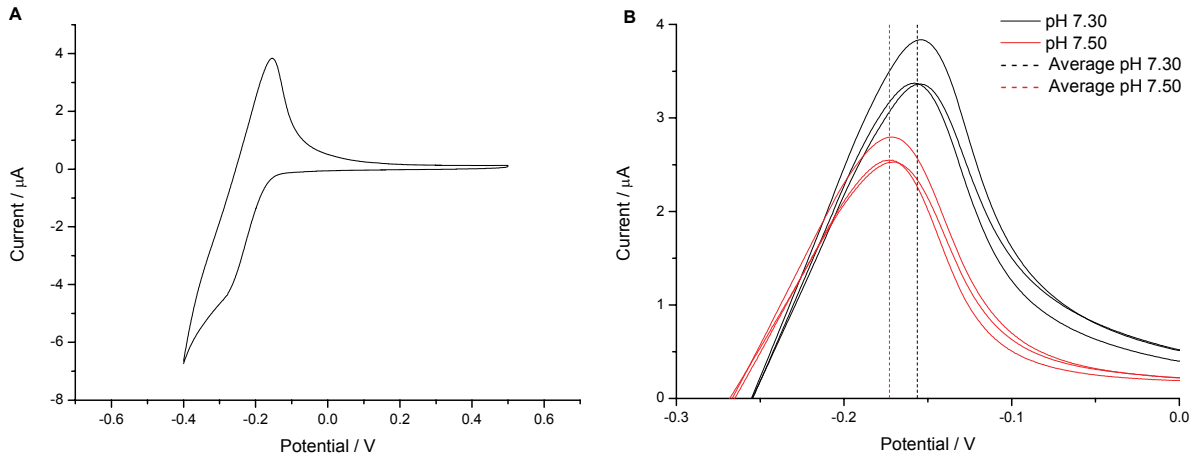

Figure 32: A. Typical cyclic voltammogram (υ = 100 mV s^{-1}) of a PAQ incorporated sensor in a pH 7.30 buffer solution. B. Zoom on the anodic peak region (three sensors were characterized at pH 7.30 and pH 7.50).

From cyclic voltammograms taken in two different pH buffer solutions, a clear shift of the anodic peak towards more negative potentials was noticed: the average potential of the peak at pH 7.30 and pH 7.50 was -0.155 ± 0.002 V and -0.171 ± 0.002 V (n=3 samples), respectively (Figure 32 B). This change in potential would actually correspond to a sensor sensitivity of approximately 0.084 V per pH unit. This response was greater than the theoretical predicted Nernstian response and is also named "Super Nernstian". Such a behavior was already observed in other works while its nature still remains rather unclear [4]. While the theoretical Nernstian response is obtained and well understood for dissolved redox species, here the species were incorporated into the electrode matrix and might involve other side processes that result in a slightly different sensor sensitivity.

- ***Fc incorporated graphite electrodes***

The cyclic voltammograms of the electrodes incorporating Fc compounds showed the presence of both anodic and cathodic peaks revealing the presence of the Fc/Fc^+ redox couple (Figure 33 A). Unexpectedly, when increasing the pH of the test solution, the anodic peak shifted towards more positive potentials whereas it should be pH-insensitive and thus stay at a constant position. The average potential of the peak at pH 7.30 and pH 7.50 was 0.220 ± 0.008 and 0.286 ± 0.004 V (n=3 samples), respectively. However, the cathodic peak kept the same position and did not shift with pH: the average potential of the peak at pH 7.30 and pH 7.50 was 0.110 ± 0.004 V and 0.111 ± 0.012 V, respectively (Figure 33 B).

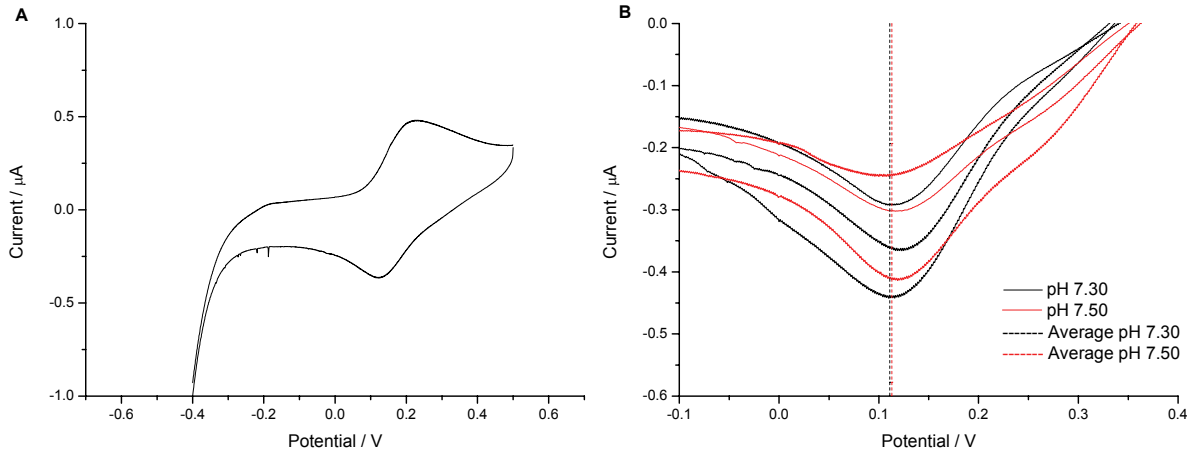

Figure 33: A. Typical cyclic voltammogram (υ = 100 mV s^{-1}) of a Fc incorporated sensor in 7.30 pH buffer solution. B. Zoom on the cathodic peak region (three sensors were characterized at pH 7.30 and pH 7.50).

- ***PAQ and Fc incorporated graphite electrodes***

The cyclic voltammograms of the electrodes incorporating both PAQ and Fc compounds revealed the combined presence of the Q/QH_2 and Fc/Fc^+ redox couples (Figure 34 A) which was in good agreement with the previous cyclic voltammograms obtained for the sensors incorporating each individual compound.

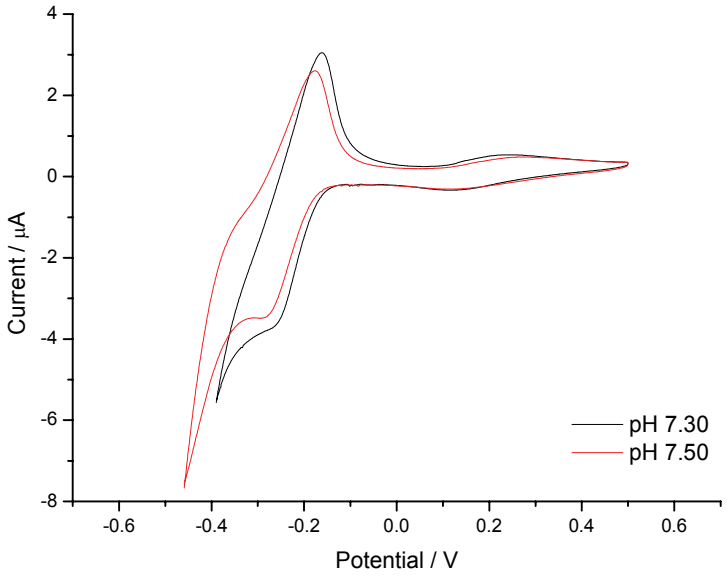

Figure 34: Typical cyclic voltammograms (υ = 100 mV s^{-1}) in pH 7.30 and pH 7.50 buffer solutions of a PAQ / Fc incorporated sensor vs. a DJRE.

From these cyclic voltammograms, a pH change of 0.2 units corresponded to an identical potential shift in the oxidation peak of Q/QH_2 as the one previously observed for the sensor that incorporated only PAQ (i.e., 16 mV). Also in agreement with what was previously observed, the oxidation peak of Fc shifted towards more positive potentials, whereas its reduction peak did not. Thus, it was clear that the difference in peak potential between the PAQ oxidation peak and the Fc reduction peak could be used for pH sensing.

3.2.2 pH monitoring

- ***Cyclic voltammetry experiments***

Next, the pH response of the developed voltammetric system (i.e., on chip sensing electrode and Ag/AgCl QRE) was investigated in more detail. Moreover, the experiments were carried out in the microfluidic flow cell (**chapter III**) in order to reduce the volume of the analyzed sample. As seen in Figure 35, the cyclic voltammograms obtained displayed the identical shape as the ones previously obtained when characterizing the sensors versus a commercial DJRE.

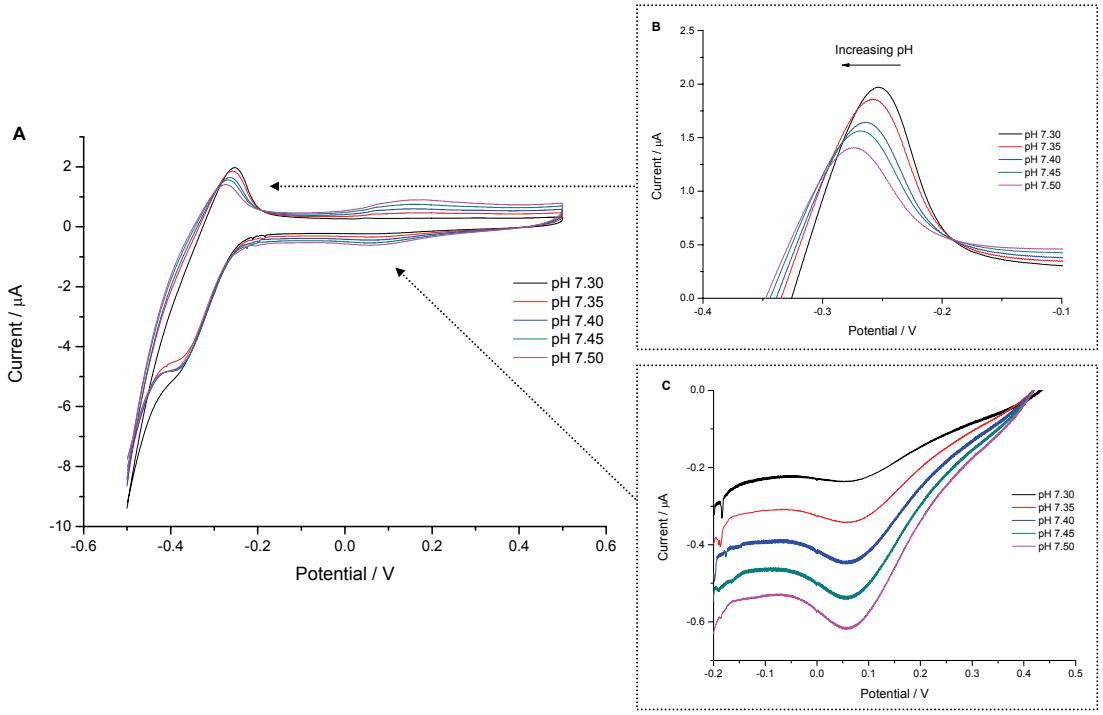

Figure 35: A. Typical cyclic voltammograms (υ = 100 mV s^{-1}) in various pH buffers of a PAQ / Fc incorporated sensor vs. an Ag/AgCl QRE. B. Zoom on the anodic peak region of the PAQ. C. Zoom on the cathodic peak region of Fc.

In accordance with the previous results, the response to pH of the PAQ compound and the "insensitiveness to pH" of the Fc compound were both confirmed (Figure 35 B and C).

In addition, the voltammetric response of three PAQ / Fc incorporated electrodes was verified in order to evaluate the reproducibility of the sensors. In Figure 36, the peak potentials of PAQ (anodic peak) and Fc (cathodic peak) as well as the potential difference between those are displayed at each pH value investigated. From this series of experiments, the pH response of PAQ was on average -89.6 mV/pH whereas taking the peak difference between the PAQ oxidation peaks and the Fc reduction peaks resulted in an average pH sensitivity of –97.0 mV/pH. These two responses were greater than that the one predicted by the Nernstian equation and thus also denoted as "Super Nernstian". Also observed by V. Lafitte et al. [4], this behavior is not fully understood.

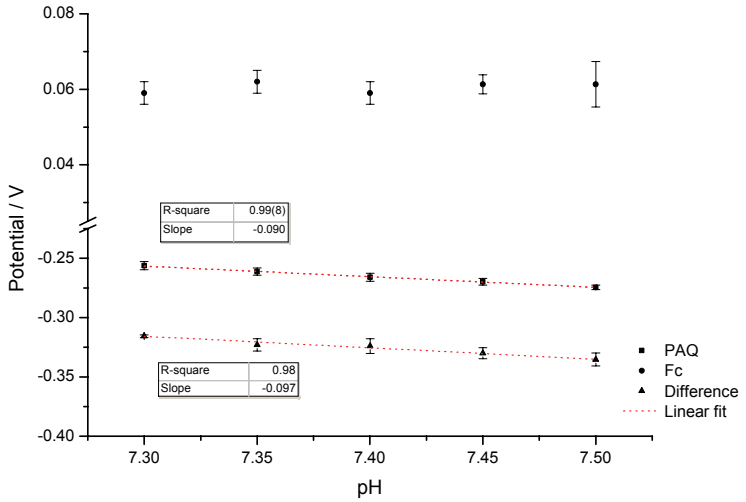

Figure 36: Plot of the peak potential against pH for the PAQ (▪), Fc (●) and the difference between the two (▲) (n=3 samples).

Taking into account the manual fabrication of the sensors, the reproducibility of the experiments (from sensor to sensor) was good as witnessed by typical error values of less than 3 mV for the PAQ peaks and 4.5 mV for the peak difference values (n=3 samples) which was in good agreement with the previous work of D. Kampouris et al. [2] and the cited references.

Moreover, for the last series of CV experiments the sensors characterized were used nine days after the first electrochemical experiments (meanwhile, the sensors were kept dry stored) and still displayed very promising results. This proved the confinement of the PAQ and Fc compounds in the graphite electrodes and also highlighted the good lifetime of sensors despite the very simple physical incorporation technique used. This was previously observed by C. Heald et al. [7], who used a more complicated chemical derivatization method of carbon nanotubes to incorporate the electroactive species on the sensors.

- ***Square-wave voltammetry experiments***

SWV was then used as a means to obtain sharper and well defined voltammetric peaks in single sweep experiments [7].

Unexpectedly, the square-wave voltammograms obtained for the PAQ / Fc incorporated sensors displayed fairly broad peaks. Investigating the influence of experimental parameters such as the frequency, potential step and amplitude did not contribute to improving the sharpness of the peaks. Even changing the content of the sensor paste (PAQ / Fc ratio in the graphite matrix) was attempted without any significant improvement of the signal sharpness.

Typical square-wave voltammetric curves carried out on a PAQ / Fc incorporated sensor versus a DJRE and a Pt CE are displayed in Figure 37 A.

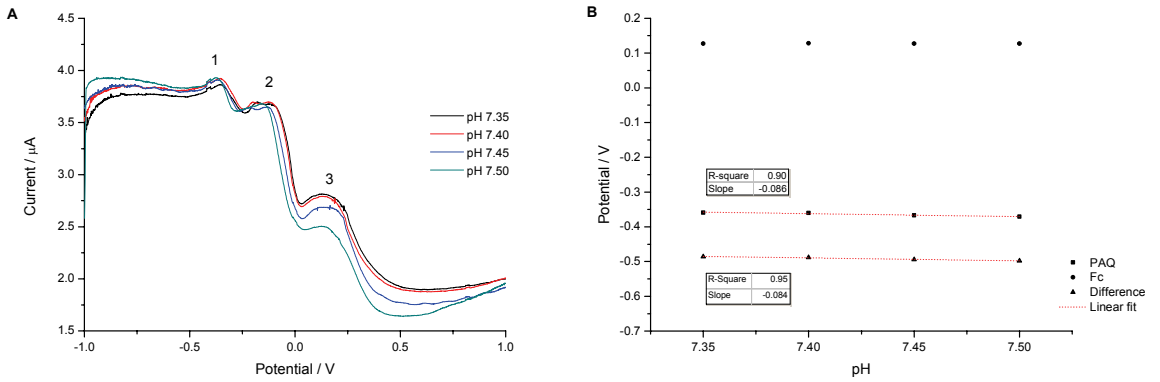

Figure 37: A. Typical square-wave voltammetric response in various pH buffer solutions of a PAQ / Fc incorporated sensor vs. a DJRE. B. Typical peak potential variation of the PAQ (▪), Fc (●) and the difference between the two (▲) in various pH buffer solutions (Peaks 1, 2, and 3 are described below)

Despite the relatively broad shape of the obtained peaks, it was possible to identify the peak responsible for the presence of PAQ (at E~ -0.361 V in a pH 7.30 buffer solution, Figure 37 A, peak 1) and the peak responsible for the presence of Fc (at E~ 0.127 V in all pH buffer solutions, Figure 37 A, peak 3).

From square-wave voltammograms taken in various pH solutions, the response to pH of the PAQ compound was –86.0 mV/pH and thus, lower but still in fairly good agreement with the previous results from the CV experiments. Moreover, the redox wave of the Fc compound only slightly shifted towards negative potential with increasing pH and could therefore be used as internal reference. As a result, a pH response of –84.0 mV/pH was obtained for the PAQ compound with respect to Fc. Figure 37 B summarizes the influence of pH on the redox peak position of the different electroactive species as well as the difference between the two peaks.

In the square-wave voltammograms, a third peak centered on E ~0.150 V was also observed (see peak 2 in Figure 37 A). This peak was not very pronounced for some of the experiments (especially for square-wave voltammogram frequencies above 25 Hz) and did not display any clear or significant correlation between its position and pH. A double peak in the square-wave voltammograms was also previously observed in other works [5,8] and tentatively attributed to the redox chemistry of PAQ. However, this phenomenon was seen at high pH (i.e., above pH 12). In [8], the shoulder in the peak currents was attributed to the reduction of quinone to semi-quinone species.

4 Conclusions

The fabrication process used to manually screen-print graphite electrodes has proven to stand for a fast, inexpensive and relatively reproducible fabrication method for electrochemical systems. The fabricated graphite based sensors displayed electrochemical properties very close to the ones of semi automatically fabricated sensors.

This means represents a much simpler way to incorporate electroactive redox components (i.e., PAQ as a pH-sensitive species and Fc as a pH-insensitive species) into graphite electrodes compared to other techniques such as covalent chemical derivatization on carbon materials with electroactive species [7,8]. Moreover, the fact that the redox species were incorporated into the electrodes and not immobilized on them presented the advantage of avoiding fast depletion of the species from the electrodes, which could shorten the lifetime the sensors. Some of the developed sensors were actually kept nine days dry stored between two electrochemical experiments and still displayed very good properties, attesting of their good lifetime despite their simple fabrication.

Moreover, a major advantage of this type of sensors featuring both sensing and reference species was that the difference between the redox peaks of the two species was taking into account. Therefore, potential drift of the reference half-cell was not as crucial as for common three electrode electrochemical setups and the use of a simple QRE was permitted.

The CV experiments showed the clear presence of the PAQ and Fc redox couples incorporated in the sensors. The oxidation peak for the Q/QH_2 redox couple shifted as expected towards more negative potentials with increasing pH and thus, validated the implementation of PAQ as the pH-sensitive species. Unexpectedly, the oxidation peak for the Fc/Fc^+ couple also shifted with pH whereas its reduction peak did not. Therefore, the use of Fc as a pH-insensitive species or internal reference species was also confirmed.

Recording the position of the oxidation peak of PAQ with respect to the reduction peak of Fc was successfully used for pH monitoring and resulted in a super Nernstian pH-response of -97.0 mV/pH. This type of response was also observed earlier by Lafitte et al. [4] for identical components and remains not yet understood.

The SWV experiments resulted in voltammograms with redox peaks broader than expected. However, the response of the sensors remained fairly identical to the one obtained from the cyclic voltammograms.

Further improvement in the final electrochemical system could be envisioned and consist in implementing other indicator molecules in the sensor paste for parallel detection of other components.

5 References

[1] R. P. Buck, E. Lindner, Analytical Chemistry, **2001**. 73(3): p. 88-97.

[2] D. K. Kampouris, R. O. Kadara, N. Jenkinson, and C. E. Banks, Analytical Methods, **2009**. 1: p. 25 - 28.

[3] J. J. Hickman, D. Ofer, P. E. Laibinis, G. M. Whitesides, and M. S. Wrighton, Science, **1991**. 252(5006): p. 688-691

[4] V. G. H. Lafitte, W. Wang, A. S. Yashina, N. S. Lawrence, Electrochemistry Communications, **2008**. 10: p. 1831-1834.

[5] N. S. Lawrence, M. Pagels, S. F. J. Hackett, S. McCormack, A. Meredith, T. G. J. Jones, G. G. Wildgoose, R. G. Compton, L. Jiang, Electroanalysis, **2006**. 19(4): p. 424-428.

[6] V. D. Parker, *Electroanalytical Chemistry*. Dekker, ed. Bard, A. J. Vol. 14. **1986**, New York.

[7] C. G. R. Heald, G. G. Wildgoose, L. Jiang, T. G. J. Jones, R. G. Compton, ChemPhysChem, **2004**. 5(11): p. 1794–1799.

[8] G. G. Wildgoose, M. Pandurangappa, N. S. Lawrence, L. Jiang, T. G. J. Jones, R. G. Compton, Talanta, **2003**. 60(5): p. 887-893

Chapter VI Conclusions and outlook

1 Conclusions and outlook

In this last chapter, the different conclusions drawn in the previous chapters are summarized. Moreover, future perspectives, potential experiments and developments that could bring valuable additional information to understand some of the phenomena left unexplained in this thesis are also envisioned.

1.1 Fabrication of electrochemical systems

Electrochemical systems are well established tools used to determine the presence of target analytes in clinical, environmental, food, or industrial samples. One of the major fabrication technologies used to develop electrochemical systems is the thick-film technology of SP. Inexpensive, simple, versatile, and highly reproducible, SP presents several advantages and thus appeared as the evident fabrication process for the development of disposable sensors in this project. Due to the popularity of this technology, many different companies propose a very expansive range of SP products, especially in terms of inks for electronically conducting materials and dielectric materials. However, the precise ink compositions are kept as proprietary information from the manufacturers.

In this thesis, an assortment of some of the most commonly used commercially available products was investigated. It was demonstrated that significant differences in terms of electrochemical, mechanical and electrical properties exist between these products. The effect of electrochemical and thermal treatments of the screen-printed materials was also investigated. This study resulted in the selection of an optimal electrochemical system used for further electrochemical investigations in this thesis.

Recently, some of the most promising future perspectives in the SP area have been highlighted by J. P. Metters et al. [1]. For instance, the increasing use of nanomaterials to further improve electron transfer processes was envisioned. Additionally, smaller printed patterns and more precise geometries could definitely be beneficial to the development of screen-printed microarrays. Additionally, in order to even further decrease the cost of the developed electrochemical devices, the use of new materials for SP platforms starts emerging. For instance, the recent fabrication of paper-based electrochemical devices or µPED has been described by Z. Nie et al. [2] and could pave the way to the development of a novel type of low cost electrochemical systems.

In order to greatly facilitate characterization and fabrication of the developed electrochemical sensors, a combination of rapid prototyping techniques was chosen to develop various polymer

based devices. Micromilling, PDMS-casting (replica molding) and CO_2 laser ablation were mainly used to fabricate a fluidic cell, a fluidic interconnect unit and a manual screen-printing platform.

1.2 Ion-selective electrodes

Based on the developed screen-printed chips, the fabrication of potentiometric pH-sensors was first studied. These sensors featured a photo-curable PUR membrane as ion-selective-membrane developed by our collaborators N. Abramova et al. [3]. The use of such membrane was very attractive from a technological point of view since it was compatible with standard photo-lithographic processes and thus easier to streamline than commonly used PVC membranes.

Prior to the membrane deposition on the screen-printed electrodes, a series of electrode treatments were used in order to increase the DL capacitance of the graphite based sensors and thereby increase their potential stability. Electrochemical activation by CV and optimized thermal treatment of the graphite sensors were used. The final potentiometric pH-sensor was composed of a CWE and a QRE and displayed the excellent pH response of -60.8 ± 1.7 mV/pH over a six day period, which is very close to the theoretical Nernstian value.

In order to further improve the stability of the CWEs and discard the potential formation of a water layer, the conducting polymer PEDOT-PSS was deposited between the graphite electrode and the ISM to act as ion-to-electron transducing material. In this type of solid-state electrochemical system, the potential stability is then defined by the redox capacitance instead of the DL capacitance as in the case of CWEs.

The dependence of the thickness of the PEDOT-PSS layer on the capacitance and the pH response of the final pH-sensor were investigated. It was observed that the thicker the PEDOT-PSS layer, the higher the capacitance of the sensor but the lower the pH-response of the final sensor. In order to support these results and understand them in depth, additional experiments are needed. The potential damage of the ISM was suspected and might have affected the pH sensitivity of the sensors. Thus, the development of new sensors would require the synthesis of a new ISM formulation to be certain that the properties of the membrane are not altered. Moreover, the choice of the CP as ion-to-electron transducer for pH-selective electrodes needs to be investigated in more details. Alternatively, polymers that have proven to be suitable for such purpose such as polyaniline or polypyrrole could be used.

1.3 Voltammetric systems with internal reference

Finally, the development of a screen-printed voltammetric system for pH monitoring was attempted. The main characteristic of this system was that it integrated both sensing and reference electroactive species in the graphite matrix of the working electrode.

Sensors were fabricated by screen-printing a graphite paste loaded with phenanthraquinone as a pH-sensitive moiety (i.e., indicator species) and dimethylferrocene (denoted as Fc) as a pH-insensitive moiety. This stood for a much simpler and faster technique compared to, for example, covalent chemical derivatization on carbon materials with electroactive species as described in other works [4,5]. Moreover, to my knowledge, the use of SP for the development of this type of voltammetric systems has surprisingly only been investigated by D. K. Kampouris et al. [6] despite its undeniable advantages.

CV and SVW measurements highlighted the promising performances of such electrochemical system. It was shown that the oxidation peak of the Q/QH_2 redox couple and the reduction peak of the Fc/Fc^+ redox couple could be successfully used to monitor pH. A super Nernstian pH response was displayed by the sensors which was already observed by V. Lafitte et al. [7] for the same electroactive components, but still remains not understood. However, here, the sensors responded to pH changes in a very reproducible way despite their very simple fabrication processes. Moreover, this voltammetric system presented the major advantage of limiting the potential issues stemming from the reference half-cell. Indeed, since the measurement principle was based on evaluating the difference between the redox peaks of the two electrochemical species, potential drift of the RE was thus not as crucial as for other common electrochemical setups.

Further development on the final electrochemical system could consist in implementing other indicator molecules in the screen-printed graphite ink for parallel detection of several components.

1.4 Side investigations and additional suggestions

Due to the lack of time, some projects and investigations had unfortunately to be left aside.

First, the development of ISEs carried out was also supposed to include the fabrication of other types of electrodes for monitoring the level of other target analytes such as K^+ and Na^+. The development of these electrodes was initiated but unfortunately not pursued.

On a fairly different topic, I also looked at the development of low-temperature-co-fired-ceramic (LTCC) based sensors. This fabrication technique appeared very interesting in terms of packaging of multilayered electrochemical systems.

A pneumatic pressure controller for microfluidic system MAESFLO (*Fluigent*, France) was attempted to be used to address different samples (up to six) in the microfluidic interconnect and cell developed in a precise and controlled way. However, the system (still under development by the manufacturer) appeared to be fairly complex to operate and some issues were encountered such as back flow of the fluid and bubble formation. Experiments were carried out in order to optimize experimental flow conditions as well as the design of the microfluidic system used. However, the MAESFLO had also to be left aside and less "elegant" ways of handling the liquid solutions were adopted (e.g., manual injection with syringes or syringe pumps).

Research and improvements could be pursued on the previously mentioned tracks and may ultimately lead towards the development of a lab-on-chip multi sensors system using the LTCC packaging technology and advanced integrated microfluidics.

1.5 Concluding remark

In this thesis, the potential of the thick-film process of SP for the development of miniaturized disposable electrochemical systems has been demonstrated. However, future investigations would allow to fully benefit from this technology by possibly combining it with other expending fields such as the field of microfluidics or the field of conducting polymers.

2 References

[1] J. P. Metters, R. O. Kadara, C. E. Banks, Analyst, **2011**. 136(6): p. 1067-1076.

[2] Z. Nie, C. A. Nijhuis, J. Gong, X. Chen, A. Kumachev, A. W. Martinez, M. Narovlyanskya, G. M. Whitesides, Lab on a Chip, **2009**. 10(4): p. 477-483.

[3] N. Abramova, A. Bratov, Talanta, **2010**. 81(1-2): p. 208-212.

[4] C. G. R. Heald, G. G. Wildgoose, L. Jiang, T. G. J. Jones, R. G. Compton, ChemPhysChem, **2004**. 5(11): p. 1794–1799.

[5] G. G. Wildgoose, M. Pandurangappa, N. S. Lawrence, L. Jiang, T. G. J. Jones, R. G. Compton, Talanta, **2003**. 60(5): p. 887-893

[6] D. K. Kampouris, R. O. Kadara, N. Jenkinson, C. E. Banks, Analytical Methods, **2009**. 1: p. 25 - 28.

[7] V. G. H. Lafitte, W. Wang, A. S. Yashina, N. S. Lawrence, Electrochemistry Communications, **2008**. 10: p. 1831-1834.

Appendix

Appendix A

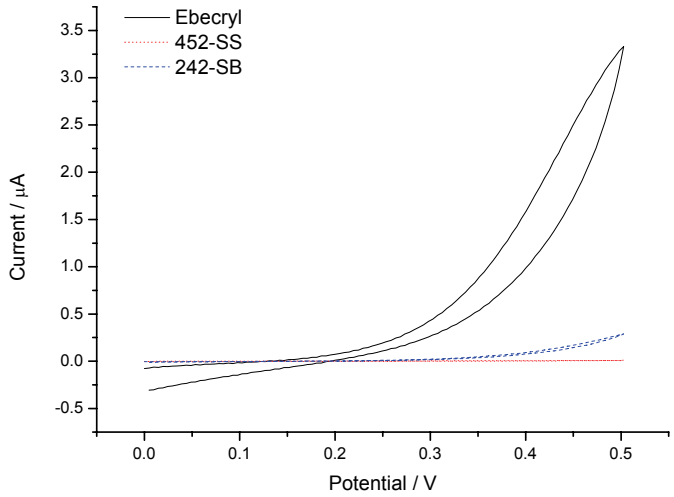

Figure 38: Cyclic voltammograms (υ: 100 mV s^{-1}, in 1 mM $K_4[Fe(CN)_6]^{4-}$, 0.1 M KNO_3) of *Acheson* graphite electrodes protected with various passivation layer materials (*452-SS*, *242-SB* and *Ebecryl*).

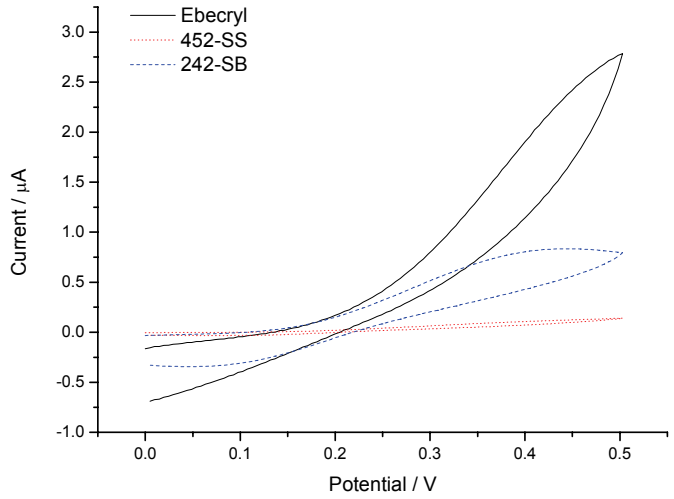

Figure 39: Cyclic voltammograms (υ: 100 mV s^{-1}, in 1 mM $K_4[Fe(CN)_6]^{4-}$, 0.1 M KNO_3) of *DuPont* graphite electrodes protected with various passivation layer materials (*452-SS*, *242-SB* and *Ebecryl*).

Appendix B

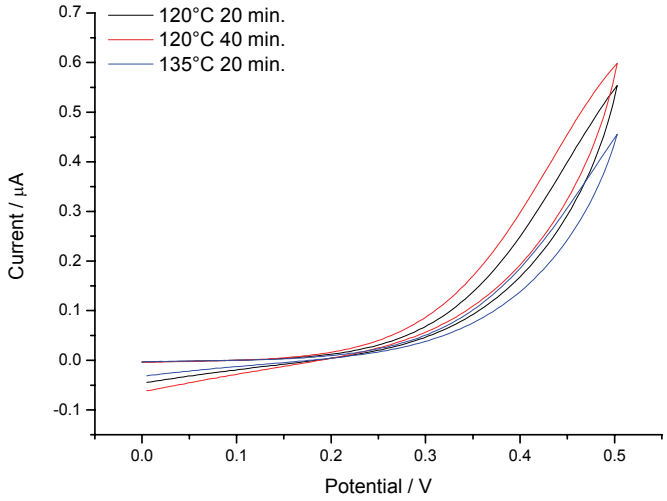

Figure 40: Cyclic voltammograms (υ: 100 mV s^{-1}, in 1 mM $K_4[Fe(CN)_6]^{4-}$, 0.1 M KNO_3) of *Acheson* graphite electrodes cured at different temperatures and times.

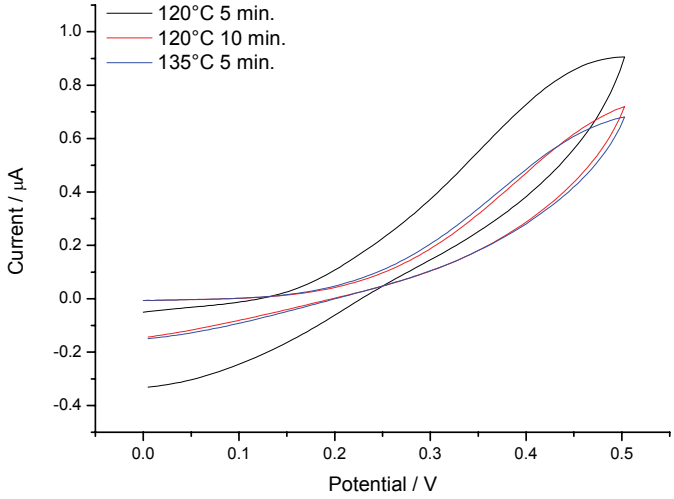

Figure 41: Cyclic voltammograms (υ: 100 mV s^{-1}, in 1 mM $K_4[Fe(CN)_6]^{4-}$, 0.1 M KNO_3) of *DuPont* graphite electrodes cured at different temperatures and times.

Appendix C

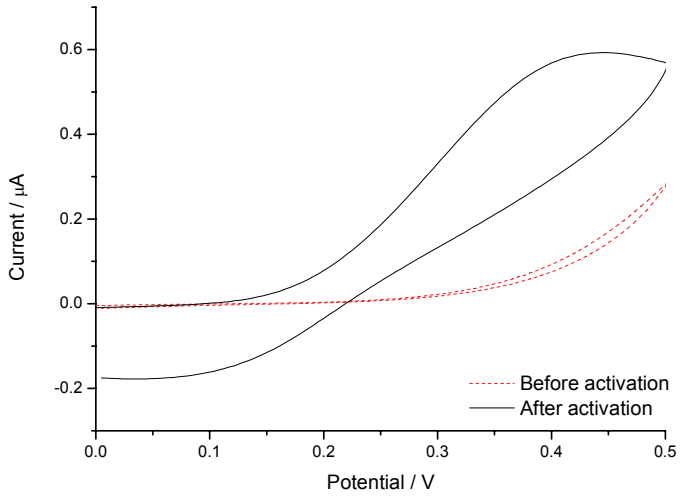

Figure 42: Example of cyclic voltammograms (υ: 100 mV s^{-1}, in 1 mM $K_4[Fe(CN)_6]^{4-}$, 0.1 M KNO_3) depicting the typical effect of the electrochemical activation of a *Acheson* graphite electrode

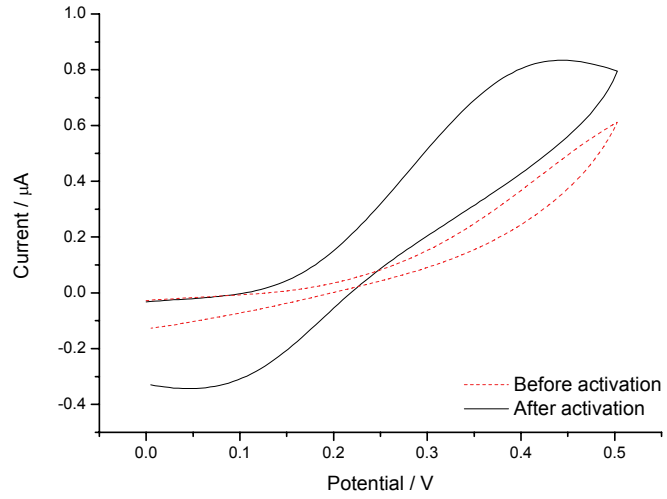

Figure 43: Example of cyclic voltammograms (υ: 100 mV s^{-1}, in 1 mM $K_4[Fe(CN)_6]^{4-}$, 0.1 M KNO_3) depicting the typical effect of the electrochemical activation of a *DuPont* graphite electrode

Publication and conference contributions

Following is the publication published in Electroanalysis.

Not enclosed to this thesis, a manuscript is in preparation regarding the work done and reported in **chapter V**.

Full Paper **ELECTROANALYSIS**

Disposable Miniaturized Screen-Printed pH and Reference Electrodes for Potentiometric Systems

Arnaud Emmanuel Musa,[a] *Francisco Javier del Campo*,[b] *Natalia Abramova*,*[b] *María Asunción Alonso-Lomillo*,[c] *Olga Domínguez-Renedo*,[c] *María Julia Arcos-Martínez*,[c] *Monica Brivio*,[a] *Detlef Snakenborg*,[a] *Oliver Geschke*,[a] *Jörg Peter Kutter*[a]

[a] DTU Nanotech, Department of Micro and Nanotechnology, Technical University of Denmark (DTU), Ørsteds Plads, 2800 Kongens Lyngby, Denmark
[b] Instituto de Microelectrónica de Barcelona, IMB-CNM (CSIC), Esfera UAB, Campus Universitat Autónoma de Barcelona, 08193 Bellaterra, Barcelona, Spain
phone: SP – 93 594 77 00 ext.: 2209, fax: SP – 93 580 14 96
[c] Departamento de Química Analítica, Facultad de Ciencias, Universidad de Burgos, Pza. Misael Bañuelos, 09001 Burgos, Spain
*e-mail: natalia.abramova@imb-cnm.csic.es

Received: July 15, 2010
Accepted: October 13, 2010

Abstract
This work describes the development of a miniaturized potentiometric system comprising a miniaturized quasi-reference electrode (QRE) coupled to a solid-state ion-selective electrode (ISE) for the monitoring of pH. We describe the optimization of materials and fabrication processes including screen-printing (SP), electrode treatments (thermal and electrochemical) and the formulation and deposition of an ion-selective membrane (ISM), to obtain a system compliant with biomedical specifications. We developed a potentiometric system composed of an Ag/AgCl QRE and a pH-electrode (ISM deposited on a graphite electrode) that can be used continuously for a period of not less than 7 days in aqueous solutions. Curing the Ag/AgCl pastes during 20 minutes at 120 °C after printing allowed the QREs to display excellent potential stability, as demonstrated by an open-circuit-potential standard deviation of ±1.2 mV over a period of 7 days ($n=3$ samples). Promoting adhesion of the pH membrane over graphite electrodes improved the pH-electrode performance. This was achieved through a combination of thermal treatment and electrochemical activation of the electrodes by cyclic voltammetry (CV). The final device integrated both the QRE and the pH-electrode, and displayed an average pH sensitivity of −60.8±1.7 mV per pH unit, over a pH range of 7.00 to 7.63.

Keywords: Screen-printed-electrode (SPE), Potentiometry, pH-electrode

DOI: 10.1002/elan.201000443

Presented at the 13th International Conference on Electroanalysis, ESEAC 2010, Gijón, Spain

1 Introduction

Adapted from the microelectronics industry, the thick-film process of screen-printing (SP) is one of the most commonly used techniques to deposit coatings in the sub-millimetre range. SP is an inexpensive, simple, versatile and highly reproducible large-scale production technique [1–3]. It involves pressing different pastes or inks through a porous screen to transfer patterns on a substrate. Originally used on ceramic materials due to their good mechanical, chemical and, especially, thermal properties, SP is today also applied on a broader range of substrates including paper, fabrics and plastics [4,5].

An important application of this technology is the fabrication of planar components for miniaturized electrochemical sensors, which have proven their suitability in biomedical, environmental and industrial applications [6–9]. In this work, we investigate the fabrication of low-cost electrochemical potentiometric systems using SP.

Potentiometric systems measure the difference in potential between an indicator electrode, also known as ion-selective electrode (ISE), and a reference electrode (RE) [10]. Due to the absence of liquid phase, solid contact (SC) ISEs present certain advantages over conventional ISEs. For instance, since they can adopt planar geometries, they are maintenance free and easily miniaturized [11]. On the other hand, their operating mechanism is more complex than conventional ISEs and their underpinning thermodynamic mechanisms (i.e., internal boundary potentials) are difficult to harness [12]. On top of that, the performance of SC ISEs is often limited by the adhesion of this membrane to the electrode, as seeping of the electrolyte between the electrode surface and the membrane impairs the sensor [13–15]. Nonetheless, from the manufacturing point of view, SC ISEs are extremely

attractive since they are compatible with low cost and mass production technologies and can be monitored with relatively simple electronic measuring apparatus [16,17] and are therefore suitable for laboratory use and biomedical applications [11].

An important feature of the ion-selective membrane (ISM) used in this work is that it is based on a photocurable polymer. Photocurable ISMs are becoming very attractive from a technological point of view because they are compatible with standard photo-lithographic processes, which makes them easier to streamline than commonly used polyvinylchloride (PVC) membranes [18].

Here, we thus present the development of a solid-state potentiometric system intended for clinical applications. In addition to responding fast to concentration changes, biomedical sensing systems must meet very stringent quality requirements in terms of accuracy, reliability and stability. We have developed a system that meets such demanding specifications over a 7-day period. We first show the construction, and optimization of individual components, namely a quasi-reference electrode (QRE) and a pH-electrode. Then, we combine them to produce a miniaturized sensing device. We describe the optimization of screen-printed QREs and solid-state ISEs by tuning the electrodes post-fabrication processes using electrochemical (activation by cyclic voltammetry (CV)) and thermal treatments (curing process of the screen-printed materials). Although chloride affects the potential of this kind of RE, the Ag/AgCl QREs fabricated here may be suitable in the future for environmental and medical applications, but the RE must be separated from the test solution. Finally, the performance of the pH-electrode integrated on a same chip as the QRE was analyzed. During the 6 days following the first 2 days of hydration, the pH response of a typical system was -60.8 ± 1.7 mV/pH. By integrating miniaturized components and automating functionalities, a final lab-on-a-chip system based on this technology may provide fast, cost effective and reliable point-of-care diagnostics.

2 Experimental

2.1 Materials, Equipments and Reagents

Commercial ionophores tridodecylamine (HI-I) and lipophilic additives (potassium tetrakis(*p*-chlorophenyl)borate (K-TpClPB), tetradodecylammonium tetrakis(4-chlorophenyl)borate (ETH 500) were purchased from Fluka, Spain. Aliphatic urethane diacrylate (oligomer Ebecryl 270) and cross-linker hexanediol diacrylate (HDDA) were from UCB Chemicals, Spain. The photoinitiator 2,2′-dimethoxyphenylacetophenone (IRG 651) was from Ciba-Geigy, Switzerland. Copolymerized plasticizer di-(*n*-hexyl)-itaconate (DHI) was synthesized as described previously [19].

All other reagents used (KOH, KCl, KH_2PO_4, KNO_3, $K_4Fe(CN)_6$, and tetrahydrofuran (THF)) were of analytical grade and were used as received from Sigma-Aldrich, Spain, without any further purification. Stock solutions were prepared weekly with deionised (DI) water of maximum conductivity of 18 MΩ cm.

The following inks for SP were supplied by Acheson Colloiden, The Netherlands, and used as received for the fabrication of electrodes: Electrodag PF-407 A (graphite ink), Electrodag 418 (Ag ink), Electrodag 6037 SS (Ag/AgCl ink), Electrodag 452 SS (dielectric ink). SP was performed on 500 μm thick polyethylene terephthalate (PET) films from HiFi Industrial Film, France.

Screen-printed electrodes (SPEs) were produced with a DEK 248 printing machine from DEK, UK, using polyester screens with appropriate stencil designs (three polyester DEK screens featuring the patterns for printing the relevant layers of the electrochemical systems were purchased).

A specially designed box under nitrogen flow was used for exposition of the samples (i.e., curing of the ISMs) to the UV-light source of a spot lamp system PC 5000 (Dymax, Germany) with irradiance of 62 mW/cm^2 at the wavelength of 365 nm.

Potentiometric measurements were carried out with a CH700 series electrochemical workstation from CH Instruments, USA, controlled by a Windows based PC. The electrodes developed were used as working electrodes and a double junction Ag/AgCl (3 M KCl) RE (Metrohm, Spain) was used for the potentiometric measurements. The pH value of solutions was monitored with a commercial pH-meter (model 827, Metrohm, Spain). All experiments were conducted inside a Faraday cage.

Images of the surface of the samples and roughness measurements were obtained with a PLμ noncontact confocal imaging profiler system attached to a Nikon microscope controlled using PLμ proprietary software (Sensofar, Spain) and a Leo 1530 (Zeiss, Spain) scanning electron-microscope (SEM).

2.2 SPEs Fabrication

Different transducers were fabricated based on an 8-electrode configuration on 500 μm thick PET films.

The basic configuration of the final electrode system consisted in 8 graphite electrodes (Figure 1A). The Ag/AgCl ink was printed over 4 of them to serve as QREs (Figure 1B). Next, the final electrode geometry was defined printing a dielectric material over the substrates (Figure 1C). This dielectric coating also provided further protection to the devices.

We also prepared few sets of SPEs (Figure 2A) with the passivation layer merely covering the connection pads (Figure 2B).

Different curing treatments of the different screen-printed pastes were investigated: 30 minutes at 90 °C and 20 minutes at 120 °C.

Moreover, for the fabrication of the QREs, different configurations were fabricated, such as Ag/AgCl electrodes printed directly on clear PET sheet, on Ag tracks, and on graphite tracks.

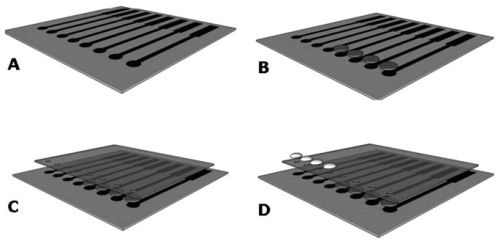

Fig. 1. A) Printing of electrical paths and working electrodes. B) Printing of the QREs. C) Printing of the insulating layer. D) Deposition of the ISMs.

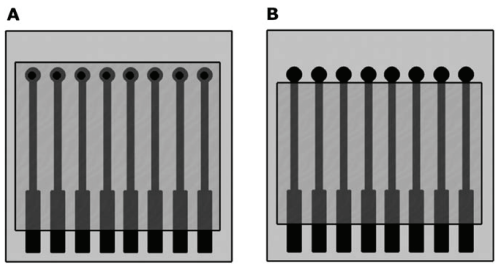

Fig. 2. A) Electrode-set with the original passivation layer design. B) Electrode-set with alternative passivating layer design.

2.3 Ion-Selective Membranes

ISMs are usually prepared from a mixture composed of a high molecular weight polymer, a plasticizer, an ionophore and lipophilic cationic or anionic salts, dissolved in an organic solvent [20]. In this work, ISMs were composed of 0.3 g of a main polymer composition mixture (polyurethane diacrylate, cross-linker and photoinitiator) dissolved in 0.2 mL of THF. Ionophore, plasticizer and lipophilic salts were then added to this solution as described in [21]. The mixture was homogenized in an ultrasonic bath and then the solvent was evaporated for several hours.

The ISMs were produced by carefully dropping 1 μL of the membrane cocktail over the electrode surface (see Figure 1D). The deposited membranes were then exposed to UV-light for 200 seconds under nitrogen. These electrodes could be stored for several days before use, but once immersed in solution the membranes must be kept hydrated.

2.4 Protocols of Electrochemical Characterization and Activation of SPEs

Characterization of the SP graphite electrodes was carried out by CV in 1 mM $K_4Fe(CN)_6$, 0.1 M KNO_3, at a scan rate ranging from 25 to 500 mV s^{-1}.

The effects of electrochemical activation of the electrodes on the pH-sensor performance were also investigated by CV. This electrochemical treatment was meant to clean the electrode pastes of impurities. This activation step consisted in 10 CV scans, ranging from −2 to 2 V, at a scan rate of 50 mV s^{-1}, in a 0.1 M KNO_3 solution.

2.5 Potentiometric Measurements

This section begins describing the potentiometric characterization of Ag/AgCl QREs and then the pH-electrodes, including a selectivity test.

First, the Ag/AgCl QREs were cleaned with deionized (DI) water, dried under mild airflow, and dipped into a stirred potassium dihydrogen phosphate solution (0.04 M KH_2PO_4) also containing potassium chloride (0.06 M KCl). The pH of this solution was raised to 7.00 by addition of potassium hydroxide (0.1 M KOH). The potential of these electrodes was recorded for 5 minutes versus an Ag/AgCl (3 M KCl) RE. The average and standard deviation of the potential during the steady regime (last minute of each measurement) were taken. The electrodes were rinsed with DI water, dried under an air stream and re-analyzed under the same conditions as just described. This protocol was repeated 4 times for each sample. This measurement was repeated over a period of 7 days.

The response of the ISEs to pH change was characterized in a test buffer solution (0.04 M KH_2PO_4, 0.06 M KCl) whose pH was raised to 7.00 by addition of 0.1 M KOH. The open-circuit-potential of each electrode was recorded during 10 minutes in the stirred buffer solution vs. Ag/AgCl (3 M KCl) RE. The solution was then titrated by adding 500 μL of 0.1 M KOH solution every 5 minutes (5 additions are made) on a pH range of 7.00 to 7.63. The pH values were followed with a pH-meter and a glass electrode (see Section 2.1).

The potentiometric response to pH in presence of sodium (i.e., selectivity test) was also studied in a test buffer containing 100 mM Tris with 140 mM sodium chloride (NaCl). The solution was titrated by addition of 500 μL aliquots of the 140 mM HCl, 140 mM NaCl mixture, every 5 minutes.

3 Results and Discussion

3.1 Fabrication of SPEs

44 electrode-sheets (an electrode sheet is composed of 8 electrode sets, each composed of 8 electrodes) were screen-printed (i.e., 2816 electrodes in total). The screens were aligned semi-automatically using the DEK align-4-vision system. As mentioned above, 3 different layers were screen-printed (electrical connector layer, electrode material and passivation layer).

1.0 mm^2 electrodes were reproduced on the PET sheets. Randles-Sevčik analysis of cyclic voltammograms confirmed an electrode size of 1.0 ± 0.1 mm^2.

Confocal images and stylus profiling of the SPEs (data not shown) revealed typical thicknesses of 7 ± 1 μm and 36 ± 3 μm for the electronically conducting materials and the dielectric material, respectively.

3.2 Ag/AgCl Quasi-Reference Electrodes (QRE)

From all the different configurations of QREs fabricated (Ag/AgCl on clear PET sheet, on Ag tracks, and on graphite tracks), the best performance (especially in terms of electrode potential stability) was obtained using Ag/AgCl on graphite tracks printed on the PET sheets. We therefore focused our attention on this material configuration for the QREs.

The curing treatment of the QREs was optimized by successively heating the graphite and then Ag/AgCl layers during 20 minutes at 120°C. SEM images (Figure 3) and confocal images of the topography of different samples revealed that the Ag/AgCl electrodes cured for 20 minutes at 120°C presented a slightly rougher surface ($Ra_{Ag/AgCl\ 120} = 3.3 \pm 0.5$ μm ($n = 8$)) than the ones cured for 30 minutes at 90°C ($Ra_{Ag/AgCl\ 90} = 2.5 \pm 0.5$ μm ($n = 8$)). This indicates that a higher curing temperature is very likely to remove more of the nonmetallic components contained in the pastes, leaving rougher electrode surfaces.

The standard deviation of the potential at these electrodes over a period of 7 days of measurement was ±1.2 mV (for 3 samples). Assuming that this type of electrode is used as QRE in combination with a strictly Nernstian pH-electrode, this deviation represents an error of 0.02 pH units only.

Reproducibility tests have been carried out on 3 different QREs. Their average open-circuit-potential after 4 consecutive experiments was 26.2 ± 0.2 mV, 26.8 ± 0.3 mV and 26.7 ± 0.1 mV, respectively. The magnitude of these errors can be considered really small; as an example, the maximum allowed uncertainty of the RE for monovalent ions in a medical environment, which is one of the most demanding, is ±0.50 mV [22].

3.3 pH-Electrode

The aim of this work is to develop a potentiometric pH-electrode with sensitivity as close as possible to the theoretical Nernstian behaviour. To determine the best configuration, our pH-membrane formulation was deposited on 3 different substrates: bare graphite SPEs, electrochemically activated graphite SPEs, and heat cured graphite SPEs. Different passivation layer designs were also investigated and selectivity tests to Na were performed.

Although direct deposition of membranes over an electrode surface has a variety of long-term negative consequences, this method affords a fast, simple and low cost ISE production process. The main drawback of this approach is the eventual appearance of a liquid layer between the membrane and its solid contact, resulting from membrane peeling, and which results in potential drifts and non-Nernstian response [23,24]. In our case, such potential drifts were insignificant, and the fact that the response was nearly Nernstian implies the absence of a water layer between the membrane and the electrode during the test period. Moreover, it has been demonstrated [25] that solid-contact ISEs, like the ones presented here, displayed performances very close to the ones of ISEs with an internal electrolyte.

Thus, in our work, the pH-membrane formulation was directly deposited on nonpretreated graphite SPEs. The potentiometric response to pH of this ISE system was characterized over 7 days. The average potentiometric response was −40.0 mV/pH, far from the theoretical Nernstian response of −59.2 mV/pH.

We then investigated by CV the effects of electrochemical activation of the electrodes on the pH-sensor performance as means to improve their sensitivity. This electrochemical treatment was meant to clean the electrode pastes of impurities via in situ generation of hydrogen at the electrode surface. Typical effects of the electrochemical activation of the graphite electrodes consisted in increases of both capacitive and faradaic current (Figure 4), which reflect the roughening of the surface and therefore

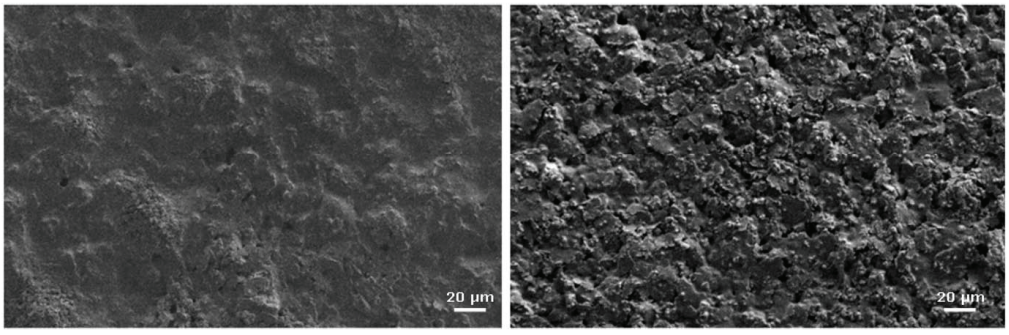

Fig. 3. SEM images of: A) an Ag/AgCl QRE cured for 30 minutes at 90°C. B) an Ag/AgCl electrode cured for 20 minutes at 120°C.

a net increase in active surface area due to the activation step.

The increase of roughness due to electrochemical activation was confirmed by confocal microscopy as well as surface roughness measurements: $Ra_{activated} = 1.7 \pm 0.5$ µm ($n = 8$), whereas $Ra_{nonactivated} = 1.0 \pm 0.1$ µm ($n = 8$).

Following electrochemical activation, the electrodes were coated with the pH-membrane and their potentiometric response to pH changes was recorded over 7 days. The average slope was −51.7 mV/pH. The activation step improved the potentiometric response of the electrodes, which became more Nernstian.

One can assume that the violence of the bubble generation from the electrochemical activation process resulted in an increase of the surface roughness of the electrodes. We believe that this allowed the electrodes to display a better pH response than nonactivated ones because it enhanced the adhesion of the polymer membranes on their surface.

Since a high resistivity of SPEs may be detrimental to the overall sensor performance and requires more expensive electronic components, we explored the effect of curing treatment on the overall resistivity of the SPEs.

Analysis of the surface of the electrodes by confocal microscopy and SEM, (data not shown) revealed that the shape of the electrodes was better defined after curing them 30 minutes at 90 °C than after curing them 20 minutes at 120 °C (where the passivation layer material seemed to partially cover the electrodes). However, curing the pastes 20 minutes at 120 °C resulted in a thinner passivation layer and allowed the resistance of the devices to decrease from 2.31 kΩ (curing at 90 °C for 30 minutes) to 1.65 kΩ.

As it has also been discussed elsewhere [26], this is likely due to the fact that more of the nonmetallic components present in the pastes either decompose or evaporate after raising the curing temperature. These phenomena cause an increase of the carbon content of the pastes and ultimately lead to an increase of their conductivity. Curing at temperatures beyond 120 °C did not seem to offer any further resistivity improvements.

One of the samples that underwent this thermal treatment was then activated by CV (same protocol as previously used) before drop-casting of the pH-membrane. Thermal treatment followed by electrochemical activation of the electrodes allowed the pH response of the ISEs to rise to an average value of −53.0 mV/pH over the 7 days of measurement.

The last step in the optimization of the pH-sensors was the verification of the passivation-layer influence around the electrodes. We prepared some other sets of SPEs (electrodes cured 20 minutes at 120 °C and subsequently electrochemically activated as described above), this time featuring the passivation layer design described in Figure 2B and ultimately drop-cast ISMs on them. Their average potentiometric pH response (only characterized 4 days) was −53.5 mV/pH. Despite displaying a potentiometric response very similar to the previous electrodes featuring the passivation layer based on the layout depicted in Figure 2A, the appearance of the ISMs changed after being immersed in the test solution for a couple of days. While one would expect the membranes to swell due to water intake during the hydration phase [27,28], they surprisingly seemed to shrink and slightly delaminate. These phenomena could probably be explained on the grounds that the ISM adheres preferentially to the

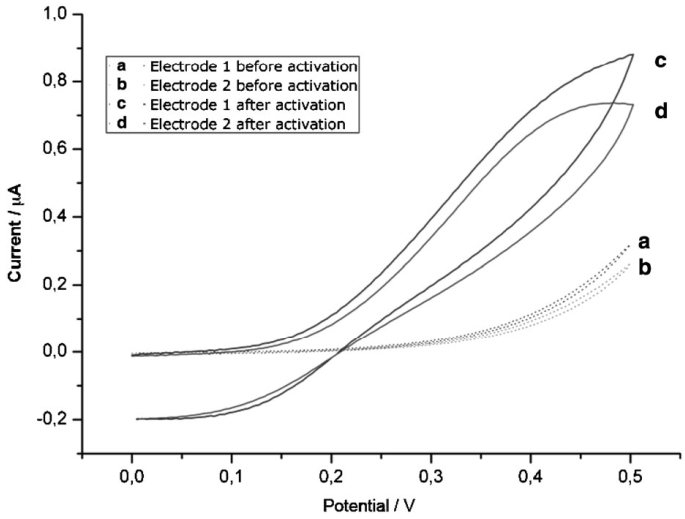

Fig. 4. Cyclic voltammograms of 2 graphite electrodes before and after electrochemical activation.

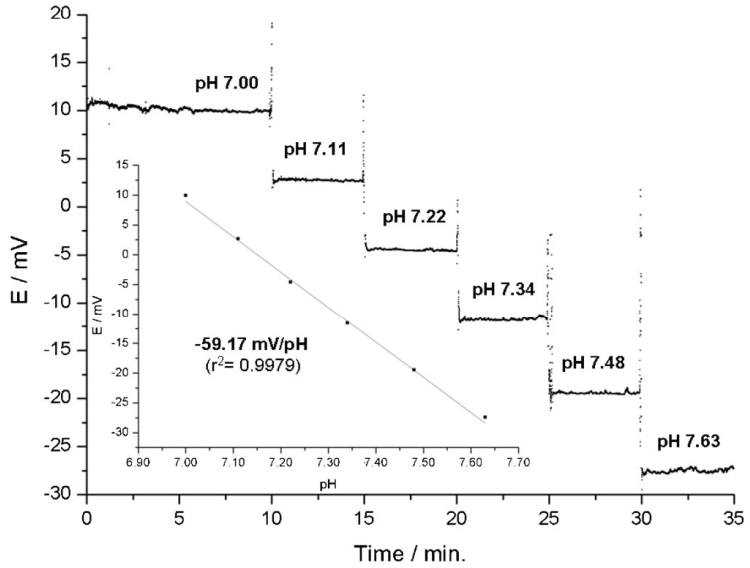

Fig. 5. Example of titration plot and its related calibration plot of the potentiometric system pH-electrode vs. Ag/AgCl QRE.

passivation layer compared to the PET substrate, and therefore the absence of the dielectric passivation layer around the electrodes results in a poorer adhesion of the membranes and a shorter electrode lifetime.

An important requirement for our pH-electrode is to be selective in the presence of physiologically important ionic species such as Li^+, Na^+, K^+, etc. The potentiometric pH response of the ISEs has been studied by titration in sodium containing solutions. We observed that the presence of 140 mM of NaCl did not interfere with the pH response. During 7 consecutive days of measurement the pH-electrode displayed a pH response of −55.1 mV/pH, which was fairly close to its response in absence of Na^+. The selectivity of our sensor was assumed to be the similar to that of the sensors presented in [21], because the same ionophore was used in both cases.

3.4 QRE/ISE System Performance

In the previous sections, we have described the individual construction of a QRE and a pH-electrode. Both of them were stable and reliable over a target period of at least 7 days. The typical potentiometric response of this system during titration and the corresponding calibration plot are displayed in Figure 5. As seen in Figure 5, the response time of the system was very short and a stable potential was reached after less than a minute after titration.

The average potentiometric response of the electrochemical system was -60.8 ± 1.7 mV/pH after the 2 first days of membrane conditioning, which is exceptionally close to the theoretical Nernstian behaviour. Indeed, our ISMs needed a preconditioning phase by immersion in the test solution for 2 days before reaching a steady potentiometric response. During this period, water is transported through the polymer membrane of the ISE until a steady state condition is reached [27]. In order to greatly decrease this preconditioning time, one could think of storing the sensors in containers with a humid atmosphere before use [29].

4 Conclusions

SP has proven to be a simple, fast and low-cost means to develop disposable potentiometric electrochemical systems.

While the effect of the electrochemical pretreatment of different SP pastes has been investigated in few other works (e.g., [30]), the effect of the thermal electrode pretreatment has only rarely been considered [9]. In our work, combining electrochemical and thermal treatments of SPEs considerably improved the performance of QREs and ISEs. Indeed, the post printing curing step of the electrode pastes (Ag/AgCl QREs and graphite working electrodes) of 20 minutes at 120 °C decreased the electrodes electrical resistance, very likely due to thermal decay of the plastic/nonconducting components of the ink.

The optimized QREs presented an excellent potential stability over 7 days (±1.2 mV, for 3 QREs characterized). Therefore, our QREs are in principle suitable for a

broad range of applications. This QRE was used in combination with our screen-printed pH-sensor in saline solutions of controlled composition and constant ionic strength. Possible applications for this system are the control of the saline solutions used in dialysis equipment or the analysis of environmental samples. However, in any final application, the RE must be separated from the test solution to ensure reference potential stability in the presence of chloride ions.

Electrochemical activation of the graphite working electrodes prior to the deposition of ISMs proved to be largely beneficial. This electrochemical activation by CV helped removing some of the impurities present on the graphite paste. In addition, the violence of hydrogen bubble generation resulted in an increase of surface roughness which enhanced the adhesion of the polymer membranes on their surface and lead to higher pH sensitivity ISEs.

The passivation layer material used to protect the electrodes also played an important role in improving the adhesion of the pH-membranes on the electrodes. Surrounding the electrodes with a layer of dielectric material not only prevented electrode delamination but also allowed the membranes to stick more strongly to their surface (adhesion of the membrane is stronger on the passivation layer than directly on the PET substrate), increasing their stability and hence, the sensor lifetime.

Last, we integrated the optimized QRE and pH-electrode on the same PET substrate. The potentiometric response to pH of the final system was in good agreement with the theoretical Nernstian behavior. During the 6 days following 2 days of hydration, the pH response of a typical system was -60.8 ± 1.7 mV/pH. This experimental error value makes this QRE potentially suitable for nearly any kind of application.

Future work will verify the influence of composition and the use of broader range of curing treatments of the SP pastes on the electrochemical performance of the sensors. In fact, all of these parameters are currently under investigation by our group in order to pave the way towards new low-cost disposable potentiometric systems for use in biomedical applications. Also, we are working on the development of a flow-system where the QRE is physically separated from the pH sensor in contact with the sample solution.

Acknowledgements

The authors would like to acknowledge *Radiometer Medical* and the *Spanish Ministry of Science and Innovation (MICINN)* (through two *Ramón y Cajal* Fellowships, Project CTQ2009-08595 and Contract Number AGL2008-05578-C05-05) for financial support.

References

[1] Ł. Tymecki, S. Glab, R. Koncki, *Sensors* **2006**, *6*, 390.
[2] M. Prudenziati, B. Morten, *Microelectr. J.* **1992**, *23*, 133.
[3] C. A. Galán Vidal, J. Munoz, C. Dominguez, S. Alegret, *Trends Anal. Chem.* **1995**, *14*, 225.
[4] Ł. Tymecki, E. Zwierkowska, R. Koncki, *Anal. Chim. Acta* **2004**, *526*, 3.
[5] S. Laschi, I. Palchetti, G. Marrazza, M. Mascini, *J. Electroanal. Chem.* **2006**, *593*, 211.
[6] O. Domínguez Renedo, M. A. Alonso-Lomillo, M. J. Arcos Martúnez, *Talanta* **2007**, *73*, 202.
[7] J. P. Hart, S. A. Wring, *Trends Anal. Chem.* **1997**, *16*, 89.
[8] M. Tudorache, C. Bala, *Anal. Bioanal. Chem.* **2007**, *388*, 565.
[9] R. O. Kadara, N. Jenkinson, C. E. Banks, *Sens. Actuators B, Chem.* **2009**, *138*, 556.
[10] C. A. Burtis, R. Ashwood, *Fundamentals of Clinical Chemistry*, 5th ed., Saunders, New York **2001**, p. 105.
[11] E. Lindner, R. E. Gyurcsányi, *J. Solid State Electrochem.* **2009**, *13*, 51.
[12] M. Vamvakaki, N. A. Chaniotakis. , *Anal. Chim. Acta* **1996**, *320*, 53.
[13] E. Lindner, V. V. Cosofret, S. Ufer, R. P. Buck, W. J. Kao, M. R. Neuman, J. M. Anderson, *Biomed. Mater. Res.* **1994**, *28*, 591.
[14] G. S. Cha, D. Liu, M. E. Meyerhoff, H. C. Cantor, A. Rees Midgley, H. D. Goldberg, R. B. Brow *n, Anal. Chem.* **1991**, *63*, 1666.
[15] H. Nam, G. S. Cha, T. D. Strong, J. Ha, J. H. Sim, R. W. Hower, S. M. Martin, R. B. Brown, *Proc. IEEE*, **2003**, *91*, 870.
[16] E. Lindner, R. P. Buck, *Anal. Chem.* **2000**, *72*, 336.
[17] S. Joo, R. B. Brown, *Chem. Rev.* **2008**, *108*, 638.
[18] N. Abramova, A. Bratov, *Sensors* **2009**, *9*, 7097.
[19] N. Abramova, A. Ipatov, S. Levichev, A. Bratov, *Talanta* **2009**, *79*, 984.
[20] W. Morf, W. Simon, *Ion Selective Electrodes in Analytical Chemistry* (Ed: H. Freiser), Plenum Press, New York **1978**, p. 211.
[21] N. Abramova, A. Bratov, *Talanta* **2009**, *81*, 208.
[22] G. J. Kost, C. Hague, *In Vitro, Ex Vivo, and In Vivo Biosensor Systems, Handbook of Clinical Automation, Robotics and Optimization*, Vol. 648, Wiley, Chichester **1996**.
[23] M. Fibbioli, W. E. Morf, M. Badertscher, N. F. de Rooij, E. Pretsch, *Electroanalysis* **2000**, 12.
[24] J. Bobacka, *Anal. Chem.* **1999**, *71*, 4932.
[25] S. Walsh, D. Diamond, J. McLaughlin, E. McAdams, D. Woolfson, D. Jones, M. Bonner, *Electroanalysis* **1997**, *9*, 1318.
[26] J. Wang, M. Pedrero, H. Sakslund, O. Hammerich, J. Pingarron, *Analyst* **1996**, *121*, 345.
[27] A. Lynch, D. Diamond, P. Lemoine, J. McLaughlin, M. Leader, *Electroanalysis* **1998**. *10*, 1096.
[28] P. Lemoine, P. Mailley, M. Hyland, J. M. McLaughlin, E. McAdams, J. Anderson, A. Lynch, D. Diamond, M. Leader, *J. Biomed. Mater.* **2000**, *50*, 313.
[29] V. V. Cosofret, M. Erdösy, E. Lindner, T. A. Johnson, R. P. Buck, W. J. Kao, M. R. Neuman, J. M. Anderson, *Anal. Lett.* **1994**, *27*, 3039.
[30] G. Cui, J. H. Yoo, J. S. Lee, J. Yoo, J. H. Uhm, G. S. Cha, H. Nam, *Analyst* **2001**, *126*, 1399.

During my Ph.D., I have been presenting my investigations at the following international conferences:

- **Arnaud Emmanuel Musa**, Francisco Javier del Campo, Natalia Abramova, María Asunción Alonso-Lomillo, Olga Domínguez-Renedo, María Julia Arcos-Martínez, Monica Brivio, Detlef Snakenborg, Oliver Geschke, Jörg Peter Kutter, ***Miniaturized screen-printed ISEs for clinical applications***, 61st Annual Meeting of the International Society for Electrochemistry (ISE), September 26th – October 1st, 2010, Nice, France, poster presentation.

- **Arnaud Emmanuel Musa**, Francisco Javier del Campo, Natalia Abramova, María Asunción Alonso-Lomillo, Olga Domínguez-Renedo, María Julia Arcos-Martínez, Monica Brivio, Detlef Snakenborg, Oliver Geschke, Jörg Peter Kutter, ***Miniaturized screen-printed ISEs for clinical applications***, 13th International Conference on Electroanalysis, Gijón, Spain, June 20th – 24th,2010, poster presentation.

- **Arnaud Emmanuel Musa**, Monica Brivio, Detlef Snakenborg, Oliver Geschke, Anders Wolff, ***Development of a lab-on-a-chip system for blood gas analysis***, Nano2life Summer Meeting, June 25th – 27th, 2008, Crete, Greece, short oral presentation and poster presentation